Ichnotaxonomy of the Eocene Green River Formation, Soldier Summit and Spanish Fork Canyon, Uinta Basin, Utah: Interpreting behaviors, lifestyles, and erecting the Cochlichnus Ichnofacies

By

© 2018

Joshua D. Hogue
B.S. Old Dominion University, 2013

Submitted to the graduate degree program in Geology and the Graduate Faculty of the University of Kansas in partial fulfillment of the requirements for the degree of Master of Science.

Chair: Dr. Stephen T. Hasiotis

Dr. Paul Selden

Dr. Georgios Tsoflias

Date Defended: May 1, 2018

The thesis committee for Joshua D. Hogue certifies that this is the approved version of the following thesis:

Ichnotaxonomy of the Eocene Green River Formation, Soldier Summit and Spanish Fork Canyon, Uinta Basin, Utah: Interpreting behaviors, lifestyles, and erecting the Cochlichnus Ichnofacies

_____

Chair: Dr. Stephen T. Hasiotis

Date Approved: May 1, 2018

ABSTRACT

The Eocene Green River Formation in the Uinta Basin, Utah, has a diverse ichnofauna. Nineteen ichnogenera and 26 ichnospecies were identified: *Acanthichnus cursorius*, *Alaripeda lofgreni*, c.f. *Aquatilavipes* isp., *Aulichnites* (*A. parkerensis* and *A. tsouloufeidos* isp. nov.), *Aviadactyla* (c.f. *Av*. isp. and *Av*. *vialovi*), *Avipeda phoenix*, *Cochlichnus* (*C. anguineus* and *C. plegmaeidos* isp. nov.), *Conichnus conichnus*, *Fuscinapeda texana*, *Glaciichnium liebegastensis*, *Glaroseidosichnus* ign. nov. *gierlowskii* isp. nov., *Gruipeda* (*G. fuenzalidae* and *G. gryponyx*), *Midorikawapeda* ign. nov. *semipalmatus* isp. nov., *Planolites montanus*, *Presbyorniformipes feduccii*, *Protovirgularia dichotoma*, *Sagittichnus linki*, *Treptichnus* (*T. bifurcus*, *T. pedum*, and *T. vagans*), and *Tsalavoutichnus* ign. nov. (*Ts. ericksonii* isp. nov. and *Ts. leptomonopati* isp. nov.). Four ichnocoenoses are represented by the ichnofossils—*Cochlichnus*, *Conichnus*, *Presbyorniformipes*, and *Treptichnus*—representing dwelling, feeding, grazing, locomotion, predation, pupation, and resting behaviors of organisms in environments at and around the sediment-water-air interface. A new Cochlichnus Ichnofacies is established to represent continental assemblages of traces produced in environmental conditions at and around the sediment-water-air interface. The Cochlichnus Ichnofacies can be identified in deposits from as old as the Carboniferous. The Cochlichnus Ichnofacies replaces the Shorebird Ichnofacies and usage of the Mermia Ichnofacies for ephemeral water bodies, and restricts the Mermia Ichnofacies to traces in deeper, perennial water bodies. A new ichnospecies of *Aulichnites* is proposed, *A. tsouloufeidos*. Three new ichnogenera with four ichnospecies are established: *Glaroseidosichnus gierlowskii*, *Midorikawapeda semipalmatus*, and *Tsalavoutichnus* (*Ts. ericksonii*, *Ts. leptomonopati*). This is the first detailed ichnotaxonomic study of the Soldier Summit and Spanish Fork Canyon localities of the Eocene Green River Formation.

ACKNOWLEDGMENTS

Thank you to the Gunther family for their donation of the slabs used in this study to the University of Kansas (KU), without which this research could not have been conducted. Thank you, also, to Mr. Ronald Voelkel for assistance with the German translation of Walter (1985) for the diagnosis of *Glaciichnium liebegastensis*. Thanks to KU IchnoBioGeoScience (IBGS) Research Group for their assistance in the early stages of the formulating of this manuscript.

TABLE OF CONTENTS

INTRODUCTION

No systematic ichnotaxonomic assessment currently exists for the Eocene Green River Formation (GRF). Trace fossils in the GRF, especially in the Uinta Basin, have been under studied despite the formation being well known for body fossils (e.g., Grande, 1984). Ichnological studies are necessary to better understand organism diversity, which may or may not be represented by body fossils (e.g., Hasiotis, 2003, 2004, 2007, 2008). Trace fossils are records of organism behaviors that reflect the physicochemical conditions at the time they were produced (e.g., Bohacs, Hasiotis, & Demko, 2007; Hasiotis & others, 2007; Hasiotis & Platt, 2012). This is the first study to systematically describe trace fossils, microbial mats, and plant traces from the GRF in the Uinta Basin at Soldier Summit and Spanish Fork Canyon, Utah (Fig. 1). Trace fossil and lithofacies associations are used to interpret the physicochemical conditions and paleoenvironmental settings.

Many studies have identified, without systematic descriptions, trace fossils in the GRF (Table 1). Only Bohacs, Hasiotis, and Demko (2007) has provided, albeit general, interpretations of the physicochemical and paleoenvironmental conditions interpreted from trace-fossil associations, describing a diverse group of invertebrate trace fossils (ITFs) and noting associations between the degree of basin fill and the types of trace fossils present. Their study areas, however, were in Wyoming and included work on the time-equivalent Wasatch Formation, therefore representing different environments than the GRF at Soldier Summit and Spanish Fork Canyon, Utah.

There has been much research on vertebrate traces in the GRF (e.g., Curry, 1957; Moussa, 1968; Langston & Rose, 1978; Grande, 1984). Systematic descriptions of bird trace fossils (BTFs), however, are lacking, with contributions being limited to: (1) descriptions based

on potential tracemaker (e.g., Erickson, 1967; Scott & Smith, 2015); and (2) only one trackway being ichnotaxonomically described (*Presbyorniformipes* Yang & others, 1995). Curry (1957) provided the first general descriptions of BTFs but did not place them into any ichnotaxa. Moussa (1968) provided general descriptions and photographs of several bird tracks, with one type assigned to the morphofamily Avipedidae by Mustoe (2002). The only systematically described BTF in the Uinta Basin, *Presbyorniformipes*, is a webbed bird track associated with dabble marks that were first photographed and discussed by Erickson (1967). The dabble marks—attributed by Erickson (1967) to feeding traces while the tracemaker was walking—have yet to be systematically described. More recently, Olson (2014) attributed fossil tracks to a stilt-like bird of the Recurvirostridae in the Charadriiformes, though the tracks were not placed into an ichnotaxon. Scott and Smith (2015) provided detailed photos of bird tracks, noting the preservation of scale impressions on tracks as well as plover-like and *Presbyornis*-like footprints.

This study aims to: (1) provide systematic descriptions and ichnotaxonomic designations to the GRF BTFs and often-associated ITFs; (2) establish ichnocoenoses and assign appropriate ichnofacies; and (3) compare the GRF ichnofossil assemblages to those of other lacustrine deposits.

GEOLOGIC SETTING

The Eocene GRF is a lacustrine deposit consisting of several independent basin systems: Piceance Creek Basin in Colorado, Uinta Basin in Utah, and Green River and Washakie basins in Wyoming (Blakey & Ranney, 2008). These basins were formed via a combination of the Sevier and Laramide orogenic events (Dickinson & others, 1988). Laramide deformation in the Late Cretaceous sedimentologically isolated the basins. Basement-cored uplifts, including the Sevier

uplift to the West, confined the isolated basins that led to the development of lacustrine systems and deposition of the GRF (Blackstone, 1983; Johnson, 1985; Dickinson & others, 1988; Crews & Ethridge, 1993).

Soldier Summit and Spanish Fork Canyon, Utah, are located near the southwestern edge of the Uinta Basin. The Uinta Basin is bounded by the Uinta uplift and the San Rafael and Uncompahgre uplifts to the North and South, respectively, and is separated from Piceance Creek Basin by the Douglas Creek Arch (Bader, 2009). The Uinta Basin is also the source of the largest oil shale deposit in the world, composed primarily of lamosite via cyanobacteria (Dyni, 2006; Berg, 2008). The GRF in the Uinta Basin overlays the Wasatch Formation and is overlain by the Uinta Formation. The precise subdivisions of the GRF in the Uinta Basin vary by locality (Keighley & others, 2003). Generally, the GRF in the Uinta Basin is composed of the Cow Ridge Member, characterized by limestone, claystone, and fine- to very fine-grained sandstone; the Douglas Creek Member, characterized by limestone, siltstone, and sandstone; and the Parachute Creek Member, characterized by oil shale, marlstone, siltstone, and tuff (Cashion, 1995).

BACKGROUND

Most studies on traces in lacustrine deposits have focused on modern and Cenozoic settings (e.g., Cohen, 2003; Hasiotis & others, 2012; Mansilla & others, 2012; Scott & Smith, 2015). Scott and Smith (2015) provided a general review of previously identified GRF trace fossils. The traces are present particularly along lake margins in subaerial and shallow-water conditions, balanced-filled lake-basin conditions, and transitions into transgressive systems (e.g., Erickson, 1967; Moussa, 1968; Bohacs, Hasiotis, & Demko, 2007).

Body fossils in the GRF represent a diverse flora and fauna (e.g., Cope, 1884; Gilmore, 1938; Jepsen, 1966; Olson, 1977; Langston & Rose, 1978; Stokes, 1978; Grande, 1984). The most diverse group of vertebrate body fossils is fish with 14 families represented (Cope, 1884; Grande, 1984) and invertebrate body fossils is insects with 14 orders represented (Scudder, 1890a, b; Cockerell, 1921; Bradley, 1931; Grande, 1984).

The diversity of GRF vertebrate trace fossils described to date is comparatively lower than that for body fossils. Trace fossils that have been reported include coprolites and traces of birds, fish (*Undichna* Anderson, 1976), lizards, and mammals (e.g., Erickson, 1967; Moussa, 1968; Stokes, 1978; Grande, 1984; Martin, Vazquez-Prokopec, & Page, 2010). Of mammals, perissodactyl tracks have been identified in the GRF from Soldier Summit (Moussa, 1968; Bohacs, Hasiotis, & Demko, 2007), and creodont tracks (*Quiritipes* Sarjeant, Reynolds, & Kissell-Jones, 2002) from the Wasatchian in Wyoming (Sarjeant, Reynolds, & Kissell-Jones, 2002).

Research on BTFs in Eocene lacustrine settings is limited (e.g., Curry, 1957; Erickson, 1967; Moussa, 1968). Bird tracks assigned to *Avipeda* Vyalov, 1965, *Gruipeda* Panin & Avram, 1962, and *Uhangrichnus* Yang & others, 1995, were described from the Eocene Fossil Hill at King George Island, Antarctica (Mansilla & others, 2012), an area interpreted as an intermontane lake system (Yaosong, Yanbin, & Erjun, 1996). Mustoe (2002) assigned bird tracks from the Eocene Chuckanut Formation in northwestern Washington to *Ardeipeda* Panin & Avram, 1962, *Avipeda*, *Charadriipeda* Panin & Avram, 1962, and the morphofamily Avipedidae. Bird tracks assigned to *Gruipeda* and *Alaripeda* Sarjeant & Reynolds, 2001, as well as an indeterminate form, were identified in the Eocene Laguna Brava Formation of Argentina (Melchor, de Valais,

& Genise, 2002, 2013; Melchor & others, 2006; Melchor, Buchwaldt, & Bowring, 2013). These Late Eocene tracks were originally misidentified as birdlike dinosaur tracks of Triassic age.

MATERIALS AND METHODS

Twenty-one slabs donated by the Gunther family from Spanish Fork Canyon and Soldier Summit, Utah, were studied (Table 2). All slabs are housed in the KU Ichnology repository. Slabs were labeled with the following methodology: GC-C-#; GC = Gunther collection, C = continental origin, # = slab number. Traces were labeled as Slab ID-Xxx-#; Xxx = abbreviated ichnogenus and ichnospecies, # = trace number. Traces were described via architectural and surficial morphologies and infill pattern and assigned to an ichnotaxon (Hasiotis & Mitchell, 1993; Bromley, 1996). New ichnotaxa were erected for traces that do not fit into those already established. Trace ethology was classified following Bromley (1996). Ichnocoenoses were established based on the unique assemblages of traces identified on each slab horizon with traces, taking into account any crosscutting relationships (e.g., Hammersburg, Hasiotis, & Robison 2018).

Traces were measured with a digital caliper (CEN-TECH item 93293) with 0.2 mm error. A maximum of 20 specimens were measured on slabs with > 20 of a given ichnotaxon. All measurements taken are presented in the appendices at the end of this manuscript. Photographs were taken using a Canon EOS Rebel T3 with a Canon EF-S 18-55mm 1:3.5:5.6 IS II SLR macro lens. Microscope photos were taken using a Nikon SMZ1000 microscope with a Nikon Digital Camera DXM1200 with 0.67x magnification.

Rhizolith branches were categorized using a system of numbered orders following conventions of Weaver and Himmel (1929), Danjon and others (1999), and Pregitzer and others

(2002), with one being the smallest diameter terminal branches, counting up with increasing branch diameter. Root hairs are projections that increase root surface area by up to 50% or more and are present on multiple root orders; however, they are so small in diameter (7–15 μm in angiosperms; Dittmer, 1949; Wulfsohn & Nyengaard, 1999) that they cannot be resolved with the binocular microscope used in this study. Any small, sub-mm scale projections of roots described in this study are, therefore, considered as part of the root branching system, and not root hairs. Rhizolith halo color were identified using Munsell Color (2009).

Such sinusoidal traces as *Cochlichnus* Hitchcock, 1858, were measured as amplitude and wavelength, with amplitude measured as the linear length from the crest of one wave to the trough of the next wave, and wavelength measured as the linear length from the crest of one wave to the crest of the next wave (Elliot, 1985).

Bird trace fossils were identified, measured, and described following morphotypes (Fig. 2.1–2.6) and methods established by Elbroch and Marks (2001), Falk, Hasiotis, and Martin (2010), Falk, Martin, and Hasiotis (2011), and Falk and others (2017). Bird trace-fossil measurements (Figs. 3.1–3.2, 4.1–4.6) include: Track width (W_t), track length (L_t), trackway width (W_{tw}), Angle of Divarication (AoD) from trackway midline (ϕ), stride length (L_s), pace length (L_p), pace width (W_p), Sinuosity Index (SI), and AoDs between digits. Adobe Illustrator Creative Cloud was used to measure trace angles from photographs.

As these samples were collected and donated to the KU Ichnology collection by a third party without horizon or formation member information, establishing representative ichnocoenoses for the sample localities is difficult. Each trace-bearing slab horizon is in and of itself a unique ichnocoenosis. We, therefore, follow the methods of Pemberton and others

(2001), Jackson, Hasiotis, and Flaig (2016), and Hammersburg, Hasiotis, and Robison (2018) in establishing overarching ichnocoenoses for the GRF samples.

SYSTEMATIC ICHNOLOGY

PLANTS

RHIZOLITHS

Figure 5.1–5.2

Material.—GC-C-5 (n = 9), GC-C-11 (n > 20).

Description.—Thin, simple to highly branching traces, 0.2–2.0 mm diameter, sub-mm to 3 cm long, preserved in concave hyporelief. On GC-C-5, traces have reddish yellow haloes (7.5YR 6/6) around concave hyporelief impressions and the impressions crosscut other traces. Branching traces on GC-C-11 slightly curvilinear and numerous, branching at least three times along their length, with each branch being smaller diameter. Diameters of the branches decreases to < 0.1 mm (within the error of the calipers), and morphology shifts from slightly curvilinear to mostly rectilinear. Crosscut other associated traces. Refer to Appendix 1 for additional measurements.

Associated ichnotaxa.—Cochlichnus anguineus Hitchcock, 1858, *C. plegmaeidos*, *Planolites montanus* Richter, 1937, *Sagittichnus linki* Seilacher, 1953, and *Treptichnus pedum* Seilacher, 1955a.

Discussion.—Rhizoliths are distinguishable from burrows by having a combination of passive fill, change in diameter between orders of branches, and distal tapering of terminal segments. Branch orders assist with determining overall branching pattern, which can assist in determining the type of plant that made the traces. Rhizoliths on GC-C-5 are branched with two

orders, taper distally, and have haloes characteristic of oxidation. Crosscutting of associated traces by rhizoliths indicates that they were made after the other traces. Rhizoliths on GC-C-11 display at least four orders of branching, with the largest diameter branches having haloes and the smallest, ~400 μm diameter and smaller branches without haloes.

Rhizoliths represent the presence of plants in the ecosystem at the time the traces were made. Ranging from the Ordovician to recent (Hasiotis, Cressler, & Beerbower, 1999; Retallack, 2001), rhizoliths have been described from a variety of terrestrial environments, both dry and aquatic (e.g., Loope, 1988; Kraus & Hasiotis, 2006). In rock samples predating the rise of aquatic flowering plants (Angiosperms), rhizoliths are good indicators of subaerial exposure (Hasiotis, 2004, 2008). As our samples are from the Eocene, the rhizoliths may have been made by semi-aquatic or aquatic angiosperm plants. The preservation of sub-mm-scale rhizoliths and associated traces is indicative of a water-margin terrestrial environment.

On GC-C-5, the associations with *Treptichnus pedum* suggests a subaerially exposed setting with or without very high-water tables, *Sagittichnus lincki* suggests a shallow aquatic setting, and *Cochlichnus anguineus* suggests periods where the water level was as at the sediment-water-air interface (SWAI). This indicates fluctuations in water level by at least a few cm, with *T. pedum* forming before rhizoliths on a subaerially exposed surface; rhizoliths, *C. anguineus*, and *Planolites montanus* being formed at the SWAI; and *Sa. lincki* and potentially some *Pl. montanus* forming underwater.

GC-C-5 is unique in that the bird track *Fuscinapeda texana* Sarjeant & Langston, 1994, on the epirelief side of the slab presses through the layers and forms a convex trace on the hyporelief of the slab. Since so many layers are punctuated by the bird track, it is not truly associated with the traces on the hyporelief of the slab.

On GC-C-11, the rhizoliths are associated exclusively with *C. anguineus* and *C. plegmaeidos,* suggesting the environment was at the SWAI. The area must have also been calm with very low sedimentation rate to preserve such small root traces.

INVERTEBRATES

Ichnogenus ACANTHICHNUS Hitchcock, 1858

Type ichnospecies.—Acanthichnus cursorius Hitchcock, 1858.

Diagnosis.—Tracks of two parallel rows of imprints, slightly turned outward; imprints short, straight, and strokelike (Hitchcock, 1858; Häntzschel, 1975).

Discussion.—Acanthichnus applies to a variety of parallel trackways whose imprints appear, per the etymology, as prickles or spines (Hitchcock, 1858). One ichnospecies (*Acanthichnus tardigradus* Hitchcock, 1858), however, was separated and established as *Pterichnus tardigradus* by Hitchcock (1865), as the tracks resembled those of myriapods. Hitchcock (1865) held reservations about this change, though his establishment of *Pt. tardigradus* has since been upheld by Keighley and Pickerill (1998).

Acanthichnus cursorius was originally described as a series of leaps with variable distances between imprints of up to eight times longer than the sample with the shortest distances and having up to four sets of imprints (Hitchcock, 1865; see plate VI, fig 1). Dalman and Lucas (2015) emended the diagnosis for *A. cursorius* to include that it can have 2 to 4 pairs of imprints. They also noted an association of *A. cursorius* with *Cheliceratichnus lockleyi* Dalman & Lucas, 2015, suggesting that some of the trackway variations were made by chelicerates. With the variation included in the original and supplemental descriptions of *A. cursorius*, there is no need to emend the diagnosis. We follow Hitchcock's (1858, 1865) diagnosis and his original

interpretations, as the trace morphologies in Dalman and Lucas (2015) represent far different behaviors with only tenuous morphological similarity to *A. cursorius*.

Hitchcock (1858) originally attributed *Acanthichnus* potentially to crustaceans, though Häntzschel (1975) later attributed it to insects. Originally ranging from Triassic–Jurassic, *Acanthichnus* has been described from deposits representing fluviolacustrine, lacustrine, and terrestrial environments (Hitchcock 1858; Lull, 1915). This is the first study to describe *Acanthichnus* from the Eocene, therefore, the new range of *Acanthichnus* is from Triassic to Eocene.

ACANTHICHNUS CURSORIUS (Hitchcock, 1858)

Figure 5.3

Material.—GC-C-15 (n=1).

Diagnosis.—Two to four parallel rows of linear tracks; short, nearly straight, strokelike impressions slightly turned outward (Dalman & Lucas, 2015).

Description.—Slightly sinuous trackway consisting of paired, repeated, elongate, scratchlike imprints turned outward from the trackway median. Width 1.9 mm, length 38.6 mm. Preserved in convex hyporelief.

Associated ichnotaxa.—Avipeda phoenix Vyalov, 1966, *Cochlichnus anguineus*, *Gruipeda gryponyx* Sarjeant & Reynolds, 2001, *Planolites montanus*, and *Protovirgularia dichotoma* McCoy, 1850.

Discussion.—Our specimen closely matches the description and diagrams of *A. cursorius* from Hitchcock (1865, see plate VI, figs. 1, 7, 8, 18; plate VII, fig. 10). This close match to the original material suggests that the GRF sample was also produced by an insect.

Acanthichnus cursorius indicates the presence of insects, potential prey items for birds. One of us (STH) has observed a similar occurrence of trace associations in modern lake sediments (Clinton Lake, Lawrence, Kansas) that became subaerial, exposing freshwater mollusk burrows (*Lockeia* James, 1879) overprinted by annelid (*Cochlichnus*), and terrestrial insect and bird tracks. Associations of *A. cursorius* with *Avipeda phoenix*, *Cochlichnus anguineus*, *Gruipeda gryponyx*, and *Protovirgularia dichotoma*, suggest that water level on GC-C-15 (hyporelief) was at the SWAI.

Ichnogenus AULICHNITES Fenton & Fenton, 1937a

Type ichnospecies.—Aulichnites parkerensis Fenton & Fenton, 1937a

Diagnosis.—Bilobate, ribbonlike trail with medial furrow preserved in convex epirelief; hyporelief surface may show unilobate, convex shape, or concave furrows with convex medial ridge (Fenton & Fenton, 1937a; Fillion & Pickerill, 1990).

Discussion.—Aulichnites is a trail that is part of a group of similar, but very distinct traces: *Gyrochorte* Heer, 1865; *Olivellites* Fenton & Fenton, 1937b; *Psammichnites* Torell, 1870; and *Scolicia* de Quatrefages, 1849 (Hammersburg, Hasiotis, & Robison, 2018). *Aulichnites* lacks the biserially plaited ornamentation or vertically stacked spreite of well-preserved *Gyrochorte* (Heinberg, 1973; Häntzschel, 1975). D'Alessandro and Bromley (1987) and Mángano, Buatois, and Rindsberg (2003) synonymized *Aulichnites* and *Olivellites* under *Psammichnites* as preservational variants. We follow the Hammersburg, Hasiotis, and Robison (2018) rejection of that synonymy due to the original establishments by Fenton and Fenton (1937a, 1937b) of *Aulichnites* as having a medial furrow in epirelief and *Olivellites* as having a medial ridge in epirelief, which are absent in *Psammichnites*. We also follow the rejected synonymy (e.g.,

Häntzschel, 1975; Hakes, 1977; Fillion & Pickerill, 1990) of *Aulichnites* under *Scolicia* by Chamberlain (1971), as no reason was given for the synonymy.

Aulichnites is interpreted as repichnia or pascichnia of gastropods or xiphosurids (Fenton & Fenton, 1937b; Yochelson & Schindel, 1978; Chisholm, 1985; Fillion & Pickerill, 1990). Ranging from the Ediacaran to recent (e.g., Narbonne & Aitken, 1990; MacNaughton, 2003; Desai & others, 2008; Zonneveld, Gingras, & Beatty, 2010; Hammersburg, Hasiotis, & Robison, 2018), *Aulichnites* has been described from deposits representing a range of aquatic environments, including shallow and deep marine, as well as brackish and freshwater (e.g., Fenton & Fenton, 1937a; Zawiskie, Collinson, & Hammer, 1983; Fillion & Pickerill, 1990).

AULICHNITES PARKERENSIS Fenton & Fenton, 1937a

Figure 5.4

Material.— GC-C-13 (n = 1).

Diagnosis.—As type (Fenton & Fenton, 1937a).

Description.—A sinuous bilobate trail with a medial ridge and lacking longitudinal transverse striations. Does not cross over itself. Width 1.1 mm, length 191.0 mm. Preserved in convex hyporelief.

Associated ichnotaxa.—Aulichnites tsouloufeidos, C. anguineus, Conichnus conichnus Männil, 1966, and *Glaciichnium liebegastensis* Walter, 1985.

Discussion.—The medial ridge is what is expected in a well-preserved convex hyporelief of *Aulichnites* (Fenton & Fenton, 1937a). The medial ridge preserved in hyporelief was produced as a function of how the snail moved along the surface with its pseudopod.

The unique crosscutting assemblage of traces on GC-C-13 is likely the result of changes in hydrology. Water level was likely cm-scale deep when associated snail trace *Co. conichnus* was produced, whereas water level was likely at or near the SWAI when the repichnial traces *C. anguineus*, and *Gl. liebegastensis* were produced. *Aulichnites parkerensis* and *Au. tsouloufeidos*, can occur at or below the SWAI in any water depth in oxic bottom water conditions (e.g., Hasiotis & others, 2012).

AULICHNITES TSOULOUFEIDOS new species

Figure 5.4

Material.—GC-C-13 (n = 1).

Etymology.—From the Greek word *tsouloúfi*, wisp, and *eidos*, appearance.

Diagnosis.—Bilobate trail with flanking and medial furrows in epirelief, or ridges in hyporelief; staggered, arcuate projections from the sides of the trail.

Description.—Nearly linear trail with medial and flanking ridges with staggered curved projections directed outwards in an arcuate pattern. Width 8.8 mm, length 79.4 mm. Preserved in convex hyporelief.

Types.—Holotype: GC-C-13.

Associated ichnotaxa.—Aulichnites parkerensis, *C. anguineus*, *Co. conichnus*, and *G. liebegastensis*

Discussion.—Trail begins from the slab margin and terminates in a resting trace, providing evidence for the direction of motion. Most of the arcuate projections point outward towards the direction of motion (Fig. 5.4). Remnants of underlying layers obscure the resting trace. The ichnotaxonomic position of the resting trace cannot be determined, as forcibly

removing those layers may damage or destroy the trace. The association with other repichnial traces and the dwelling trace *Co. conichnus* on GC-C-13 indicate that water level was likely cm-scale deep when *Co. conichnus* was produced, and water level was likely at or near the SWAI when the other repichnial traces were produced.

Ichnogenus COCHLICHNUS Hitchcock, 1858

Type ichnospecies.—Cochlichnus anguineus Hitchcock, 1858.

Diagnosis.—Smooth trails, regularly meandering, resembling a sine curve (Häntzschel, 1975).

Discussion.—Cochlichnus appears similar to, but differs from, the zig-zagging trail *Belorhaphe* Fuchs, 1895, due to lacking its characteristic sharp corners with potential projections at the crests and troughs. *Sinusia* Krestew 1928 and *Sinusites* Demanet and van Straelen, 1938, were moved into *Cochlichnus* by Häntzschel (1975) after being originally placed in *Belorhaphe* by Michelau (1955), as they are sinuous trails whose edges more closely resemble smooth sine curves than sharp corners.

Cochlichnus was originally interpreted as locomotion of an annelid worm (Hitchcock, 1858); though at the time no existing annelid was known to move in such a serpentine pattern. *Cochlichnus* has been attributed to nematodes from observations of trail-making in modern lake-margin and floodplain deposits (Moussa, 1970; Chamberlain, 1975). Metz (1987, fig. 1) shows sinusoidal trails made by modern ceratopogonid (biting midge) larvae at the SWAI. This is supported by Hasiotis (2004, 2008), which interprets that *Cochlichnus* can be made at the SWAI, due to its association with pterosaur traces in the Morrison Formation. *Cochlichnus* ranges from

Ediacaran to recent in marine and Carboniferous to recent in freshwater environments (e.g., Hitchcock, 1858; Häntzschel, 1975; Hasiotis, 2002, 2004, 2008; Lucas & others, 2004).

COCHLICHNUS ANGUINEUS (Hitchcock, 1858)

Figure 5.1, 5.4–5.6, Figure 6.1, 6.3–6.4, 6.6, Figure 7.4, Figure 11.2

Material.— GC-C-1 (n > 20), GC-C-2 (n = 3), GC-C-3 (n = 8), GC-C-5 (n > 20), GC-C-6 (n > 20), GC-C-7 (n > 20), GC-C-10 (n = 7), GC-C-11 (n > 20), GC-C-12 (n > 20), GC-C-13 (n > 20), GC-C-14 (n > 5), GC-C-15 (n > 10), GC-C-16 (n > 10), GC-C-18 (n = 1).

Emended Diagnosis.—Smooth trails with regular to irregular meanders, generally resembling a sine curve.

Description.—Sinusoidal-shaped trails with wavelengths 0.7–2.9 mm and amplitudes 0.3–1.9 mm. These traces often crosscut each other but never crosscut themselves. Irregularities in wavelengths and amplitudes can lead to turns in the trackway axes. Very large masses of crosscutting traces deform each other, as on GC-C-6 (epirelief). Some trails exhibit isolated waves of extended amplitude, ballooning the wave outwards from the rest of the trail and often leading to a change in the direction of the trackway axis. Other trails exhibit isolated waves of flattened amplitude, which also often leads to a change in the direction of the trackway axis. Traces are preserved in concave hyporelief, convex hyporelief, concave epirelief, and concave hyporelief. Refer to Appendix 2 for additional measurements.

Associated ichnotaxa.—Acanthichnus cursorius, *Alaripeda lofgreni* Sarjeant & Reynolds, 2001, c.f. *Aquatilavipes* Currie, 1981, isp., c.f. *Aviadactyla* Kordos, 1985, isp., *Au. parkerensis*, *Au. tsouloufeidos*, *Aviadactyla vialovi* Kordos *in* Kordos & Prakfalvi, 1990, *Avipeda phoenix*, *C. plegmaeidos*, *Co. conichnus*, *G. liebegastensis*, *Gl. gierlowskii*, *Gruipeda fuenzalidae*

Covacevich & Lamperein, 1970, *Gruipeda gryponyx*, *Midorikawapeda semipalmatus*, *P. montanus*, *Pr. dichotoma*, *S. linki*, *Treptichnus bifurcus* Miller, 1889, and *T. pedum*.

Discussion.—We emend this ichnospecies to reflect irregularity in the pattern of the type specimen of *C. anguineus*, which was not clearly defined in the original description of the ichnospecies. Irregularities often occur where segments of wavelengths do not have regular sinusoidal morphology of either flattening patterns of increasing amplitude and/or increases to wavelengths (Fig. 5.5). The overall variation in morphology reflects the locomotion of the organism in response to media consistency and surface microtopography. The resultant pattern is analogous in form to meandering rivers before they form oxbows. Any changes in course of the trail must be accomplished through a flattening of amplitudes for the turn.

Cochlichnus anguineus is the most abundant trace in the GRF samples. Counting the total number of individual trails on each slab, however, is exceedingly difficult due occurrences of extremely high density of trails. On GC-C-6, there is such high density and overlap that the traces deform each other and resolving individual specimens is unrealistic. Other slabs are difficult to get accurate counts for due to the extremely small size and sheer number of traces across a surface. One trail on GC-C-13 appears similar to *Belorhaphe*, however upon closer inspection, the trail is deformed along a small change in elevation. What appear to be extensions from the peaks and troughs of the trail are ridges that are part of the slab and not part of the trail. The trail does, however, have sharper corners than usual due to the surface topography at the time of deposition, likely from slight differences in the wetness and consistency of the media. On GC-C-14, GC-C-15, and GC-C-16, many specimens are difficult to discern as they are cryptic. The number of specimens on those samples is, therefore, inexact and likely greater than the number measured.

On slab horizons where *C. anguineus* is not associated with other traces (including GC-C-7 epirelief, GC-C-13 epirelief, and GC-C-18 epirelief) as well as those where it is only associated with *C. plegmaeidos* and/or *P. montanus* (including GC-C-1 hyporelief, GC-C-2 epirelief, GC-C-3 hyporelief, GC-C-10 hyporelief, GC-C-11 hyporelief, and GC-C-12 epirelief), the environments were likely at the SWAI.

Associations with only bird tracks and no other invertebrate traces—c.f. *Aviadactyla* isp. on GC-C-3 (epirelief); *Gruipeda gryponyx* on GC-C-6 (epirelief); *Alaripeda lofgreni*, and *Gr. gryponyx* on GC-C-6 (hyporelief); *Gr. gryponyx* on GC-C-7 (hyporelief); *Avipeda phoenix* and *Gr. gryponyx* on GC-C-14 (epirelief); *Al. lofgreni*, *Av. vialovi*, *Ap. phoenix*, and *Gr. gryponyx* on GC-C-15 (epirelief)—is indicative of water level at the SWAI.

On GC-C-5 (hyporelief) trace-fossil associations with *P. montanus*, rhizoliths, *S. linki*, and *T. pedum* suggest variation in water level above the SWAI (*T. pedum* and possibly rhizoliths and *P. montanus*), at the SWAI (*C. anguineus* and possibly *P. montanus* and rhizoliths), and below the SWAI in cm-scale water depths (*S. lincki*). Though *Fuscinapeda texana* appears to be present on GC-C-5 (hyporelief), it is not part of the associations when interpreting the environment as it was impressed from the epirelief of the slab.

On GC-C-13 (hyporelief), where *Cochlichnus* is not associated with bird tracks, but with arthropod, gastropod, and bivalve repichnial and domichnial traces (i.e., *Au. parkerensis*, *Au. tsouloufeidos*, *Co. conichnus*, and *G. liebegastensis*), the water level likely fluctuated, with *Co. conichnus* being formed when water level was deeper and *C. anguineus* and other repichnial traces being formed while at the SWAI.

On GC-C-14 (hyporelief), associations with *Al. lofgreni*, *Av. vialovi*, *Co. conichnus*, *Gr. gryponyx*, *P. montanus*, and *T. bifurcus* indicates fluctuation in water level around the SWAI: *T.*

bifurcus and potentially bird tracks and *P. montanus* produced above the SWAI; *C. anguineus*, bird tracks, and potentially *P. montanus* produced at the SWAI; and *Co. conichnus* and potentially *P. montanus* produced in cm-scale water depths.

On GC-C-15 (hyporelief), trace fossil associations with *A. cursorius*, *Ap. phoenix*, *Gr. gryponyx*, *P. montanus*, and *Pr. dichotoma* suggest water level was at the SWAI.

On GC-C-16 (hyporelief), the trace-fossil associations with c.f. *Aquatilavipes* isp., *Av. vialovi*, *Gl. gierlowskii*, *Gr. fuenzalidae*, and *Midorikawapeda semipalmatus* indicates that that environment underwent a fluctuation in water depth. Water was deeper when *Gl. gierlowskii* was produced and at the SWAI when the other traces were produced.

COCHLIHCNUS PLEGMAEIDOS new species

Figure 5.6

Material.—GC-C-1 (n = 4), GC-C-10 (n = 1), GC-C-11 (n = 1), GC-C-12 (n = 3).

Etymology.—From the Greek words *plegma*, braided, and *eidos*, appearance.

Diagnosis.—Mostly straight, horizontally oriented trail with a helical form and a central sinusoidal pattern.

Description.—Trails preserved in hyporelief as convex coils and concave sinusoidal furrows (GC-C-1, GC-C-10, and GC-C-11), and in epirelief as concave coils and convex sinusoidal ridges (GC-C-12). Trail widths range from 1.4–2.2 mm, averaging 1.6 mm, and lengths range from 8.2–79.8 mm, averaging 37.4 mm. Refer to Appendix 3 for additional measurements.

Types.—Holotype: GC-C-1; Paratypes: GC-C-10, GC-C-11, GC-C-12.

Associated ichnotaxa.—Cochlichnus anguineus and *P. montanus*.

Discussion.—The effect of the internal sinusoidal furrow on the helical coils gives the trace a braidlike appearance, though the trace is not truly a braided form. *Cochlichnus plegmaeidos* differs from *Helicolithus* Azpeitia-Moros, 1933, due to following a straighter course, whereas *Helicolithus* meanders and exhibits self-looping patterns. *Cochlichnus plegmaeidos* further has no gap between coils as in *Helicolithus* or related *Helicodromites* Berger, 1957, though this is not to be mistaken for the tightly packed, high coil density of *Helicorhaphe* Książkiewicz, 1970. *Helicodromites* has a corkscrew-shaped morphology along a straight horizontal axis (Poschmann, 2015). *Cochlichnus plegmaeidos* differs from *Helicodromites* in that the visible coils are bisected by the sinusoidal furrow. *Cochlichnus plegmaeidos* is always present with other forms of *Cochlichnus* among our samples.

In our samples, some *C. plegmaeidos* exhibit short transitions to forms similar to the sinusoidal *C. anguineus* along the same trace due to the loss of the helical form. One of the examples on GC-C-1 has a segment where the sinusoidal furrow is barely visible and appears in some lighting angles as *Helicorhaphe*. The morphology of *C. plegmaeidos* is more similar to *Cochlichnus* than helical ichnotaxa due to the highly characteristic central sinusoidal pattern along the trace.

Cochlichnus plegmaeidos is likely a burrow of a vermiform organism made just under the sediment surface. The medium was wet and soft, forcing the tracemaker down into the sediment to continue locomotion. Points of transition indicate local areas of increasing or decreasing wetness depending on transitions to more helical or sinusoidal forms, respectively. The size of the central sinusoidal pattern is consistent with the co-occurring *C. anguineus*, indicating that these trails were likely made by nematode-size organisms. The surface was, therefore, likely at or near the SWAI on slabs horizons.

Ichnogenus CONICHNUS (Männil, 1966)

Type ichnospecies.—Conichnus conichnus Männil, 1966.

Diagnosis.—Conical or subcylindrical vertical structures with a base that is either rounded or a papillalike protuberance. Infill may have such internal structures as chevron laminations, but not radial medusoid symmetry (Männil, 1966; Frey & Howard, 1981; Pemberton, Frey, & Bromley, 1988).

Discussion.—In Häntzschel (1975), Männil was written as Myannil, and that spelling has permeated the literature (e.g., Frey & Howard, 1981, Pemberton, Frey, & Bromley, 1988). Jensen (2001), however, points out that that spelling was based on a transliteration of the original name from Estonian to Cyrillic, and that the spelling should be as Männil.

Pemberton, Frey, and Bromley (1988) synonymized 15 ichnogenera of similar plug-shaped morphologies into five: *Astropolichnus* Crimes & Anderson, 1985, *Bergaueria* Prantl, 1945, *Conichnus*, *Conostichus* Lesquereux, 1876, and *Dolopichnus* Alpert & Moore, 1975. Lack of radial medusoid symmetry distinguishes *Conichnus* from *Bergaueria* and *Conostichus* (Frey & Howard, 1981). *Conichnus* also lacks the characteristic ridged rim of *Astropolichnus* and does not terminate in an expanded chamber, as in *Dolopichnus*.

Conichnus is interpreted as domichnia or cubichnia of actinians or clams (e.g., Männil, 1966; Frey & Howard, 1981). Ranging from the early Cambrian to recent (e.g., Hiscott, James, & Pemberton, 1984; Pemberton & Jones, 1988; Jackson, Hasiotis, & Flaig 2016; Hammersburg, Hasiotis, & Robison, 2018), *Conichnus* is known from deposits representing shallow marine, intertidal, fluvial, or lacustrine depositional environments (e.g., Frey & Howard, 1981; Hiscott, James, & Pemberton, 1984).

CONICHNUS CONICHNUS (Männil, 1966)

Figure 5.4, Figure 6.1, Figure 7.3

Material.—GC-C-13 (n = 25), GC-C-14 (n > 10).

Diagnosis.—Tapered, cone-shaped traces indistinctly to thinly lined with a smooth, rounded, distinct basal apex (Frey & Howard, 1981).

Description.—Short, plug-shaped protuberances with smooth fill preserved as endichnia on hyporelief of slab (Fig. 6A, B, E). Diameters average 0.8 mm. Traces do not fully penetrate the slab. Refer to Appendix 4 for additional measurements.

Associated ichnotaxa.—Alaripeda lofgreni, *Au. parkerensis*, *Au. tsouloufeidos*, *Av. vialovi*, *Ap. phoenix*, *C. anguineus*, *G. liebegastensis*, *Gr. gryponyx*, *P. montanus*, and *T. bifurcus*.

Discussion.—Spacing between individual *Co. conichnus* traces is inconsistent with such U-shaped tubes as *Arenicolites* Salter, 1857, and *Diplocraterion* Torell, 1870. Since the traces do not penetrate the slab they are more likely plug-shaped traces rather than vertical burrows like *Skolithos* Haldeman, 1840.

Conichnus conichnus is the only vertically oriented trace of the GRF samples. Due to the small size of the traces, water flow and sediment accumulation were likely low to allow the mm-scale tracemaker, likely a snail, as well as other tracemakers, to construct these and other traces.

Associations with repichnial and grazing traces including *Au. parkerensis*, *Au. tsouloufeidos*, *C. anguineus*, and *G. liebegastensis* on GC-C-13 (hyporelief) suggests fluctuations in water level: deeper, likely cm-scale water depth with the development of *Co. conichnus* and likely the SWAI with the development of the other traces.

On GC-C-14 (hyporelief), associations with *Al. lofgreni*, *Av. vialovi*, *Ap. phoenix*, *C. anguineus*, *Gr. gryponyx*, *P. montanus*, and *T. bifurcus* indicate fluctuations in water level around the SWAI, with *Co. conichnus* indicating cm-scale water depth, *C. anguineus* and possibly *P. montanus* and bird tracks indicating the SWAI, and *T. bifurcus* and possibly *P. montanus* and bird tracks indicating subaerial exposure.

Ichnogenus GLACIICHNIUM Walter, 1985

Type ichnospecies.—Glaciichnium liebegastensis Walter, 1985.

Diagnosis.—Paired and staggered, C-shaped impressions oblique to the trackway axis forming narrow track widths < 5-mm diameter.

Discussion.—The patterns characteristic of *G. liebegastensis* differentiate it from similar repichnial trails, such as *Diplichnites* Dawson, 1873, and *Lithographus* Hitchcock, 1858. In *Diplichnites*, the impressions lack the C-shaped pattern, and tracks have two rows of paired imprints, as opposed to a single row of staggered or paired impressions in *Glaciichnium*. *Lithographus* impressions are more J shaped, with each impression comprised of multiple segments, as opposed to just one in *Glaciichnium*.

Glaciichnium is interpreted as a repichnial trace of arthropods, including many forms of insect larvae or nymphs, such as ephemeropterans (mayflies), plecopterans (stoneflies), and megalopterans (alderflies, dobsonflies, etc.), though the trace has been shown to be made by *Asellus aquaticus*, an isopod crustacean typical of glacial lakes (e.g., Schwarzbach, 1938; Gibbard & Stuart, 1974; Uchman, Kazakauskas, & Gaigalas, 2009). Ranging from Eocene–Pleistocene, *Glaciichnium* is known exclusively from lacustrine deposits (Walter, 1985; Uchman, Kazakauskas, & Gaigalas, 2009).

GLACIICHNIUM LIEBEGASTENSIS Walter, 1985

Figure 5.4, Figure 6.2

Material.—Fig. 6. GC-C-13 (n = 14).

Diagnosis.—Gauge and step width 3 mm; those with varying regularity of alternating C impressions form approximately 1-mm-wide double groove (Walter, 1985).

Description.—Trails consist of paired parallel or offset V-shaped markings, with or without central ridges down the center of the trail that can deform the markings; widths from 1–1.9 mm, averaging 1.5 mm; lengths from 25.3–272.5 mm, averaging 108.3 mm; preserved in convex hyporelief. Refer to Appendix 5 for additional measurements.

Associated ichnotaxa.—Aulichnites parkerensis, Au. tsouloufeidos, C. anguineus, Co. conichnus.

Discussion.—Trail morphologies are consistent with *G. liebegastensis* following Uchman, Kazakauskas, and Gaigalas (2009), who applied this ichnotaxon to a range of similar morphologies of the V-like patterns. They attributed the differences in morphology to differing ventral anatomical features of tracemakers exhibiting the same locomotive behavior. The central ridges are attributed to drag marks.

Arthropods are the likely tracemakers of these samples, likely feeding on a variety of aquatic and semiterrestrial annelids and arthropods, including those that produced the associated *C. anguineus* trails and burrows. Associations with the repichnial and domichnial traces on GC-C-13 are indicative of variations in water depth, with *Co. conichnus* being produced in cm-scale water depth, whereas the repichnial traces likely at the SWAI.

Ichnogenus GLAROSEIDOSICHNUS new genus

Type ichnospecies.—Glaroseidosichnus gierlowskii

Etymology.—From the Greek, Gláros, for seagull, eidos, for appearance, and ichnus, for trace.

Diagnosis.—Series of paired, arcuate impressions, directed outward from center; small gap (~0.5 mm) between impressions in center; gap between impression sets approximately 7 mm; preserved in convex hyporelief or concave epirelief.

Discussion.—Impressions form a shape similar to simple, V-shaped seagull wing drawings with a small gap in the middle. *Broomichnium flirii* Benner, Ridge, & Taft, 2008, is a similar trace made by fish pectoral fins, which differs from *Glaroseidosichnus* in that the gap between imprints is much wider and the holotype has extra linear lines between the paired impressions, interpreted as anal fin impressions. *Glaroseidosichnus* instead seems to be made from the hind legs of swimming insect nymphs or adults, such as diving beetles (Coleoptera, Dytiscidae), water boatmen (Hemiptera, Corixidae), and other aquatic hemipterans. *Glaroseidosichnus* is interpreted as a repichnial trace from an Eocene shallow lacustrine environment.

GLAROSEIDOSICHNUS GIERLOWSKII new species

Figure 6.3

Material.—GC-C-16 (n = 1)

Etymology.—Named after Elizabeth Gierlowski-Kordesch, professor at Ohio University who passed away in 2017.

Diagnosis.—As ichnogenus.

Description.—Trail of paired, C-shaped impressions, directed outward from the center; ~0.5 mm gap between center of each paired impression; space between impression sets approximately 7 mm; width 8.5 mm; length 58.7 mm; preserved in convex hyporelief.

Types.—Holotype: GC-C-16.

Associated ichnotaxa.—c.f. *Aquatilavipes* isp., *Av. vialovi*, *C. anguineus*, *Gr. fuenzalidae*, and *M. semipalmatus*.

Discussion.—Appear as seagull wing drawings with a small gap between the wings. Both ends of the trail are more cryptically preserved on the slab surface, indicating that the tracemaker swam close to medium surface, leaving the imprints, and then rose into the water column. The insect tracemaker likely fed on other aquatic arthropods and annelids but was also itself likely a food source for birds. Trace-fossil associations on GC-C-16 (hyporelief) suggests water level fluctuated between the SWAI (*C. anguineus* and bird tracks) and below the SWAI, with depth up to ~5 cm for swimming insects (*Gl. gierlowskii*).

Ichnogenus PLANOLITES Nicholson, 1873

Type ichnospecies.—Planolites beverleyensis Billings, 1862.

Diagnosis.—Straight to curvilinear, horizontal burrows, rarely lined or branching; smooth to irregular walls, and circular to semicircular cross sections. Infill is unstructured and may differ from host lithology (e.g., Pemberton & Frey, 1982; Fillion & Pickerill, 1990; Uchman, 1998).

Discussion.—Pemberton and Frey (1982) differentiated *Planolites* from *Palaeophycus* Hall, 1847, by diagnosing *Planolites* as having no wall linings and active infilling. Keighley and Pickerill (1995) argued for using the lack of a lining as the primary differentiating criterion as well as for synonymizing *P. montanus* Richter, 1937, under *P. beverlyensis* on the basis that the

only appreciable difference between the two is size, though this synonymy has been largely ignored (e.g., Pickerill & Fyffe, 1999; Uchman, 1999; Hofmann & others, 2012).

Planolites is attributed to a variety of burrowing vermiform organisms and arthropods (e.g., Häntzschel, 1975; Hasiotis, 2004, 2007, 2008; Smith & others, 2008a, 2009). Ranging from Ediacaran to recent, *Planolites* has been described from deposits representing both marine and continental (terrestrial and aquatic) environments (e.g., Häntzschel, 1975; Fillion & Pickerill, 1990; Ekdale, Bromley, & Loope, 2007; Hasiotis, 2004, 2007, 2008; Smith, Carroll, & Singer, 2008; Smith & others, 2009).

PLANOLITES MONTANUS (Richter, 1937)

Figure 5.2, Figure 6.1, 6.4, 6.6, Figure 7.3, 7.6

Material.—GC-C-1 (n = 1), GC-C-2 (n = 4), GC-C-5 (n > 25), GC-C-14 (n > 5), GC-C-15 (n = 3).

Diagnosis.—Bent to distorted relatively small burrows (Pemberton & Frey, 1982**)**.

Description.—Straight to slightly curved, unlined, and unbranching horizontal burrows. On GC-C-1, length of trace 16.8 mm, width 1.5 mm, convex hyporelief. On GC-C-2, lengths from 67.9–173 mm, averaging 99.8 mm; widths from 0.8–3.5 mm, averaging 2.3 mm, convex epirelief. On GC-C-5, two forms of preservation present: one with different texture infill than the host lithology preserved in convex hyporelief; and one as casts in concave hyporelief. The convexly preserved samples exhibit a high degree of overlapping; widths ~0.4–0.7 mm. Concavely preserved samples < 0.1-mm scale, with varying lengths of a few mm, and tend to be slightly curved. On GC-C-14, widths from 0.6–1.0 mm, averaging 0.8 mm; lengths from 2.8–44.4 mm, averaging 16.4 mm; convex hyporelief. On GC-C-15, widths from 0.4–0.6 mm,

averaging 0.67 mm; lengths from 29.8–54.1 mm, averaging 39.5 mm; convex hyporelief. Refer to Appendix 6 for additional measurements.

Associated ichnotaxa.—Acanthichnus cursorius, *Al. lofgreni*, *Av. vialovi*, *Ap. phoenix*, *C. anguineus*, *C. plegmaeidos*, *Gr. gryponyx*, *Pr. dichotoma*, rhizoliths, *S. linki*, *T. bifurcus*, and *T. pedum*.

Discussion.—Planolites montanus lacks annulations, is smaller size than *P. beverlyensis*, and is mostly straight (Billings, 1862; Pemberton & Frey, 1982). On its own, *P. montanus* is not a particularly good indicator of the paleoenvironment because it is ubiquitous across varying environments of deposition in the rock record (e.g., Hasiotis, 2004, 2008; Smith & others, 2009). On GC-C-5 (hyporelief), the convexly preserved traces are similar to, but differentiated from *Thalassinoides* Ehrenberg, 1944, by their lack of branching, as their degree of overlapping produces false branching. The concavely preserved traces also on GC-C-5 (hyporelief) appear similar to slightly curved strands of hair in small groups of three or more. The concave *P. montanus* were not formally measured as their widths were within the error range of the measuring equipment. The concave traces were subsurface burrows likely produced by juvenile vermiform organisms, such as juvenile horsehair worms (phylum Nematormorpha, class Gordiadae), in a stable medium.

The associations with *C. anguineus* and *C. plegmaeidos* on GC-C-1 (hyporelief) and *C. anguineus* on GC-C-2 (epirelief) suggest that water level was at the SWAI. On GC-C-5 (hyporelief), the trace-fossil associations indicate water-level fluctuation from subaerial (rhizoliths, *T. pedum*), to the SWAI (*C. anguineus*, rhizoliths), to shallow water depths (*S. lincki*). While *F. texana* is apparent on GC-C-5 (hyporelief), it is impressed from the epirelief of the slab and is not associated with this horizon. On GC-C-14 (hyporelief), the trace-fossil

associations also indicate water-level fluctuation from subaerial (*T. bifurcus*), to the SWAI (bird tracks, *C. anguineus*), to shallow water depths (*Co. conichnus*). On GC-C-15, the trace-fossil associations with *A. cursorius*, *Ap. phoenix*, *C. anguineus*, *Gr. gryponyx*, and *Pr. dichotoma* suggest water level was at the SWAI.

Ichnogenus PROTOVIRGULARIA (McCoy, 1850)

Type ichnospecies.—Protovirgularia dichotoma McCoy, 1850.

Diagnosis.—Straight to slightly curved, unbranched trail with paired, wedge-shaped, lateral projections from a medial ridge or furrow (Han & Pickerill, 1994).

Discussion.—Protovirgularia is a unique trail that was originally interpreted as octocoral and graptolite body fossils (McCoy, 1850). Many ichnogenera were synonymized under *Protovirgularia* by Seilacher and Seilacher (1994), including: *Imbrichnus* Hallam, 1970; *Pennatulites* de Stefani, 1885; *Uchirites* Macsotay, 1967; and *Walcottia* Miller & Dyer, 1878, as they are all morphologically similar and more appropriately represent different ichnospecies of the same ichnogenus.

Neoichnological experiments by Seilacher and Seilacher (1994) showed that bivalves and scaphopods produced trails that looked like *Protovirgularia*, and thus interpreted *Protovirgularia* as a push-pull locomotion (repichnia) and feeding (fodinichnia) trace of those organisms. Ranging from the early Cambrian to recent, *Protovirgularia* is known from marine and brackish water settings (e.g., Han & Pickerill, 1994; Seilacher & Seilacher, 1994; Carmona & others, 2010; Jackson, Hasiotis, & Flaig, 2016; Hammersburg, Hasiotis, & Robison, 2018).

PROTOVIRGULARIA DICHOTOMA (McCoy, 1850)

Figure 6.5

Material.— GC-C-15 (n = 1).

Diagnosis.—Linear bilobate trails with medial furrow and paired, V-shaped projections oblique to trail axis (Han & Pickerill, 1994).

Description.—Unbranched, slightly curved burrow with medial furrow and paired, wedge-shaped crests extending laterally from the furrow. Cut off by slab margins on both ends. The trace fades in two areas along length to be barely visible. Length 168.2 mm, width 2.0 mm. Preserved in convex hyporelief.

Associated ichnotaxa.—Acanthichnus cursorius, *Ap. phoenix*, *C. anguineus*, *Gr. gryponyx*, and *P. montanus*.

Discussion.—The chevron morphology of the sample is similar to that of analogous experimental undertraces illustrated by Seilacher and Seilacher (1994, pl. 1, fig. a). Our specimen also lacks a terminal *Lockeia*-like object, differentiating it from *Pr. rugosa*. *Protovirgularia dichotoma* is attributed to fodinichnia and cubichnia movement of a mollusk across the surface (Uchman, 1998). Small mollusks, such as snails, are common along the banks and shores of modern lakes and ponds, so the presence of *Pr. dichotoma* associated with bird tracks in this part of the GRF is reasonable. The mollusks would have been a potential food item for small shorebirds, represented by *Avipeda* and *Gruipeda*. The associations with bird tracks and other repichnial invertebrate traces indicates that the environment was at or near the SWAI.

Ichnogenus SAGITTICHNUS Seilacher, 1953

Type ichnospecies.—Sagittichnus lincki Seilacher, 1953.

Diagnosis.—Arrowhead-shaped to ovoid to subcircular, convex mounds or concave pits sometimes with a median keel; occur in small to large groups (e.g., Häntzschel, 1975; Gluszek, 1995; Garvey & Hasiotis, 2008).

Discussion.—*Sagittichnus* was described for keeled, arrowhead-shaped pits and mounds (Seilacher, 1953; Głuszek, 1995; Garvey & Hasiotis, 2008). Jones and Hasiotis (2018) have shown that bat trackways can have marks that look similar to *Sagittichnus*.

Retrum, Hasiotis, and Kaesler (2011) showed *Sagittichnus*-like morphologies being formed by freshwater ostracodes. *Sagittichnus* has also been associated with small arthropod trackways (Głuszek, 1995). Ranging from the Cambrian to recent (Bednarczyk & Przybyołwicz, 1980; Retrum, Hasiotis, & Kaesler, 2011; Hammersburg, Hasiotis, & Robison, 2018), *Sagittichnus* has been described from deposits representing a range of wet settings, from shallow marine and brackish to freshwater continental, such as estuaries, lakes, or rivers (e.g., Bromley & Asgaard, 1979; Głuszek, 1995; Garvey & Hasiotis, 2008; Jackson, Hasiotis, & Flaig, 2016).

SAGITTICHNUS LINCKI Seilacher, 1953

Figure 6.6

Material.—GC-C-5 (n > 20).

Diagnosis.—Subcircular–ovoid or arrowhead-shaped small convex mounds lacking discrete medial keels (as type; Garvey & Hasiotis, 2008).

Description.—Sub-mm scale, arrowhead- to ovoid-shaped protrusions generally aligned in orientation with widths from 0.5–0.9 mm; average 0.7 mm. Grouped in sets of up to approximately 10 per cm^2. Preserved in convex hyporelief. Refer to Appendix 7 for additional measurements.

Associated ichnotaxa.—Cochlichnus anguineus, *P. montanus*, *T. pedum*, and rhizoliths.

Discussion.—Specimens were assigned to *S. lincki* due to their small, arrowhead- to ovoid-shaped morphology and concentrated groupings on the slab, though none had a medial keel. The *S. linki* traces are most closely associated in scale with *C. anguineus* and concavely preserved *P. montanus*. The presence of *S. linki* on GC-C-5 represents the medium being stable and the environment being a calm, shallow nearshore lacustrine setting whose sediments were left undisturbed even in burial. In contrast, *C. anguineus* is representative of the SWAI, and rhizoliths and *T. pedum* indicate subaerial exposure. The environment on GC-C-5 (hyporelief), therefore, fluctuated from a shallow water setting, to the SWAI, to being subaerially exposed. While *F. texana* is apparent, the track is impressed from the epirelief side of the slab, pushing through the entire slab and deforming the bottom, and is therefore not truly associated with the hyporelief trace fossil assemblage.

Ichnogenus TREPTICHNUS (Miller, 1889)

Type ichnospecies.—Treptichnus bifurcus Miller, 1889.

Diagnosis.—Horizontal to subhorizontal chains of straight to curved, zigzagging burrow segments with vertical to oblique tubes representing a three-dimensional burrow structure with possible pits and nodules near the base or top of burrow segments at sediment interfaces (Buatois & Mángano, 1993; Uchman, Bromley, & Leszczyński, 1998).

Discussion.—Treptichnus and its ichnospecies have undergone numerous emendations over time, a summary of which is reviewed in Hammersburg, Hasiotis, and Robison (2018): Buatois and others (1998) synonymized *Plangtichnus* Miller, 1889, under *Treptichnus* due to being interpreted as preservational variants of the same structure. This synonymy was upheld and

refined by Rindsberg and Kopaska-Merkel (2005), placing *Plangtichnus* as a junior synonym in *T. bifurcus* due to possessing the key projections of *T. bifurcus*. Rindsberg and Kopaska-Merkel (2005) also suggested that *Haplotichnus* Miller, 1889, *Treptichnus*, and *Plangtichnus* indicate the possibility of a single species of tracemaker forming these differing structures through ontogeny. Getty and Bush (2017) synonymized *Haplotichnus* under *T. bifurcus* after finding that the holotype of *Haplotichnus* also possessed projections key to *T. bifurcus*. The suggestions of ontogeny explaining differences in morphology from Rindsberg and Kopaska-Merkel (2005) can, thus, now be applied solely within *Treptichnus*.

Ontogenesis resulting in the variation of morphologies within *Treptichnus* has, in fact, been shown in a study by Muñiz Guinea and others (2014) utilizing a modern Dipteran, *Symplecta* (a crane fly larva). Muñiz Guinea and others (2014) show that a larva can create a compound trace system starting with *T. bifurcus*-like morphology, transitioning to *T. pedum*-like morphology, then terminating at the surface. Those transitions are resultant from life-stage transitions from larva to pupa to adult, with the pupal stage being responsible for the *Treptichnus*-like forms. The *T. pedum* form is likely the result of searching for a position for final metamorphosis to the adult stage. Modern traces made by midge larvae on river banks and point bars are also similar in form to *Treptichnus* (Uchman, 2005; Martin, 2009).

Treptichnus has been interpreted to represent a variety of behaviors, such as deposit feeding, agriculture, grazing, predation, scavenging, and reproduction (e.g., Seilacher, 2007; Vannier, Gaillard, & Żylińska, 2010; Wilson & others, 2012; Muñiz Guinea & others, 2014; Getty & others, 2016). Potential tracemakers include annelid worms in marine settings and insect larvae and pupae in terrestrial settings (e.g., Miller, 1889; Uchman, Bromley, & Leszczyńsky, 1998; Vannier, Gaillard, & Żylińska, 2010; Muñiz Guinea & others, 2014; Getty & others,

2016). Ranging from the Ediacaran to recent (e.g., Germs, 1972; Uchman, Bromley, & Leszczyński, 1998; Droser & others, 2002; Vannier, Gaillard, & Żylińska, 2010; Hammersburg, Hasiotis, & Robison, 2018), *Treptichnus* has been reported from deposits representing shallow and deep marine, as well as floodplain and proximal lacustrine settings (e.g., Jensen, 1997; Uchman, Bromley, & Leszczyński, 1998; Wilson & others, 2012; Muñiz Guinea & others, 2014; Getty & others, 2016).

TREPTICHNUS BIFURCUS (Miller, 1889)

Figure 6.1, Figure 7.1–7.2

Material.—GC-C-9 (n = 35), GC-C-14 (n = 2).

Diagnosis.—Straight to slightly curved burrow with short projections between elongate, thin, and horizontal burrow segments (Buatois and Mángano, 1993; Uchman, Bromley, & Leszczyński, 1998); may occur as zigzagging chain of evenly spaced alternating beads or depressions around a central axis (Hammersburg, Hasiotis, & Robison, 2018).

Description.—Alternating offset ridge or furrow segments forming mostly linear trails. Another form is a series of alternating offset convex bulbs. On GC-C-9, trail width from 0.5–8.0 mm, averaging 1.5 mm; lengths from 6.4–260.2 mm, averaging 90.2 mm; trails can have >20 segments. On GC-C-14, trail widths 0.2 mm and 0.3 mm; lengths 14.4 mm and 11.5 mm. Some trails irregularly meander and have short projections. Other trails are mostly straight with short projections that alternate on each side of the trace. Preserved in concave epirelief and convex hyporelief. Refer to Appendix 8 for additional measurements.

Associated ichnotaxa.—Alaripeda lofgreni, *Av. vialovi*, *Ap. phoenix*, *C. anguineus*, *Co. conichnus*, *Gr. gryponyx*, *P. montanus*, *T. pedum*, and *T. vagans* Książkiewicz, 1977.

Discussion.—Treptichnus bifurcus is the most common ichnospecies of *Treptichnus* of the GRF samples. Convex or concave alternating bulbs represent the ends of probe chambers characteristic of the morphology of *Treptichnus* (Fig 8A, B, D). Among our samples, a single trail of alternating offset chamber bulbs grades into *T. vagans* and overall forms a semicircular pattern (Fig. 8A). Another burrow transitions into *T. pedum* as described in Muñiz Guinea and others (2014). This pattern indicates that these were likely dipteran pupation traces, made by larvae searching for a place to pupate. The GRF *Treptichnus* trace samples on GC-C-9 (epirelief and hyporelief) are indicative of subaerial exposure. On GC-C-14, *T. bifurcus* is indicative of subaerial exposure, whereas associated traces indicate water-level fluctuation to the SWAI (bird tracks, *C. anguineus*) and cm-scale water depths (*Co. conichnus*).

TREPTICHNUS PEDUM (Seilacher, 1955a)

Figure 7.1

Material.—GC-C-5 (n = 4), GC-C-9 (n = 1).

Diagnosis.—Straight to curved primary burrow system consisting of intervals regularly branching successive burrow segments (Fillion & Pickerill, 1990; Jensen, 1997).

Description.—Offset furrows or ridges forming curved or circular patterns. GC-C-5 specimens 0.6, 0.6, 0.8, and 0.7 mm wide segments; 4.8, 3.4, 5.1, and 4.0 mm diameter; convex hyporelief. GC-C-9 specimens 1.7 mm wide segments; 21.9 mm diameter; concave epirelief.

Associated ichnotaxa.—Cochlichnus anguineus, *P. montanus*, rhizoliths, *S. lincki*, *T. bifurcus*, and *T. vagans*.

Discussion.—The circular pattern of furrows in our samples is common in *T. pedum*. The offset furrows or ridges to only one side differentiates *T. pedum* from the strictly alternating

furrows or ridges of *T. bifurcus*. The *T. pedum* on GC-C-9 are not associated with any other traces besides other ichnospecies of *Treptichnus* and is, therefore, consistent with the interpretation of the environment being subaerially exposed. The environment preserved on GC-C-5 (hyporelief) underwent a fluctuation in water level, from shallow with the production of *S. lincki*, to the SWAI with the production of *C. anguineus*, to potentially subaerially exposed with the production of rhizoliths and *T. pedum*. The *F. texana* track apparently present on the hyporelief of GC-C-5 is an undertrack that originates from the epirelief side of the slab and is not associated with this horizon.

TREPTICHNUS VAGANS (Książkiewicz, 1977)

Figure 7.1

Material.—GC-C-9 (n = 2).

Diagnosis.—Discontinuous, irregularly meandering or looping trail of variably spaced, short to elongate, ovoid, irregular, or circular beads or depressions (Hammersburg, Hasiotis, & Robison, 2018).

Description.—Meandering trail of linearly aligned concave furrows, each with a terminal pit preserved in epirelief (Fig 8A). Width 1.4 and 1.5 mm, length 85.7 and 165.4 mm, respectively.

Associated ichnotaxa.—Treptichnus bifurcus, T. pedum.

Discussion.— Hammersburg, Hasiotis, and Robison, (2018) placed *Pteichoplasma vagans* Książkiewicz, 1977, into *Treptichnus* based on samples from the Spence Shale and observation of GC-C-9, where the morphology was used in support for the transfer of the ichnospecies to *Treptichnus*. Hammersburg, Hasiotis, and Robison (2018) focused their

reasoning based on a compound trace on our GC-C-9, where a *T. bifurcus* with the morphology of a chain of alternating concave beads transitions into a morphology otherwise consistent of former *Pt. vagans*. The alternating beaded pattern transitions to a linear single chain of beads, which then is lost and replaced with a series of concave furrows. In this case, *T. vagans* begins the moment the alternating pattern of beads is lost. The variance in morphology of our *T. vagans*, from a single chain of concave beads to a series of concave furrows, is a result of preservational variation of the three-dimensional burrow structure. This trace was likely made by a similar dipteran pupa as with the other forms of *Treptichnus* on GC-C-9 (epirelief), the environment being subaerially exposed along the lake margin.

VERTEBRATES

Ichnogenus ALARIPEDA Sarjeant & Reynolds, 2001

Type ichnospecies.—Alaripeda lofgreni Sarjeant & Reynolds, 2001.

Diagnosis.—Tridactyl or tetradactyl tracks; digit III directed forward and may curve sharply; digit I short, < 0.5x length digit III, often oriented reverse to digit III axis but can deviate up to 20°; digits II and IV directed laterally, may also curve; digits united or separate proximally; length digit III comparable to (or < 25% longer than) digits II and IV; lacks webbing; no indication of a metatarsal pad (Sarjeant & Reynolds, 2001).

Discussion.—Alaripeda was established for tracks with laterally oriented digits II and IV, meaning very high AoD II–IV, even exceeding 180° (Sarjeant & Reynolds, 2001). The curvature of digits II–IV is a defining character of this ichnogenus compared to such similar ichnotaxa as *Aquatilavipes* and *Gruipeda gryponyx*.

Alaripeda is attributed to small shorebirds along proximal shorelines (Sarjeant & Reynolds, 2001). Previously known from the Miocene (Sarjeant & Reynolds, 2001), the GRF specimens extend the range of *Alaripeda* to the Eocene.

ALARIPEDA LOFGRENI Sarjeant & Reynolds, 2001

Figure 7.3, 7.6

Material.—GC-C-6 (n = 3), GC-C-14 (n = 1), GC-C-15 (n = 2).

Diagnosis.—Tetradactyl tracks with digits II–IV curving forward; digit III directed forward and inward toward track axis; digit I very short when present, oriented reverse of digit III axis; digits II and IV oriented laterally; digits slender, lacking distinct claws; digital pads not distinguishable; lacks webbing; digit III shorter, curves more strongly than lateral digits; digit I < 0.5x length and width of digit III; digits united proximally, slightly forward of backward curve of lateral digits; no metatarsal pad; trackway narrow; stride moderate (Sarjeant & Reynolds, 2001).

Description.—Tracks of three or four digits, with digits II–IV united proximally; digits II–IV somewhat to strongly curved, especially in digit III; no webbing. Small digit I preserved on one track on GC-C-6. Lengths from 12.2–21.6 mm, averaging 16.2 mm; widths from 16.6–24.5 mm, averaging 21.9 mm; AoD II–IV from 126.2–200.2°, averaging 144.8°. Preserved in concave epirelief and convex hyporelief. Refer to Appendix 9 for additional measurements.

Associated ichnotaxa.—Aviadactyla vialovi, *Ap. phoenix*, *C. anguineus*, *Co. conichnus*, *Gr. gryponyx*, *P. montanus*, and *T. bifurcus.*

Discussion.—Alaripeda lofgreni is the only ichnospecies of *Alaripeda* (Sarjeant & Reynolds, 2001), with no others yet established for some of the broader morphologies suggested by the ichnogenus diagnosis.

Some of the GRF tracks, especially on GC-C-15, are very cryptic in their preservation, though the characteristic curvature in at least digit III is present in all GRF tracks assigned to this ichnotaxon. The curving of digit III and smaller size are the primary characters that distinguish these tracks from the very similar c.f. *Aquatilavipes* isp. tracks present on GC-C-16 (hyporelief).

On GC-C-6 (hyporelief) and GC-C-15 (epirelief), associations with other bird tracks and *C. anguineus* suggest the environment was at or near the SWAI. On GC-C-14 (hyporelief), associations with other bird tracks, *C. anguineus*, *Co. conichnus*, and *T. bifurcus* indicates that water level varied above, at, and below the SWAI.

Ichnogenus AQUATILAVIPES (Currie, 1981)

Type ichnospecies.—Aquatilavipes swiboldae (Currie, 1981).

Diagnosis.—Small to large footprints with three proximally united digits with a metatarsal pad, lacking webbing and hallux. Maximum width of digits <15% of length. Digit III >25% longer than other digits. Digit IV longer than digit II. All digits have claw marks curved inwards to digit axis. When digital pads visible, three to four on digit III and two on other digits (McCrea & Sarjeant, 2001).

Discussion.—McCrea and Sarjeant (2001) emended the diagnosis of *Aquatilavipes* to provide a clear differentiation from *Fuscinapeda* Sarjeant and Langston, 1994, and note that the preservation of the digital pads can vary based on media. *Aquatilavipes* has thinner digits than *Fuscinapeda* that are always proximally united and have a less sticklike character than *Aviadactyla* Kordos, 1985 (McCrea & Sarjeant, 2001).

Aquatilavipes is interpreted as a repichnial trace of large wading birds (McCrea and Sarjeant, 2001). Described thus far only from the Cretaceous (e.g., Currie, 1981; McCrea &

Sarjeant, 2001; Azuma & others, 2002; Huh & others, 2012), the GRF samples potentially extends the range of *Aquatilavipes* to the Eocene. *Aquatilavipes* is known from coastal plain, deltaic, and lacustrine shoreline environments (e.g., Currie, 1981; McCrea & Sarjeant, 2001; Azuma & others, 2002; Huh & others, 2012).

c.f. AQUATILAVIPES isp.

Figure 7.4

Material.—GC-C-16 (n = 2).

Description.—Tracks large, width 86.9 mm and 91.2 mm, length 60.2 mm and 70.3 mm, AOD II–IV 137.7° and 134.4°, respectively. Three digits preserved on both tracks in convex hyporelief. One track has cryptic indication that the digits are proximally united, whereas the other has no preserved indication of proximally united digits.

Associated ichnotaxa.—*Aviadactyla vialovi*, *C. anguineus*, *Gl. gierlowskii*, *Gr. fuenzalidae*, *M. semipalmatus*.

Discussion.—No clear preservation of proximally united digits on the tracks precludes formally classifying these tracks as *Aquatilavipes*. The tracks are similar in size and morphology to the associated *Gr. fuenzalidae* track, though lack a preserved hallux impression and thus precludes assignment to *Gruipeda*.

Association with *C. anguineus* and the other bird tracks is indicative of the SWAI, whereas *Gl. gierlowskii* is indicative of a shallow water depth. This indicates that GC-C-16 (hyporelief) underwent a fluctuation in water depth from relatively shallow to the SWAI.

Ichnogenus AVIADACTYLA (Kordos, 1985)

Type ichnospecies.—Aviadactyla media Kordos, 1985.

Diagnosis.—Three digits; digit width slender to moderate, tapering distally and sometimes with claw or digital pad impressions; digits convergent; II and III may be proximally united; digit III < 25% longer than digits II and IV; AoD II–IV > 95°; no metatarsal pad or webbing between digits (Sarjeant & Reynolds, 2001).

Discussion.—Aviadactyla is a wide, incumbent anisodactyl bird track similar to *Avipeda* and *Koreanaornis* Kim, 1969. Mustoe (2002) assigned Eocene tracks from the Chuckanut Formation in northwestern Washington with AoD II–IV > 95° to the morphofamily Avipedidae. He compared those tracks to other North American Paleogene BTFs and found that they were most similar to GRF tracks in Moussa (1968, pl. 178, fig. 5). While he assigned similar tracks with AoD II–IV ≤ 95° to *Avipeda*, the tracks with AoD > 95° were not assigned to an ichnotaxon, pending better descriptions of tridactyl bird tracks from other Paleogene and Neogene (*sic* Tertiary) localities. Such tracks with AoD > 95° were defined by Sarjeant and Reynolds (2001) as belonging to *Aviadactyla*. The tracks from Mustoe (2002) and Moussa (1968), therefore, belong to *Aviadactyla* under the emended diagnosis by Sarjeant and Reynolds (2001).

Díaz-Martinez and others (2015) proposed synonymizing *Aviadactyla* under *Koreanaornis*, citing that differences in AoDs and hallux preservation are dependent upon tracemaker pace and media consistency. We do not follow this synonymy, however, as *Aviadactyla* can have tracks with proximally united digits. As originally described and displayed, the *Koreanaornis* holotype does not have proximally united digits (Kim, 1969; Sarjeant & Reynolds, 2001). There is an argument for synonymizing *Aviadactyla* under an emended *Avipeda* for the same reasons used by Díaz-Martinez and others (2015) for synonymizing

Aviadactyla under *Koreanaornis*, however, this would require extensive study of pace behavior and media consistency on track morphology using modern birds with incumbent anisodactyl feet, which is beyond the scope of this study.

Carpathipeda vialovi Kordos *in* Kordos & Prakfalvi, 1990, was emended to be under *Aviadactyla* by Sarjeant and Reynolds (2001) based on: 1) that the diagnoses of *Carpathipeda* and *Aviadactyla* were extremely similar; and 2) *Carpathipeda* was diagnosed through an ichnospecies despite having a second, simultaneously described ichnospecies, thereby violating Recommendation 13C of the *International Code of Zoological Nomenclature* (Ride & others, 1985). Unnamed tracks illustrated in figure 11 in Curry (1957) were designated as *Aviadactyla* by Sarjeant and Reynolds (2001) and specifically assigned to *Av*. *vialovi*.

Aviadactyla is interpreted as a repichnia trace of small, incumbent anisodactyl shoreline birds, such as sandpipers (family Scolopacidae) and Dunlin (*Calidris alpine*) (Jaeger, 1948; Weidmann & Reichel, 1979; Sarjeant & Reynolds, 2001). Ranging from the Eocene to the Miocene, *Aviadactyla* is known from North America and Europe in ancient shoreline environments (e.g., Curry, 1957; Kordos & Prkvalfi, 1990; Sarjeant & Reynolds, 2001). The term shoreline can be applied to a variety of water-margin settings along lakes, rivers, beaches, bays, and lagoons.

***c.f.* AVIADACTYLA isp.**

Figure 7.5

Material.—GC-C-3 (n = 6)

Description.—Tridactyl tracks with digits not proximally united. Lengths 24.4 mm; widths from 34.8–35.2 mm, averaging 35 mm; AoD II–IV from 111.8–123.6°, averaging 119.5°.

Two partial trackways of two tracks each. L_p 11.5 cm, 9.7 cm; W_{tw} 3.8 cm, 6.3 cm; W_p 0.9 cm, 2.5 cm; ϕ 2.1° and 27.9°, 4.3° and 9.4°. Preserved in concave epirelief, with some digits impressing through to hyporelief of the slab. Refer to Appendix 10 and 17 for additional measurements.

Associated ichnotaxa.—Cochlichnus anguineus.

Discussion.—These are very likely tracks of an ichnospecies of *Aviadactyla*, as AoD II–IV is ≥ 95°, though the lack of further morphological detail prevents specificity. As some tracks impress through the slab, the hyporelief convex impressions are not considered to be part of the trace-fossil assemblage on that horizon. Associations on GC-C-3 (epirelief) with *Cochlichnus anguineus* suggest that the environment was at or near the SWAI.

AVIADACTYLA VIALOVI (Kordos *in* Kordos & Prakfalvi, 1990)

Figure 7.6

Material.—GC-C-14 (n = 7), GC-C-15 (n = 1), GC-C-16 (n = 6).

Diagnosis.—Three slender, flexible digits similar in length, though III longest; digits converge proximally, II sometimes contacting III, and IV always separate; claws slender and curved from digit axis; no space between digital pads; no webbing or metatarsal pad; moderate trackway width and stride length; AoD II–IV 80° to >155°; AoD II–III < III–IV (Sarjeant & Reynolds, 2001).

Description.—Slender digits with digit III longest. Some tracks may have a circular hallux claw impression. Lengths from 14.6–37.3 mm, averaging 21.9 mm; widths from 17.4–34.5 mm, averaging 25.3 mm, AoD II–IV from 97–137.8°, averaging 109.9°. Tracks are

preserved in concave epirelief and convex hyporelief. Refer to Appendix 11 for additional measurements.

Associated ichnotaxa.—Alaripeda lofgreni, c.f. *Aquatilavipes* isp., *Ap. phoenix, C. anguineus, Co. conichnus, Gl. gierlowskii, Gr. fuenzalidae, Gr. gryponyx, M. semipalmatus, P. montanus,* and *T. bifurcus.*

Discussion.—The range in AoD II–IV is so large that these tracks were likely left by several different kinds of birds. Preservation of the tracks required a low energy environment due to their small size. Associated invertebrate tracemakers are indicative of potential predator-prey relationships.

One track on GC-C-14 (hyporelief) appears to have a long hallux. The impression that appears to be a hallux on this track is *P. montanus.* This slab horizon also has many variably preserved digit impressions that are overlapping and do not form complete tracks. The digits are of indeterminate ichnotaxon and sometimes obscure complete tracks. These digits, as well as a few complete tracks of *Av. vialovi* have scutellate-scale patterns preserved.

On GC-C-14 (hyporelief), the trace-fossil associations suggest water level fluctuated above (*T. bifurcus*), at (*C. anguineus,* bird tracks), and below (*Co. conichnus*) the SWAI. On GC-C-15 (epirelief), the associations with bird tracks and *C. anguineus* suggest water level was at the SWAI. On GC-C-16 (hyporelief), the trace-fossil associations suggest water level fluctuated below (*Gl. gierlowskii*) and at (*C. anguineus,* bird tracks) the SWAI.

Ichnogenus AVIPEDA (Vyalov, 1965)

Type ichnospecies.—Avipeda phoenix Vyalov, 1965.

Diagnosis.—Tridactyl tracks with central digit III < 25% longer than digits II and IV, AoD II–IV ≤ 95°. Digits convergent or united proximally. Webbing not present or limited to proximal areas between digits (Sarjeant & Langston, 1994).

Discussion.—Avipeda is a narrow, incumbent anisodactyl or semipalmated bird track similar to *Aviadactyla*, though with a smaller AoD II–IV. This ichnogenus formerly encompassed all BTFs (Vyalov, 1965) until emended to be more specific and split up into three separate ichnogenera of *Ardeipeda*, *Avipeda*, and *Fuscinapeda* by Sarjeant and Langston (1994) and Sarjeant and Reynolds (2001). *Ardeipeda* was defined for much larger tracks with a prominent and long hallux, whereas *Fuscinapeda* lacks a hallux and has wider digits. *Avipeda* is still broadly defined and is used to place myriad different types of tracks that could be better suited in newly established or other existing ichnotaxa (Lockley & Harris, 2010).

Avipeda is interpreted as a repichnia trace of small wading birds, comparable to the little stint sandpiper (*Calidris minuta*; Weidmann & Reichel, 1979; Sarjeant & Reynolds, 2001). Ranging from Cretaceous to Miocene (Sarjeant & Langston, 1994, Lucas & Schultz, 2007, Morgan & Williamson, 2007), *Avipeda* is known from water-margin environments (Sarjeant & Langston, 1994, Morgan & Williamson, 2007).

AVIPEDA PHOENIX (Vyalov, 1966)

Figure 7.6, Figure 8.1

Material.—GC-C-14 (n = 3), GC-C-15 (n = 3), GC-C-16 (n = 1).

Emended Diagnosis.—Small, incumbent anisodactyl tracks; digits short, may or may not unite proximally; AoD II–IV up to 95°; rare claw impression or scratch from digit I.

Description.—Tridactyl tracks with thin digits. Some tracks have claw markings anterior to the forward three digits. Claw impressions at tips of digits II–IV sometimes present, usually curving towards track axis. Lengths from 19.1–37.6 mm, averaging 24.7 mm; widths from 17.4–33 mm, averaging 24.7 mm; AoD II–IV from 72.5–94.8°, averaging 86.9°. Preserved in concave epirelief and convex hyporelief. Refer to Appendix 12 for additional measurements.

Associated ichnotaxa.—Alaripeda lofgreni, c.f. *Aquatilavipes* isp., *Av. vialovi*, *C. anguineus*, *Gl. gierlowskii*, *Gr. gryponyx*, *M. semipalmatus*, *P. montanus*, and *T. bifurcus*.

Discussion.—The holotype slab in Vyalov (1965) of *Ap. phoenix* displays proximally united digits. Vyalov (1966), however, which established the diagnosis for *Ap. phoenix*, has a photograph with digits not united proximally (see pl. 53 in Vyalov, 1966). We emend the diagnosis of *Ap. phoenix* to reflect this variation in morphology, as well as to add that an indication of a hallux claw mark may be present, primarily due to preservational variation and environmental factors, and to eliminate the irrelevant precise length limitation of 1.6 cm. The hallux claw mark is not a viable digit for measuring interdigital angles from it and the whole of the track can still be considered as tridactyl (specifically incumbent anisodactyl) for the purposes of the ichnogenera diagnosis.

Our samples more closely match that photograph of material of *Ap. phoenix* in Vyalov (1966). *Avipeda phoenix* is, therefore, a broad ichnospecies of *Avipeda*, covering tracks with digits separate and proximally united, with AoD II–IV only limited by the ichnogenera diagnosis.

One track on GC-C-14 appears to have a long hallux. This is not a hallux, but a digit of an oppositely oriented track of indeterminate ichnotaxon preserved as just two digits. A side digit on this track also has a slip mark with lines from scutellate scales preserved.

On GC-C-14 (epirelief) and GC-C-15 (hyporelief), associations with other bird tracks and *C. anguineus* suggests water level was at the SWAI. On GC-C-14 (hyporelief), trace-fossil associations suggest water level fluctuated below (*Co. conichnus*), at (*C. anguineus*, other bird tracks), and above (*T. bifurcus*) the SWAI. On GC-C-15 (epirelief), associations with, *A. cursorius*, *C. anguineus*, *Gr. gryponyx*, and *Pr. dichotoma* suggest the water level was at the SWAI. On GC-C-16 (hyporelief), associations suggest water level fluctuated below (*Gl. gierlowskii*) and at (*C. anguineus*, other bird tracks) the SWAI.

Ichnogenus FUSCINAPEDA (Sarjeant & Langston, 1994)

Type ichnospecies.—Fuscinapeda sirin (Vyalov, 1966) Sarjeant & Langston, 1994.

Emended Diagnosis.—Small to large tridactyl tracks. Digits proximally united with no webbing or hallux, slim to moderately thick with maximum width >15% their length. Digit III >25% longer than other digits, and digit IV frequently somewhat larger than digit II. AoD II–IV >95°, often exceeding 120°. When present, claw impressions often curved towards digit axis. When digital pads present, three or four on digit III and two on II and IV.

Discussion.—The diagnosis is emended so that claw impressions are not a requirement of the ichnogenus. This corrects an incongruity with *F. texana* Sarjeant and Langston, 1994, not having claw impressions yet belonging to an ichnogenus that had been emended to require them (Sarjeant & Langston, 1994; McCrea & Sarjeant, 2001). While claw impressions are not mentioned in their original diagnosis of *F. texana*, Sarjeant and Langston (1994) stated that the tracks could not be made by Falconiformes due to the lack of clear claw impressions in the samples. Birds in this order have claws that would have created impressions in the medium. We

preserve the remaining previous emendations by McCrea and Sarjeant (2001), who clarified the increased digit width in *Fuscinapeda* compared to *Aquatilavipes*.

Fuscinapeda is attributed to large shoreline birds, including potential flamingo relatives (Sarjeant & Langston, 1994). Ranging from Eocene to Miocene (McCrea & Sargeant, 2001; Krapovickas & others, 2009), *Fuscinapeda* is known from water-margin environments (McCrea & Sarjeant, 2001).

FUSCINAPEDA TEXANA Sarjeant & Langston, 1994

Figure 8.2

Material.—GC-C-5 (n = 1).

Diagnosis.—Moderate to large footprints with pronounced angular heel; three digits (II to IV) of moderate thickness; II has convex sides, expands slightly from base to just below center, then tapers to its tip; III ~1.5x the length of II, tapering from base to tip and slightly flexing outward at center; IV short, broad based and similar to II; webbing proximally confined; AoD II–IV ~105°, II–III < III–IV; trackway narrow, stride long (Sarjeant & Langston, 1994).

Description.—Tridactyl track with angular heel; no preserved indications of webbing; width 10.82 cm; length 8.67 cm; length digit II 4.5 cm, digit III 6.5 cm, digit IV 4.3 cm; AOD II–IV 111.9°, II–III 47.53°, III–IV 64.41°; preserved as concave epirelief.

Associated ichnotaxa.—None.

Discussion.—The track was pressed down through the slab leaving convex markings of digits on the hyporelief side of the slab. Large size of the track is indicative of the size of the wading bird. Such a bird would need access to a larger food supply, likely vermiforms, insects, and other arthropods that left *C. anguineus*, *P. montanus*, *S. lincki*, and *T. pedum* on the

underside of the slab. The sole presence of *F. texana* on GC-C-5 (epirelief) indicates shallow water ranging in depth a few centimeters to the depth the bird would swim instead of wade.

Ichnogenus GRUIPEDA (Panin & Avram, 1962)

Type ichnospecies.—Gruipeda maxima Panin & Avram, 1962.

Emended Diagnosis.—Tri- or tetradacytl tracks; when present, digit I axis differs from digit III; AoD II–III and III–IV < 70°, I–II < I–IV; phalangeal pad impressions, when present, are 2 for digit I, 2 for digit II, 3 for digit III, and 4 for digit IV; webbing absent.

Discussion.—Mansilla and others (2012) incorrectly stated and followed their claim that Sarjeant and Langston (1994) attributed *Gruipeda* tracks to tridactyl and tetradactyl morphology when, in fact, there is no mention of tridactyl morphology. We emend the most recent diagnosis by de Valais and Melchor (2008) of *Gruipeda* to reflect that the presence or absence of a hallux impression is often a function of differential preservation and environmental factors (Lockley & Harris, 2010).

Sarjeant and Langston (1994) originally emended *Gruipeda* to provide a morphological diagnosis as opposed to the original diagnosis by Panin and Avram (1962), which was based on a potential tracemaker. This was subsequently modified by de Valais and Melchor (2008) to include the potential for phalangeal pad impressions and their number when present. De Valais and Melchor (2008), while emeding *Gruipeda*, placed *Antarctichnus* Covacevich & Lamperein, 1970 (consisting of one ichnospecies, *An. fuenzalidae* Covacevich & Lamperein, 1970), and *Trisauropodiscus aviforma* Ellenberger, 1972, as junior synonyms of *Gruipeda* due to morphological similarity, which we follow, and established *Gr. dominguensis* de Valais and Melchor, 2008. The study area of de Valais and Melchor (2008) has since been determined to be

Eocene in age as part of the Laguna Brava Formation rather than the Santo Domingo Formation (Upper Triassic), as per their retraction of a previous paper discussing bird tracks from the region (Melchor, de Valais, & Genise, 2002, 2013).

Gruipeda dominguensis was established for tracks with a wider AoD II–IV and proximally united digits, with variably preserved digit I (de Valais & Melchor, 2008). A similar trace, *Avipeda gryponyx*, has proximally united digits, similarly wide AoD II–IV, and relatively thin digits (Sarjeant & Reynolds, 2001). *Avipeda gryponyx* is unique for *Avipeda* in that it has a range of AoD II–IV that exceeds 95°, upwards of 120°, while the diagnosis of the ichnogenus requires AoD II–IV ≤ 95°. As thickness of digits may be resultant from preservational variation, the diagnosis, description, and photographs of the holotype of *Ap. gryponyx* are significantly similar to that of *Gr. dominguensis*. We, therefore, move *Ap. gryponyx* to *Gruipeda* and synonymize *Gr. dominguensis* under the new *Gr. gryponyx*, as *Ap. gryponyx* was established prior to *Gr. dominguensis*.

Gruipeda is repichnial trace attributed to shorebirds (Charadriiformes), rails (Gruiformes Rallidae), and storks (Ciconiiformes; Sargeant & Langston, 1994). Known only from the Eocene, *Gruipeda* is found in fluviolacustrine and lacustrine environments (e.g., Sarjeant & Langston, 1994; de Valais & Melchor, 2008; Mansilla & others, 2012).

GRUIPEDA FUENZALIDAE Covacevich & Lamperein, 1970

Figure 8.3–8.4

Material.—GC-C-16 (n = 1).

Diagnosis.—Tetradactyl tracks; II–IV narrow, straight subequal, consistently diverging and forward facing; I short, directed posteriorly offcenter towards trackway midline; no webbing (Covacevich & Lamperein, 1970).

Description.—Track of four digits, with digit I posteriorly directed and offset from axis of digit III; no impressions between digits; AoD II–IV 138.6°, II–III 69.9°, III–IV 68.7, I–II 81.32°, I–IV 140.1°; track width 86.1 mm, track length 60.9 mm. Track oversteps *Midorikawapeda semipalmatus*. Preserved in convex hyporelief.

Associated ichnotaxa.—Aviadactyla vialovi, c.f. *Aquatilavipes* isp.*, C. anguineus, Gl. gierlowskii, M. semipalmatus.*

Discussion.—Doyle, Wood, and George (2000) applied *Gr. fuenzalidae* (formerly *Antarctichnus fuenzalidae*) to specimens of GRF tracks from Soldier Summit, Utah, by Moussa (1968), though the exact specimens were not articulated. We place our specimen into *Gr. fuenzalidae* due to its similarity to the tracks from Moussa (1968) that were identified by Doyle, Wood, and George (2000).

The track is similar in size and digit morphology to the associated c.f. *Aquatilavipes* isp. tracks, though it has a preserved hallux impression and proximally united digits consistent with *Gr. fuenzalidae*. Associations with other shorebird tracks, as well as invertebrate traces *C. anguineus* and *Gl. gierlowskii* suggest GC-C-16 underwent water-level fluctuations below (*Gl. gierlowskii*) and at the SWAI (*C. anguineus* and other bird tracks).

GRUIPEDA GRYPONYX (Sarjeant & Reynolds, 2001)

Figure 8.5

Avipeda gryponyx—Sarjeant & Reynolds, 2001, p. 24, pl. 2, 3, 4, fig. 4, 5.

Bird-like footprint type A—Melchor & others, 2006, p 270, fig. 9C.

Gruipeda dominguensis—De Valais & Melchor, 2008, p. 153, fig. 4, 5.

Material.—GC-C-6 (n = 13), GC-C-7 (n = 2), GC-C-14 (n = 3), GC-C-15 (n = 8).

Emended diagnosis.—Tri- or tetradactyl tracks with length:width ratios generally 0.7–0.9; digits II–IV proximally united; trackways may display inward rotation to midline, pace angulation range 150–182°, and stride length 2.5–5x track length; tracks slightly asymmetric, typically AoD II–III > III-IV, AoD II–IV 90–135°; relative digit length is I < II < IV < III; hallux impression, when present, in posterior to posteromedial position; occasional rhomboid to rounded sole.

Description.—Mostly tetradactyl tracks with proximally united digits II–IV. Digit I, when present, directed backwards at an angle to track axis, short. Lengths from 14.0–37.6 mm, averaging 21 mm; widths from 17.4–41.4 mm, averaging 26.7 mm; AoD II–IV from 93.4–126.7°, averaging 106.9°. One trackway of four tracks on GC-C-6: L_s average 10.0 cm; L_p average 5.7 cm; W_{tw} 3.6 cm; W_p average 1.6 cm; ϕ average 12.1°. Preserved in concave epirelief and convex hyporelief. Refer to Appendix 13 and 17 for additional measurements.

Associated ichnotaxa.—Acanthichnus cursorius, *Al. lofgreni*, *Av. vialovi*, *Ap. phoenix*, *C. anguineus*, *Co. conichnus*, *P. montanus*, *Pr. dichotoma*, and *T. bifurcus.*

Discussion.—We emend the diagnosis to reflect the moving of *Ap. gryponyx* into *Gruipeda* and synonymization of *Gr. dominguensis* with *Gr. gryponyx*. The key characteristics of *Gr. gryponyx* are the wider AoD II–IV with proximally united digits and small, posteriorly directed digit I, which is usually present. AoD II–IV generally falls between *Avipeda* on the low end and *Alaripeda* and *Aquatilavipes* on the high end, filling a gap for traces with proximally united digits and a wide AoD II–IV not quite as high as the more laterally-oriented digits in

Alaripeda and *Aquatilavipes*. *Gruipeda gryponyx* is the most abundant of the GRF vertebrate traces at 27 samples, with *M. semipalmatus* second at 26.

GC-C-6 (epirelief) and GC-C-7 (hyporelief) trace fossil associations with only *C. anguineus* suggest that water level was at the SWAI. GC-C-6 (hyporelief), GC-C-14 (epirelief), and GC-C-15 (epirelief) trace-fossil associations with other bird traces and *C. anguineus* suggests that water level was at the SWAI. GC-C-14 (hyporelief) trace-fossil associations suggest water-level fluctuations above (*T. bifurcus*), at (*C. anguineus*, other bird traces), and below (*Co. conichnus*) the SWAI. GC-C-15 (hyporelief) trace-fossil associations with other repichnial traces (i.e., *A. cursorius*, *Ap. phoenix*, *C. anguineus*, and *Pr. dichotoma*) suggest water level was at the SWAI.

Ichnogenus MIDORIKAWAPEDA new genus

Type ichnospecies.—Midorikawapeda semipalmatus

Etymology.—From the Japanese *midori*, Green, and *kawa*, river, and the Latin *ped*, foot.

Diagnosis.—Avian tracks with three to four digits. All digits slim, ~1.0–5.0 mm wide; digits II–IV forward and proximally united; digit I, if present, typically smaller and directed backward, offset or parallel to the track axis; digit II straight or curved towards digit III axis; AoD II–IV ranges from approximately 100° to 135°; webbing incomplete, preserved between digits III–IV.

Discussion.—This new ichnogenus and ichnospecies is necessary to accommodate semipalmated tracks that do not fit well within existing ichnotaxa. The digits are too slim for *Gruipeda*, which also requires no webbing. *Aviadactyla* does not have all three forward digits proximally united. *Alaripeda* is a significantly wider track than it is long. *Goseongornipes*

Lockley & others, 2006, is the closest morphologically but has much wider AoD II–IV (140°–150°) and a much shorter, spurlike hallux angled such that AoD I–II is ~75°. *Koreanornis* is also close morphologically but contains a wide range of morphologies. For example, when the hallux is preserved, it is not necessarily elongate, digits II and IV can curve away from the trackway axis, digits II–IV need not be proximally united, and, importantly, there is no partial webbing requirement.

Midorikawapeda is a repichnial trace of a semipalmated, possible shoreline bird. *Midorikawapeda* can potentially be found along any type of ancient shoreline, though here is described from a lacustrine shoreline in the GRF.

MIDORIKAWAPEDA SEMIPALMATUS new species

Figure 8.3–4, 8.6, Figure 10.1

Material.—Fig. 11 D–F. GC-C-2 (n = 5), GC-C-16 (n = 8), GC-C-20 (n = 13).

Etymology.—From Latin for semipalmate. Full name means the Green River semipalmate track.

Diagnosis.—As ichnogenus.

Description.—Tracks with three to four digits preserved, with digit I posteriorly directed and offset from yet parallel to track axis.. Track widths from 25–38.2 mm, averaging 32.4 mm; track lengths from 18.0–46.7 mm, averaging 30.6 mm; AoD II–IV from 105.2–176°, averaging 126.5°. Preserved in concave epirelief or convex hyporelief. All tracks preserve a crescent-shaped impression between digits III and IV. The impression connects to the digits at up to a third of the total digital length and curves distally between them. Digit II curves towards digit III axis whereas digit IV is straight by comparison. On GC-C-2 there are three complete tracks and

two cut off by the slab margins, all in convex hyporelief (Fig 11 D). One complete track has hallux impression. One complete trackway of three tracks: L_s 14.8 cm; L_p average 7.4 cm; W_{tw} 3.3 cm; W_p 1.6 cm; ϕ average 14.3°. One incomplete trackway of two tracks, one of which is cut off by the slab margin: W_p 1.5 cm; ϕ 18.4°. On GC-C-16, two complete trackways, one of four tracks, the other of three: L_s average 14.0 cm, 17.4 cm; L_p average 6.9 cm, 8.3 cm; W_{tw} 6.3 cm, 4.3 cm; W_p average 2.6 cm, 2.6 cm; ϕ average 12.6°, 19.2°. On GC-C-20, tracks are on a dark, bumpy to wavy textured portion of the slab surface, all in concave epirelief (Fig 11.3). Refer to Appendix 14 and 17 for additional measurements.

Types.—Holotype: GC-C-2; Paratypes GC-C-16, GC-C-20.

Associated ichnotaxa.—Aviadactyla vialovi, c.f. *Aquatilavipes* isp., *C. anguineus, Gl. gierlowskii*, *Gr. fuenzalidae*, and *Tsalavoutichnus leptomonopati*.

Discussion.—The five tracks of *M. semipalmatus* on GC-C-2 (hyporelief) represent parts of two trackways. Two of the complete tracks are of the right foot, whereas the other complete track and the two incomplete tracks are those of a left foot. The crescent-shaped impression on every track are webbing impressions, indicating that the tracks are semipalmated between digits III and IV. The association with only *Ts. leptomonopati* on GC-C-2 (hyporelief) suggests the environment was below the SWAI in cm-scale water depth.

On GC-C-16 (hyporelief), the trace-fossil associations suggest water level fluctuated between the SWAI (bird tracks, C. anguineus) and below the SWAI (*Gl. gierlowskii*).

The dark texturing on GC-C-20 can best be described as elephant skin texturing (Fig. 11.1). This and the darker coloration are indicative of microbial mats. Deformed tracks of *M. semipalmatus* on this part of the slab indicate that the texture developed after the tracks were produced. The track deformation not only curves individual digits but also skews interdigital

angles and alters the axis of digit I to not align with digit III. The tracks do, however, clearly indicate webbing between digits III–IV extending up to about a third of the lengths of the digits, as on GC-C-2. Long track hallux impressions of the *M. semipalmatus* on GC-C-20 are characteristic of *Ardeipeda*, however, track sizes are uncharacteristically small, by a factor of ~10. These longer hallux impressions are more akin to drag marks produced by the claw of an incumbent anisodactyl digit I during slippage at the time the tracks were produced. The surface of GC-C-20, therefore, had a wet, slippery surface from extracellular polymeric substance produced by a microbial mat on which the tracemakers walked. As this surface dried, the tracks were further deformed through subaerial shrinking of the mat.

Ichnogenus PRESBYORNIFORMIPES (Yang & others, 1995)

Type ichnospecies.—Presbyorniformipes feduccii Yang & others, 1995.

Emended diagnosis.—Tetradactyl tracks with palmate webbing impressions between digits II–IV; AoD digits II–IV averages ~95°; digits II–IV convergent proximally; digits II and IV slightly inward curved with posterolaterally directed digit I.

Discussion.—While Yang and others (1995) first named and described this ichnogenus, they did not provide a formal diagnosis, but rather gave descriptions of the holotype and available paratypes. No diagnosis has yet been provided for *Presbyorniformipes*, and thus, one is provided here based on descriptions from Yang and others (1995) as well as samples studied in this report and following the general diagnosis conventions from Sarjeant and Reynolds (2001).

Yang and others (1995) describes *Pe. feduccii* as the following: tetradactyl tracks with palmate webbing impressions between digits II–IV and with faint claw impressions on all digits; digits II and IV slightly curved inwards, with posterolaterally directed hallux impression

separated from the other digit impressions without indications of webbing; average AoD between digits II and IV of 100.7°, II and III of 50.8°, and III and IV of 49.3°. We, however, were not able to obtain the same measurements from GC-C-21, which is a cast of holotype used by Yang and others (1995). The major issue between the AoD measurements in Yang and others (1995) and ours presented in the diagnosis is that they did not report the methodology used for calculating AoDs, which is 9° higher than our calculated average of 91.1° for that slab and 5° higher than the average across all our *Presbyorniformipes* samples of 95.7°. We, therefore, propose that ~95° is the average measure for the AoD digits II–IV of *Presbyorniformipes*.

Presbyorniformipes tracks are closely associated with sinuous dabbling features, though they are not part of the formal diagnosis. The dabbling traces are their own feature of a searching behavior and have yet to be formally described as an ichnotaxon. Dabble traces are not always present with *Presbyorniformipes* tracks.

Presbyorniformipes is a repichnial trace of a palmated shorebird described as being similar to *Presbyornis* (Erickson, 1967; Yang & others, 1995). Described only from the Eocene, *Presbyorniformipes* is known exclusively from lacustrine shoreline deposits of the GRF (Erickson, 1967; Yang & others, 1995).

PRESBYORNIFORMIPES FEDUCCII Yang & others, 1995

Figure 9.1–9.4, Figure 10.1–10.2

Material.—GC-C-4 (n = 5), GC-C-8 (n = 1), GC-C-10 (n = 4), GC-C-17 (n = 4), GC-C-18 (n = 1), GC-C-19 (n = 2), GC-C-21 (n = 6). GC-C-21 is a cast of holotype slab BYU B20.

Diagnosis.—As type.

Description.—These webbed tracks are associated with dabbling feeding traces on the holotype and on GC-C-10 and GC-C-17 (Fig. 9.1–9.2). Lengths from 44–63.4 mm, averaging 59.2 mm; widths from 63.7–77.4 mm, averaging 69.4 mm; AoD II–IV ranges from 78.4–117.7°, averaging 95.7°. On GC-C-4, one trackway of two tracks, one incomplete: L_p 16 cm; W_{tw} 19 cm; W_p 1.5 cm; ϕ 4.8° and 6.9°. On GC-C-10, one trackway of three tracks, one incomplete: L_p 9.9 cm; W_{tw} 10.1 cm; W_p average 3.4 cm; ϕ 4.2° and 8.8°. On GC-C-17, one trackway of two tracks, one incomplete: W_{tw} 9.9 cm, W_p 1.5 cm; ϕ 5.1°. On GC-C-21, one trackway of seven tracks, two incomplete: W_{tw} 9.9 cm, W_p 1.5 cm; ϕ average 6.1°. Preserved in concave epirelief and convex hyporelief. Refer to Appendix 15 and 17 for additional measurements.

Associated ichnotaxa.—Tsalavoutichnus ericksonii.

Discussion.—GC-C-21 is a cast of the original slab described by Erickson (1967), which was established as the holotype when the ichnogenus and ichnospecies were erected (Yang & others, 1995). Preservation of the tracks is variable across the samples, with webbing impressions varying between slabs, indicating differing media wetness at the time the tracks were produced. Individual tracks exhibit indications of webbing, slip marks, and scale impressions on the bottom of the toes (Figs. 9.3–9.4) The webbing appears to have scutellate scale impressions, while the undersides of the digits appear to have reticulate scale patterns (Fig. 10.1–10.2).

Associated dabbling feeding traces (*Ts. ericksonii*) signify a predatory relationship between the tracemaker and epi- and endofauna. Furthermore, the water level on all *Presbyorniformipes* slabs was shallow enough to allow the tracemaker to walk, sometimes while dabbling, yet deep enough to prevent the development of invertebrate traces such as *C.*

anguineus. Apparent mud cracks on GC-C-4 (hyporelief) and GC-C-21 (epirelief) indicate that the environment transitioned to being subaerially exposed before burial on those slab horizons.

Ichnogenus TSALAVOUTICHNUS new genus

Type ichnospecies.—Tsalavoutichnus ericksonii

Etymology.—From the Greek tsalavoutó, wade or dabble, and -ichnus, trace.

Diagnosis.—Sinuous to slightly sinuous trail or series of discontinuous to continuous impressions (epirelief) or mounds (hyporelief). Impressions may overlap within a single trail. Does not usually cross over itself.

Discussion.—Usually associated with palmated bird tracks, Erickson (1967, see pl. 1–2) originally photographed and interpreted this trace as a dabbling feeding trace of waterfowl. A dabble is a forward directed, sinuous feeding pattern common in modern Anseriformes. This trace, therefore, represents searching and predation behavior (praedichnia). Other, unnamed, types of feeding patterns include peck marks from probing for food, which can be indistinguishable from vertical invertebrate burrows, and side-to-side motions of the beak on the sediment surface, which can leave V-shaped scratches beside bird trackways (Elbroch & Marks, 2001; Kim & others, 2012).

Kim and others (2012) refused to describe as a separate ichnotaxon V-shaped searching and feeding traces associated with bird tracks in the Cretaceous Haman Formation. They followed the example of Yang and others (1995), who did not establish a separate ichnotaxon for the dabble marks associated with *Presbyorniformipes* on the basis that tracks and are clearly made by the same tracemaker. As feeding traces of searching and predation behaviors clearly represent different behaviors than repichnial tracks, irrespective of the tracemaker, we establish

Tsalavoutichnus to represent dabble feeding behavior. Traces are defined to represent behaviors, not tracemakers, as a single tracemaker can make several different types of traces with differing behaviors and each trace can be made by many different types of tracemakers exhibiting the same or similar behavior or set of behaviors (e.g., Ekdale, Bromley, & Pemberton, 1984; Hasiotis, 2007). That Yang and others (1995) chose not to establish a new ichnotaxon for dabble traces when defining *Presbyorniformipes* is not a valid reason for not doing so for all feeding traces associated with bird tracks.

The tracemaker of *Tsalavoutichnus* is likely a shorebird similar to *Presbyornis*, or a bird similar to such modern water fowl as ducks, geese, and swans. This trace ranges from the Eocene to recent, as the behavior is present in modern water fowl, but may range to an earlier age.

TSALAVOUTICHNUS ERICKSONII new species

Figure 9.1–9.2

Material.—GC-C-10 (n = 2), GC-C-17 (n = 1), GC-C-21 (n = 1)

Etymology.—Named after B. R. Erickson for initial descriptions and photographs of this trace when first describing webbed-footed tracks later named *Presbyorniformipes*.

Diagnosis.—Sinuous trail of consecutive, linearly aligned, teardrop- to ovoid-shaped impressions (epirelief) or mounds (hyporelief). Impressions may overlap within a single trail.

Description.—Sinuous series of linearly aligned, teardrop- to ovoid-shaped impressions preserved in concave epirelief or mounds in convex hyporelief. Trails turn usually with sharper corners, approaching right angles. Impressions are connected on all of GC-C-17 (Fig. 9.1) and most of GC-C-10 and GC-C-21 (Fig. 9.2). On GC-C-10 and GC-C-21, a segment of the trail has separated impressions. On GC-C-21 a segment of the trail is more sinuous (Fig. 9.3). Widths

from ~5.2–9.5 mm; total lengths from ~8.99–79.28 cm; linear lengths from 22.4–65 cm; SIs from 0.76–0.97. All trails are overstepped by *Pe. feduccii* tracks. Refer to Appendix 16 for additional measurements.

Types.—Holotype: BYU B20 (GC-C-21); Paratypes: GC-C-10, GC-C-17.

Associated ichnotaxa.—Presbyorniformipes feduccii.

Discussion.—GC-C-21 is a cast of the holotype of *Presbyorniformipes feduccii* (via Yang & others, 1995) tracks with the *Ts. ericksonii* trail originally collected and described by Erickson (1967). The *Ts. ericksonii* trail becomes significantly more sinuous in one section, suggesting that the tracemaker encountered a prey item and increased its search pattern more laterally. Not described by Erickson (1967) are approximately eight impressions, within and near the end of the trail, of which three form pairs similar to tuning-fork-shaped impressions that resemble the leg imprints of an aquatic insect (Fig. 9.4). The increase in local sinuosity associated with the insect leg imprints is evidence of a predatory behavior and thus signifies praedichnia.

On GC-C-10 (epirelief), a *Pe. feduccii* track destructively overprints an otherwise continuous *Ts. ericksonii* trail on a segment where the impressions are discontinuous and not as deeply impressed. The trail is considered as two separate trails for the purposes of measurements, though they are really two parts of one discontinuous trail associated with a single *Pe. feduccii* trackway.

Tsalavoutichnus ericksonii is always overstepped by *Pe. feduccii* tracks, denoting that the trail came before the tracks. This suggests that the trails were made by the same tracemaker as the tracks. Presence of *Ts. ericksonii* with bird tracks indicates a saturated medium where water depth was not deeper than the depth at which the tracemaker would swim instead of walk and dabble.

TSALAVOUTICHNUS LEPTOMONOPATI new species

Figure 8.6

Material.—GC-C-2 (n = 1).

Etymology.—From the Greek, leptós, slim; monopáti, trail or path.

Diagnosis.—Slightly sinuous (SI close to 1), thin trail of elongate ovoid impressions (epirelief) or mounds (hyporelief); ovoid impressions or mounds may overlap forming a continuous trail, or there may be small gaps between them; preserved in concave epirelief or convex hyporelief.

Description.—Slightly sinuous, thin trail of elongated ovoid mounds preserved in convex hyporelief. At the start of the trail, the ovoid impressions overlap forming a continuous trail. The overlapping lessons down the trail until there are small gaps of a few millimeters between impressions until the trail terminates. Trail width 1.7 mm; amplitude 10.2 mm; total length 12.96 cm; linear length 12.84 cm, SI 0.99. Overstepped by *M. semipalmatus*.

Types.—Holotype: GC-C-2.

Associated ichnotaxa.—Midorikawapeda semipalmatus

Discussion.—This ichnospecies is established for a very thin, slightly sinuous trail associated with two *M. semipalmatus* tracks. The small width of *Ts. leptomonopati* is indicative of the small size of the beak of the tracemaker. Being overstepped by *M. semipalmatus* indicates that the *Ts. leptomonopati* trail came before the tracks, suggesting the same tracemaker made both. The thin beak size and morphology of the tracks, therefore, indicates that these traces were made by shorebirds, likely resembling modern Sandpipers. The association with *M.*

semipalmatus on GC-C-2 (hyporelief), without any invertebrate traces, indicates the environment was below the SWAI in water depths < 5 cm.

OTHER FEATURES

ELEPHANT SKIN TEXTURING

Figure 11.1–11.2

Material.—GC-C-13, GC-C-20.

Description.—Areas of wrinkled, elephant skinlike texturing. On GC-C-13 (epirelief) and GC-C-20 (epirelief), blackened discoloration of the textured surface. Overlying traces deformed on both samples. Present in epirelief.

Discussion.—Dark discoloration is likely indicative of higher levels of carbon. Elephant skin texturing is the result of debated processes. Noffke (2010) suggested this texturing is the result of desiccation after burial of a microbial mat, whereas Seilacher (2007) suggested they are load casts under microbial mats. Davies and others (2016) suggested they result from abiotic loading irrespective of the presence of a mat. Due to the deformation of the overlying traces and dark discoloration, we follow Noffke (2010) in interpreting the texturing structures as desiccation of a microbial mat postburial for both GC-C-13 and GC-C-20. Texturing on the epirelief of GC-C-6 (Fig. 11.4) may be biotic, though we interpret this texturing as abiotic due to its similarity to an abiotic process of the accretion of wind-blown sediment in water depths of 1–2 mm, as photographed on a modern beach in Holkham, Norfolk, England (Davies & others, 2016, fig. 14A).

RAINDROP TRACES

Figure 11.3

Material.—GC-C-13.

Description.—Irregularly circular, concave pits with raised edges. Structures destructively overlap each other. Structures occur on one layer of GC-C-13 in epirelief.

Discussion.—The layer of these structures underlies the exposed layer on most of the slab, which has numerous *C. anguineus* trails and bird track digits. A section of the top layer is broken away, exposing these structures. As the structures are not perfectly circular and relatively densely overlapping, they do not appear to be consistent with the release of gas from the subsurface in a drying media. Raindrop traces described and photographed in Twenhofel (1921, fig. 1), Metz (1981, fig. 2), Lanier, Feldman, and Archer (1993, fig. 12A), and Davies and others (2016, fig. 11B) are similar to the GC-C-13 structures. Modern degassing pits from an evaporating body of water in Australia as photographed and described in Hasiotis (2008) are much more perfectly circular, have far less overlapping. Further, degassing structures often result in mounds, collapsed mounds, and cracks, not present on GC-C-13 (e.g., Twenhofel, 1921; Furniss, Rittel, & Winston, 1998; Hasiotis, 2008; Davies & others, 2016).

The absence of invertebrate traces is also notable, as the degassing structures of an evaporating water body are generally associated with traces, as shown in Hasiotis (2008). The modern analogue of raindrop impressions in Metz (1981, see fig. 2) does not have indications of co-occurring invertebrate traces, which makes sense given that any traces that were there would be destroyed during the rain event, leaving the vestiges of droplets as it ends. The lack of invertebrate trace fossils suggests that the If the layer raindrop-impression-bearing layer was buried relatively rapidly, or hardened before organisms moved across the surface, not allowing any traces to be recorded.

TEAR FABRIC

Figure 5.4, Figure 6.2

Material.—GC-C-13

Description.—Parallel-oriented, elongated pits present across slab horizon, hyporelief, GC-C-13. Pits ~1 mm long and ~0.3 mm wide.

Discussion.—These structures are more likely to be incipient tears in a microbial mat resulting from desiccation shrinkage (Noffke, 2010). Fully developed tear textures appear similar to mud crack networks in pattern, though known incipient cracks tend to be bifurcating and trifurcating (e.g., Shrock, 1948; Bohn, Pauchard, & Couder, 2005; Parizot & others, 2005; Noffke, 2010; Davies & others, 2016). The structures here likely represent the earliest stages of mat desiccation due to wind, earlier than the incipient cracks in Shrock, 1948.

The tears appear similar to casts of setulf, a wind-based feature also known as inverted flutes or sand shadows (e.g., Bottjer & Hagadorn, 2007; Sarkar, Samanta, & Altermann, 2011; Davies & others, 2016). These tears, however, are nowhere near as dense as what has been described as setulf, nor are they in sandstone, nor are they at remotely similar scale. These tears may be examples of silt setulf, the smaller size and lower density being a function of the grain size, though this is unlikely.

DISCUSSION

Ichnotaxa

Twenty-six ichnospecies are represented from 19 ichnogenera (Table 3). There are 14 ichnospecies, three of which are newly established, from 10 invertebrate ichnogenera, one of

which is newly established: *Acanthichnus*, *Aulichnites*, *Cochlichnus*, *Conichnus*, *Glaciichnium*, *Glaroseidosichnus*, *Planolites*, *Protovirgularia*, *Sagittichnus*, and *Treptichnus*. There are 12 ichnospecies, three of which are newly established across nine avian ichnogenera, two of which are newly established: *Alaripeda*, c.f. *Aquatilavipes*, *Aviadactyla*, *Avipeda*, *Fuscinapeda*, *Gruipeda*, *Midorikawapeda*, *Presbyorniformipes*, and *Tsalavoutichnus*.

Behaviors

Ichnofossils from the GRF of Soldier Summit and Spanish Fork Canyon represent various established ethological categories of behaviors (e.g., Bromley, 1996; Gingras & others, 2007; Table 3): cubichnia (resting), domichnia (dwelling), fodinichnia (feeding), pascichnia (grazing), praedichnia (predation), pupichnia (pupation traces), and repichnia (locomotion). Cubichnia is represented by *Sagittichnus*. Domichnia is represented by *Conichnus*. Fodinichnia is represented by *Planolites* and *Tsalavoutichnus*. Pascichnia is represented by *Aulichnites*. Praedichnia is represented by *Tsalavoutichnus*. Pupichnia is represented by *Treptichnus*. Repichnia is represented by *Acanthichnus*, *Alaripeda*, c.f. *Aquatilavipes*, *Aviadactyla*, *Avipeda*, *Cochlichnus*, *Fuscinapeda*, *Glaciichnium*, *Glaroseidosichnus*, *Gruipeda*, *Midorikawapeda*, *Presbyorniformipes*, and *Protovirgularia*.

Ichnocoenoses

Ichnocoenoses are assemblages of ichnofossils resultant from individual communities of tracemaking organisms that can be used to interpret the physicochemical conditions during deposition (e.g., Ekdale, Bromley, & Pemberton, 1984; Bromley, 1996; Hasiotis, 2004, 2007, 2008; Hammersburg, Hasiotis, & Robison, 2018). Four ichnocoenoses are established from our

GRF samples that are indicative of environments above, at, and below the SWAI (Table 4; Fig. 12.1–12.4). In all four ichnocoenoses, sample lithologies include very thin, planar-laminated mudstones to fine siltstones with or without microbial laminations and mud cracks.

The *Conichnus* ichnocoenosis (Fig 12.1) includes *Co. conichnus, Sagittichnus linki*, *Glaroseidosichnus gierlowskii*, and potentially *Aulichnites parkerensis, Au. tsouloufeidos*, and *Planolites montanus*. Representatives are found on GC-C-5 (hyporelief), GC-C-13 (hyporelief), GC-C-14 (hyporelief), and GC-C-16 (hyporelief). This ichnocoenosis represents cubichnia, domichnia, and repichnia (swimming traces) in an aquatic environment below the SWAI in water depths < ~5 cm.

The *Presbyorniformipes* ichnocoenosis (Fig. 12.2) includes bird tracks that occur only with other bird traces, and includes *Fuscinapeda texana*, *Midorikawapeda semipalmatus*, *Presbyorniformipes feduccii*, *Tsalavoutichnus ericksonii*, and *Ts. leptomonopati*. Representatives are found on GC-C-2 (hyporelief), GC-C-4 (hyporelief), GC-C-5 (epirelief), GC-C-8 (epirelief), GC-C-10 (epirelief), GC-C-17 (epirelief and hyporelief), GC-C-18 (epirelief), GC-C-19 (epirelief), and GC-C-21 (epirelief). This ichnocoenosis represents avian repichnia, fodinichnia, and praedichnia in an aquatic environment below the SWAI in water depths < ~5 cm.

The *Cochlichnus* ichnocoenosis (Fig. 12.3) includes *Acanthichnus cursorius*, *Alaripeda lofgreni*, c.f. *Aquatilavipes* isp., *Aviadactyla vialovi*, *Avipeda phoenix*, *C. anguineus*, *C. plegmaeidos*, *Glaciichnium liebegastensis*, *Gruipeda fuenzalidae*, *Gruipeda gryponyx*, *Midorikawapeda semipalmatus*, *Protovirgularia dichotoma*, and potentially *Aulichnites parkerensis*, *Au. tsouloufeidos*, and *Planolites montanus* and rhizoliths. Representatives are found on GC-C-1 (hyporelief), GC-C-2 (epirelief), GC-C-3 (epirelief), GC-C-6 (epirelief and hyporelief), GC-C-7 (epirelief and hyporelief), GC-C-10 (hyporelief), GC-C-11 (hyporelief),

GC-C-12 (epirelief), GC-C-13 (epirelief), GC-C-14 (epirelief), GC-C-15 (epirelief and hyporelief), GC-C-16 (hyporelief), and GC-C-18 (hyporelief). This ichnocoenosis represents invertebrate repichnia and pascichnia and avian repichnia in an aquatic environment indicative of the SWAI.

The *Treptichnus* ichnocoenosis (Fig. 12.4) includes *T. bifurcus*, *T. pedum*, *T. vagans*, rhizoliths, and potentially *Planolites montanus*. Representatives are found on GC-C-5 (hyporelief), GC-C-9 (epirelief and hyporelief), and GC-C-14 (hyporelief). This ichnocoenosis represents pupichnia in subaerial exposure above the SWAI with a moist medium.

Certain traces, such as *Planolites*, rhizoliths, and bird tracks are assemblage crossing and are present in multiple ichnocoenoses. *Planolites* is a ubiquitous trace present in a variety of environments and could be part of the *Cochlichnus*, *Conichnus*, or *Treptichnus* ichnocoenoses. Ichnocoenoses with rhizoliths can be considered as incipient Entisols (or Protosols, *sensu* Mack, James, & Monger, 1993) formed either at or above the SWAI as part of the *Cochlichnus* or *Treptichnus* ichnocoenoses, as the rhizoliths indicate short-term subaerial exposure beginning when the water table is at or just below the SWAI (e.g., Hasiotis, Kraus, and Demko 2007). The bird tracks may have been produced either at the SWAI or in shallow water depths as part of the *Cochlichnus* or *Presbyorniformipes* ichnocoenoses. None of these traces, therefore, are particularly good indicators of environmental conditions or precise trace assemblages.

These ichnocoenoses also often overprint each other, likely due to fluctuating environmental conditions typical of lake margins, an example of which is shown in Figure 12.5 (e.g., Wetzel, 2001; Cohen, 2003; Ainsworth & others, 2012; Hasiotis & others, 2012). The order of ichnocoenosis occurrence can sometimes be determined by crosscutting relationships of the

traces. Determining exactly to which ichnocoenosis the assemblage-crossing traces ultimately belong on a given horizon due to ichnocoenosis overprinting can be difficult.

For example, GC-C-14 hyporelief displays overprinting of the *Cochlichnus*, *Conichnus*, and *Treptichnus* ichnocoenoses (Fig. 12.5). Some or all of the bird traces may have been made at the SWAI as part of the Cochlichnus Ichnocoenosis, or in deeper water depths, potentially of the *Conichnus* or *Presbyorniformipes* ichnocoenoses. Even though the bird tracks cannot be accurately assigned, as crosscutting relationships on this horizon are lacking, *Cochlichnus*, *Conichnus*, and *Treptichnus* are all present and represent their respective ichnocoenoses. This horizon, therefore, experienced varying water depths above, at, and below the SWAI.

Comparative Ichnotaxonomy

Ichnology of the GRF.—A diverse ichnofauna has been documented from the Parachute Creek Member of the GRF despite the lack of full ichnotaxonomic descriptions. Curry (1957) showed a mammal track, at least five bird ichnogenera, and one invertebrate ichnogenus. The invertebrate and bird tracks appear to belong to *Anatapeda*, *Aquatilavipes*, *Aviadactyla*, *Avipeda*, *Cochlichnus*, and *Midorikawapeda*. Erickson (1967) first showed the BTFs *Presbyorniformipes* and *Tsalavoutichnus*. Moussa (1968) published photographs of at least four avian ichnogenera and three invertebrate ichnogenera, which we interpret as *Aquatilavipes*, *Aviadactyla*, *Avipeda*, *Cochlichnus*, *Conichnus*, *Gruipeda* and *Planolites*. Moussa (1970) showed traces best assigned to *Cochlichnus anguineus*. Olson (2014) described bird tracks that appear to be *Aquatilavipes*. Nine ichnogenera of the GRF Parachute Creek Member are shared with our GRF samples: *Aquatilavipes*, *Aviadactyla*, *Avipeda*, *Cochlichnus*, *Conichnus*, *Gruipeda*, *Midorikawapeda*, *Planolites*, and *Presbyorniformipes*.

The Tipton Member of the GRF in the Washakie Basin, Wyoming, contains a differing variety of ichnotaxa, few of which are similar to our GRF samples. Roehler, Hanley, and Honey (1988) identified what appear to be *Planolites* and rhizoliths from sandstone at Cottonwood Creek Delta, in the Washakie Basin, Wyoming. Leggitt and Cushman (2001), Leggitt and Loewan (2002), and Leggitt, Biaggi, and Buchheim (2007) described caddisfly larval cases in the Greater Green River Basin, Wyoming, best assigned to *Tektonargus* Hasiotis & others, 1998. Lamond and Tapanila (2003) described bioclaustration cavities in stromatolites in the Washakie Basin, Wyoming. Only *Planolites* and rhizoliths are shared with our GRF samples.

Martin, Vazquez-Prokopec, and Page (2010) described, though did not name, *Undichna* from the Fossil Butte Member of the GRF in Fossil Basin, Wyoming, which is not shared with our GRF samples.

Bohacs, Hasiotis, and Demko (2007) identified 11 ichnogenera from the GRF and time-equivalent Wasatch Formation in Wyoming, of which one is shared with our GRF samples (*Planolites*). Bird tracks appear to be *Aviadactyla* and *Avipeda*, both of which are shared with our GRF samples.

Due to the amount of overlap between ichnogenera, our traces are more consistent with what has been described from the Parachute Creek Member of the GRF.

Comparison with other ancient lacustrine environments.—The Upper Cretaceous Haman Formation is rich in ichnodiversity, particularly of bird tracks. Kim (1969) erected *Koreanornis* from the upper part of the Upper Cretaceous Haman Formation in South Korea, as well as noted the presence of sinuous worm trails (*Cochlichnus*), and gastropod trails, likely *Protovirgularia*. He used the traces and lithology to interpret a fluvio-lacustrine setting. Lim and others (2000) further identified *Koreanornis* and webbed bird tracks. Kim and others (2012)

ichnotaxonomically described more BTFs of the Gajin Tracksite in Jinju, Korea, identifying *Aquatilavipes, Goseongornipes, Ignotornis* Mehl, 1931, and *Koreanornis* tracks. The GRF samples share the invertebrate ichnogenera *Cochlichnus* and bird ichnogenera *Aquatilavipes* with the Haman Formation.

Robison (1991) described, but did not formally name, bird and frog tracks from lacustrine to fluvial-lacustrine sections of the Upper Cretaceous Blackhawk Formation in Utah. The bird tracks, based on photographs, appear to belong to *Aquatilavipes* and *Avipeda*, with two indeterminate semipalmated morphologies.

Buatois and others (1995) described and named *Vagorichnus* from lacustrine turbidites of the Jurassic Anyao Formation, China. Two other ichnogenera are noted, though not described, from the samples, *Gordia* Emmons, 1844, and *Tuberculichnus* Książkiewicz, 1977. None of the ichnotaxa are shared with the GRF samples.

De Gibert and others (2000) described invertebrate trace fossils from Lower Cretaceous lacustrine deposits in El Montsec, Spain. Five ichnogenera are described, of which only *Cochlichnus* is shared with the GRF samples.

Metz (1998, 2000) described trace fossils from lacustrine shoreline deposits of the Triassic Passaic Formation. Six ichnogenera are described, of which *Cochlichnus* and *Treptichnus* are shared with the GRF samples.

Foster (2001) described fossil salamander tracks in lacustrine shoreline deposits of the Eocene Wasatch Formation, Wyoming. Photographed, but not described or identified, are apparent *Cochlichnus* (fig. 3.3) and other invertebrate traces. *Cochlichnus* is shared with the GRF samples.

Azuma and others (2002) identified *Aquatilavipes* from the Lower Cretaceous Tetori Group in Japan, interpreting them as being produced on a lake margin. *Aquatilavipes* is shared with the GRF samples.

Melchor, de Valais, and Genise (2002) described bird tracks originally posited as being Late Triassic in age as part of the Santo Domingo Formation in Argentina. Melchor, de Valais, and Genise (2013) retracted the 2002 paper, as the study area was determined via radiometric dating in Melchor, Buchwaldt, and Bowring (2013) to be Eocene in age and part of the Laguna Brava Formation. Melchor and others (2006) further described ITFs and BTFs from the same study area. De Valais and Melchor (2008) ichnotaxonomically described the bird tracks first described in the 2002 paper. Melchor and others (2006) and de Valais and Melchor (2008) have photographs of bird tracks modified from the 2002 retracted paper (e.g., see fig. 1C, Melchor, de Valais, & Genise, 2002, vs. fig. 9C, Melchor & others, 2006, vs fig. 5D, de Valais & Melchor, 2008). The study area and results of Melchor and others (2006) and de Valais and Melchor (2008), therefore, are now be evaluated in terms of an Eocene age for their identified traces. Two BTF ichnogenera, nine ITF ichnogenera, two nonavian vertebrate ichnogenera, and rhizoliths were identified. Unidentified BTF ichnospecies appear to be *Aquatilavipes* and *Avipeda*. Five ichnogenera are shared with the GRF samples along with rhizoliths: *Alaripeda*, *Aquatilavipes*, *Avipeda*, *Cochlichnus*, and *Gruipeda*.

Hasiotis (2004, 2008) identified 75 ichnofossil morphotypes from the Upper Jurassic Morrison Formation in the Rocky Mountain region of the United States, 25 of which were from deposits interpreted as proximal lacustrine environments. *Cochlichnus*, *Conichnus*, *Planolites*, and rhizoliths are shared with the GRF samples.

Melchor (2004) described trace fossils from lacustrine deltaic deposits in the Triassic Ischigualasto-Villa Unión basin, Argentina. Nineteen ichnogenera are identified, of which only *Cochlichnus* is shared with the GRF samples.

Uchman, Pika-Biolzi, and Houchuli (2004) described traces from Oligocene floodplain pond deposits in the Lower Freshwater Molasse of Switzerland. Five invertebrate ichnogenera were described, along with several unnamed traces, of which *Cochlichnus* and *Treptichnus* are shared with our GRF samples. One vertebrate ichnogenus is described, along with four unnamed traces, none of which are shared with our GRF samples.

Kim and others (2005) described a diverse array of traces from lake-margin deposits of the Cretaceous Jinju Formation, Korea. Ten invertebrate ichnogenera were described, along with sauropod tracks. *Cochlichnus*, *Planolites*, and *Protovirgularia* are shared with our GRF samples.

Uchman, Kazakauskas, and Gaigalas (2009) described trace fossils from a Lithuanian Upper Pleistocene varved proglacial lake deposits. Four invertebrate ichnogenera were described, of which *Cochlichnus* and *Glaciichnium* are shared with the GRF samples. *Undichna* is also photographed, though is described as cf. *Warvichnium* isp. (see fig 6E in Uchman, Kazakauskas, and Gaigalas, 2009).

Huh and others (2012) described bird tracks from Cretaceous lake margin strata in the Yeosu Islands Archipelago, Korea. *Aquatilavipes* and *Koreanornis*, dinosaur tracks, and *Cochlichnus* traces have been described from this locality (Huh & others, 2001, 2002, 2012). *Aquatilavipes* and *Cochlichnus* are shared with the GRF samples.

Minter and others (2012) described *Lithographus* Hitchcock, 1858, from a lacustrine horizon in the Cretaceous Haenam tracksite, Uhangri Formation, Korea. At least two other invertebrate ichnogenera, *Planolites* and *Skolithos*, have been previously described from this

locality (Hwang & others, 2002). The site is also known for vertebrate trace fossils of dinosaurs, pterosaurs, and birds (e.g., Yang & others, 1995; Lockley & others, 1997; Hwang & others, 2002; Thulborn, 2004; Song, 2010). Only *Planolites* is shared with the GRF samples.

Mansilla and others (2012) described bird tracks from Antarctica's Eocene Fossil Hill in lacustrine sediments, identifying *Avipeda*, *Gruipeda*, and c.f. *Uhangrichnus* Yang & others 1995. *Avipeda* and *Gruipeda* are shared ichnogenera with the GRF samples.

Melchor, Cardonatto, and Visconti (2012) described flamingolike tracks (*Phoenicopterichnum* Aramayo & Manera de Bianco, 1987) from the Oligocene–Miocene Vinchina Formation in Argentina, as well as assigning three ITF ichnogenera, none of which are shared with the GRF samples.

Getty and others (2016) described Jurassic *Treptichnus* from continental playa and perennial lake sediments of the East Berlin Formation, Massachusetts, which is shared with the GRF samples.

Our samples share the most BTF ichnogenera with the Eocene Laguna Brava Formation of Argentina (de Valais & Melchor, 2008) and the most ITF ichnogenera with the Cretaceous Jinju Formation of Korea (Kim & others, 2005).

Cochlichnus Ichnofacies

Ichnofacies are recurring trace-fossil associations that represent characteristic environmental conditions and ecological types of behaviors (Seilacher, 1953, 1955b, 1967; Bromley, 1996). In marine settings, ichnofacies are well defined and clearly represent unique depositional and physicochemical conditions. Marine ichnofacies were defined based on trace-fossil distribution patterns paralleling the distribution of characteristic modern traces in similar

environmental conditions and associated lithofacies (e.g., Seilacher, 1953, 1967; Häntzschel, 1975).

The Cochlichnus Ichnofacies.—We propose a new ichnofacies, the Cochlichnus Ichnofacies, to represent continental environments where locomotion, resting, dwelling, feeding, grazing, predation, and pupation traces are produced just below, at, or just above the SWAI—also referred to as periaquatic settings (Hasiotis, 2007)—in fine-grained sediments deposited in low-energy settings, often overprinting one another (Fig. 12.5–12.6). The Eocene GRF ichnocoenoses constructed herein are representative examples of the assemblages characteristic of the Cochlichnus Ichnofacies, primarily occurring on planar-laminated beds with or without mud cracks, microbial laminations, and incipient pedogenesis (Entisols or Protosols). These ichnocoenoses represent conditions intimately associated with the SWAI where the groundwater profile and lake level fluctuate below, at, or above the SWAI at any one time. Conditions associated the SWAI, therefore, represent low-energy settings such that traces produced in all three hydrologic conditions overprint each other, and appear to co-occur together.

The Mermia, Scoyenia, and Shorebird ichnofacies are poorly defined and have either very broad or incomplete environmental interpretations for the assemblages of traces represented (e.g., Hasiotis 2004; 2008, Hasiotis & others, 2012; Hasiotis, McPherson, & Reilly, 2013). Establishing the Cochlichnus Ichnofacies assists with resolving some of the problems associated with these continental ichnofacies. The Cochlichnus Ichnofacies: (1) restricts the Mermia Ichnofacies to water depths further below the SWAI (~ >5–10 cm) and replaces its usage for temporary water bodies; (2) removes traces from the Mermia Ichnofacies produced at or above the SWAI, including *Cochlichnus*, *Treptichnus*, and arthropod crawling traces (e.g., *Helminthoidichnites* Fitch, 1850, *Glaciichnium*, *Maculichna* Anderson, 1975); (3) restricts the

Scoyenia Ichnofacies to media with lower moisture levels further above the SWAI; (4) replaces the Shorebird Ichnofacies; (5) fixes the dilemmas encountered in such works as Buatois, Jalfin, and Aceñolaza (1997), Uchman, Pika-Biolzi, and Houchuli (2004), and Kim and others (2005) with regards to placing their trace-fossil assemblages into either the Scoyenia or Mermia ichnofacies due to an overlapping of traces characteristic of both.

The Mermia Ichnofacies was originally defined to represent permanently subaqueous nonmarine (continental) environments and potentially fjords during glacial melting (Buatois & Mángano, 1995; Pazos, 2002). This ichnofacies was later redefined to include temporary water body environments (Buatois & Mángano, 2002, 2003, 2004). These settings are so different from each other that there should be differences in trace-fossil associations (e.g., Hasiotis & others, 2012). In continental settings, *Cochlichnus* and arthropod crawling traces are produced at the SWAI (e.g., Moussa, 1970; Chamberlain, 1975; Metz, 1987), whereas *Treptichnus* is produced subaerially above the SWAI (e.g., Muñiz Guinea & others, 2014), which is problematic for interpreting supposedly fully subaqueous environments. In modern settings, few traces form in temporary water bodies in water depths >10 cm (Hasiotis, 2008). Establishing the Cochlichnus Ichnofacies and removing from the Mermia Ichnofacies *Cochlichnus*, *Treptichnus*, and arthropod crawling traces produced at the SWAI, as well as the environments in which they are characteristic, helps in redefining Mermia as an ichnofacies representative of a more characteristic set of environmental conditions. Diagnostic traces typical of the Mermia Ichnofacies now include: *Circulichnus*, *Gordia*, *Helminthopsis* Heer, 1877, *Undichna*, and *Vagorichnus*; one ichnospecies of *Tuberculichnus* has been synonymized with *Treptichnus*. Such traces as *Aulichnites*, *Lockeia*, *Palaeophycus*, and *Planolites* can occur in environments further below, below, at, and just above the SWAI, as well as well above the SWAI (i.e., *Palaeophycus*

and *Planolites*) in a variety of imperfectly- to well-drained environments (e.g., Hasiotis 2004, 2008; Smith & others, 2008a, 2009; Hamer & Sheldon, 2010; Hasiotis & others, 2012).

The Scoyenia Ichnofacies was originally described by Seilacher (1963, 1967) as traces commonly found in redbeds, and was used to represent nearly all continental ichnocoenoses (Frey & Seilacher, 1980, table 4). This ichnofacies has been modified extensively over time such that it now represents continental, low-energy environments that may be periodically exposed or inundated (e.g., Frey, Pemberton, & Fagerstrom, 1984; Frey & Pemberton, 1987; Buatois & Mángano, 1995, 1998, 2004, 2011). The problem with this ichnofacies, as currently defined, is that it includes nearly all continental environments except for dry dunes and interdunes and profundal lacustrine environments (e.g., Hasiotis, 2007, 2008; Hasiotis & others, 2012). The potential environments represented by this ichnofacies also include many types of paleosols, which vary greatly in characteristics and are the products of vastly different environmental conditions (e.g., Birkeland, 1999; Retallack 2001; Schaetzl & Anderson, 2005; Hasiotis, Kraus, & Demko, 2007; Hasiotis, 2008; Hasiotis & others, 2012). Restricting the Scoyenia Ichnofacies to less moist environments further above the SWAI with the establishment of the Cochlichnus Ichnofacies is a step towards refining a characteristic set of environmental and physicochemical conditions for this ichnofacies.

Lockley, Hunt, and Meyer (1994) defined ichnofacies under a differing methodology from ichnofacies established by Seilacher (1967), preferring to define them on a per-unit scale—i.e., at the ichnocoenosis scale. The Shorebird Ichnofacies was established as a catch-all term for local ichnofacies representing conditions consistent of continental shorelines. This ichnofacies does not consider the overlapping of traces representing differing environmental conditions on a single horizon, a characteristic of many continental settings. Vertebrate tracks, and especially

shorebird tracks, are also not the most important indicators of physicochemical conditions, as terrestrial vertebrates (especially birds) are not as restricted to particular physicochemical conditions as are invertebrates (e.g., Hasiotis, 2004, 2008; Hasiotis & others, 2012; Hasiotis, McPherson, & Reilly, 2013). We reject the concept of naming ichnofacies based on facies-crossing terrestrial vertebrates and further replace the Shorebird Ichnofacies in favor of the more specifically defined and broadly applicable Cochlichnus Ichnofacies, which accounts for the overprinting of traces representative of environmental conditions around the SWAI.

Applications of the Cochlichnus Ichnofacies.—Ichnofacies were originally supported by comparisons with modern distributions of their respective diagnostic traces, as they were good indications of water depth (e.g., Seilacher, 1967). The distribution of trace fossils and lithofacies, however, is recognized as a function of physicochemical and ecological factors in the environment (e.g., Pemberton & Frey, 1985; Ekdale 1988; MacEachern, Raychaudhuri, & Pemberton, 1992; MacEachern & others, 2007; Hasiotis and Platt, 2012). The following are examples of modern environments with trace-fossil assemblages at and around the SWAI, consistent with the Cochlichnus Ichnofacies. In Hasiotis (2008), an evaporating water body in Australia includes traces that developed in very shallow and wet surface (SWAI) conditions, including simple biogenic structures similar to *Planolites* and *Cochlichnus*. Martin (2009) described and photographed surface trails similar to *Aulichnites*, *Cochlichnus*, *Gordia*, *Helminthoidichnites*, and *Treptichnus*, as well as bird and mammal tracks, on a wet, exposed Arctic fluvial point bar in North Slope, Alaska. Not noted, however, is how wet or dry the observed surfaces were at the time of observation; *Treptichnus* likely developed just above the SWAI after the other traces where produced in conditions below or at the SWAI. Hamer and Sheldon (2010) studied modern lake margins at Ruby Reservoir, Montana, and La Sotonera,

Spain, describing a diverse array of traces. Traces similar to *Cochlichnus* and *Helminthoidichnites* are found together with bird tracks in the eulittoral zone of both lakes, an assemblage consistent with the Cochlichnus Ichnofacies. Hasiotis and others (2012) described surface and subsurface burrows of mole crickets (i.e., *Steinichnus* Bromley & Asgaard, 1979), lizard trackways, and bird trackways and feeding traces (i.e., shorebirds) at and just above the swash zone (i.e., SWAI) along the shoreline of Lake Tanganyika, at Kigoma, Tanzania. Hasiotis and Jensen (in preparation, 2018) observed *Cochlichnus* and *Treptichnus* and roots at and just above the SWAI along the margins of temporary shallow (< 20 cm) freshwater pools on the alluvial plain near Svea, Svalbard.

As ichnofacies must also be broadly applicable through time, the following are examples of ancient environments with the specific set of periaquatic conditions and trace-fossil assemblages characterizing the Cochlichnus Ichnofacies, broadening the variety of traces that may be included within this ichnofacies (Table 6). Trace-fossil assemblages discussed in previous work from the Parachute Creek Member of the GRF from Soldier Summit and Spanish Fork Canyon, Utah (e.g., Curry, 1957; Erickson, 1967; Moussa, 1968), fit our *Cochlichnus* and *Presbyorniformipes* ichnocoenoses, indicating environments at and below the SWAI, consistent with the Cochlichnus Ichnofacies.

Tasch (1968) described *Cochlichnus* from the Permian Antarctic Ohio Range. The environment of deposition is described as a floodplain, following Long (1965). The presence of *Cochlichnus* indicates environments at the SWAI and is consistent with the Cochlichnus Ichnofacies.

Gibbard (1977) described *Cochlichnus* in Holocene varved lacustrine deposits, Finland. The presence of *Cochlichnus* is indicative of conditions at the SWAI and is consistent with the Cochlichnus Ichnofacies.

Buatois, Jalfin, and Aceñolaza (1997) described a Permian trace-fossil assemblage from the Laguna Polino Member of the La Golondrina Formation, Argentina. The assemblage has abundant *Cochlichnus* traces associated with *Ctenopheleus* Seilacher & Hemleben, 1966, *Helminthoidichnites*, *Helminthopsis*, and *Palaeophycus*. The assemblage was noted as having characteristics of both the Scoyenia and Mermia ichnofacies, an issue resolved by placing this assemblage and environment into the Cochlichnus Ichnofacies.

The assemblages described by Doyle, Wood, and George (2000) of BTFs from Miocene marls (lagoonal and salt marsh) of the Sorbas Member, Sorbas Basin, Spain, are best characterized in part as the Cochlichnus Ichnofacies. Not discussed, though noted, are co-occurring mammalian, invertebrate (*Cochlichnus*), and root traces, which is indicative of the environment at or near the SWAI.

Salamander tracks and *Cochlichnus* trails in Foster (2001) from the lacustrine deposits of the Eocene Wasatch Formation indicate conditions at the SWAI. This assemblage is characteristic of the Cochlichnus Ichnofacies.

Hasiotis (2004, 2008) described many trace-fossil assemblages from the Morrison Formation. Traces listed as belonging to a proximal lacustrine ichnocoenosis include: rhizoliths, adhesive meniscate burrows (now known as *Naktodemasis* Smith & others, 2008b), *Camborygma litonomos* Hasiotis & Mitchell, 1993, *Celliforma* Brown, 1934, *Cochlichnus*, *Conichnus*, *Cylindrichum* Linck, 1949, dinosaur tracks, *Fuersichnus* Bromley & Asgaard, 1979, gastropod traces, horizontal U-tubes, *Kouphichnium* Nopcsa, 1923, *Planolites*, *Pteraichnus*

Stokes, 1957, shallow U-tubes, *Steinichnus*, and stromatolites with or without borings. Periods where the surface was further above the SWAI would include *Celliforma*, *Cylindrichum*, *Fuersichnus*, *Naktodemasis*, *Planolites*, and the rhizoliths. Periods just above or near the SWAI would include *Planolites* and *Steinichnus*. Periods at the SWAI would include *Camborygma litonomos*, *Cochlichnus*, dinosaur tracks, gastropod traces, *Planolites*, and *Pteraichnus*. Periods below the SWAI would include *Conichnus*, horizontal U-shaped tubes, shallow U-shaped tubes, and stromatolites with or without borings. This broad Proximal Lacustrine ichnocoenosis for the Morrison Formation, primarily applying to the Tidwell Member, is best described as at least three separate ichnocoenoses representing environments around the SWAI, together being representative examples of the Cochlichnus Ichnofacies. The fourth ichnocoenosis (further above the SWAI) would be a representative of the Scoyenia Ichnofacies.

Lucas & others (2004) described a diverse assemblage of traces from what is described as freshwater tidal-flat deposits of the Middle Pennsylvanian Keota Sandstone Member of the McAlester Formation, Oklahoma. Invertebrate traces *Cochlichnus*, *Diplichnites*, *Diplopodichnus* Brady, 1947, *Gordia*, *Paleohelcura* Gilmore, 1926, *Tonganoxichnus* Mángano & others, 1997, *Treptichnus* and vertebrate traces *Notalacerta* Butts, 1891, *Pseudobradypus* Matthew, 1903, and *Undichna*. This is a diverse set of traces described as having elements of the Scoyenia and Mermia ichnofacies. The arthropod crawling traces and *Cochlichnus* are indicative of the SWAI, and *Treptichnus* just above the SWAI, consistent of the Cochlichnus Ichnofacies, whereas *Undichna* is characteristic of Mermia. This environment likely underwent larger fluctuations in water level from above, to at, to further below the SWAI.

Uchman, Pika-Biolzi, and Houchuli (2004) described vertebrate tracks and invertebrate traces, including *Cochlichnus* and *Treptichnus*, from Oligocene floodplain pond deposits. They

had difficulty establishing exactly to which ichnofacies their assemblages ultimately belong as they had vertebrate trackways, representative of the Scoyenia Ichnofacies, associated with *Cochlichnus* and *Treptichnus*, representative of the Mermia Ichnofacies. At the end of their discussion, the trace associations for the locality were described as belonging to the Mermia Ichnofacies, however, the first sentence of the conclusions section stated they are comparable to the Scoyenia Ichnofacies. This assemblage closely matches the overlapping *Cochlichnus* and *Treptichnus* ichnocoenoses in our GRF samples and are best placed in the Cochlichnus Ichnofacies, representing the overprinting of ichnocoenoses in periaquatic settings.

Kim and others (2005) described four ichnocoenoses from the Cretaceous Jinju Formation of Korea. Two of those assemblages were classified as Mermia-Scoyenia composite for having traces which overlap both ichnofacies. Of note, these two assemblages have *Cochlichnus*, *Diplichnites*, and trackways of sauropods. As with Uchman, Pika-Biolzi, and Houchuli (2004), these assemblages are best placed in the Cochlichnus Ichnofacies, as they represent an overlapping of conditions at and around the SWAI.

Uchman, Kazakauskas, and Gaigalas (2009) described traces fossils from varved lacustrine settings in the late Pleistocene of Lithuania. The assemblage is diverse, including arthropod trackways, grazing traces, and fish traces. The *Undichna* is unusually small, and a central body trace indicates that water level was likely very shallow, likely within the limits of our *Conichnus* ichnocoenosis of ~5 cm. The assemblages represent overlapping of conditions just below and at the SWAI as evidenced by the swimming traces and the presence of *Cochlichnus*. These assemblages are best characterized as part of the Cochlichnus Ichnofacies.

Huh and others (2001, 2002, 2012) described bird and dinosaur tracks from Cretaceous lake margin strata in the Yeosu Islands Archipelago, Korea. Of note, a *Koreanornis* assemblage

includes associated *Cochlichnus* traces. The *Koreanornis* assemblage likely occurred with water level at the SWAI, whereas a separate *Aquatilavipes* assemblage, lacking *Cochlichnus* and other trails, likely occurred below the SWAI. These assemblages are representative of the Cochlichnus Ichnofacies.

Lerner and Lucas (2015) described trace fossils from the early Permian Robeldo Mountains Formation, New Mexico. While they described the environment as tidal flats, the setting was likely freshwater (Voight & others, 2013). *Cochlichnus* is present along with other invertebrate traces including *Helminthopsis*, *Kouphichnium*, and *Selenichnites* Romano & Whyte, 1990. Vertebrate traces include *Characichnos* Whyte & Romano, 2001, and *Undichna*. This area likely underwent larger fluctuations in water depth from the SWAI to deeper water depths.

Getty & others (2017) described fourteen ichnotaxa from lake margin and lacustrine deposits in the Pennsylvanian Rhode Island Formation, Massachusetts. Two ichnocoenoses were described, with one regarded as consistent of the Mermia Ichnofacies and the other the Scoyenia Ichnofacies. The assemblage originally assigned to the Mermia Ichnofacies includes *Cochlichnus*, *Diplichnites*, *Narragansettichnus* Getty & others, 2017, and *Undichna*. This assemblage is likely an overlapping of ichnocoenoses representing both the Cochlichnus and Mermia ichnofacies, reflective of water level fluctuation from at to farther below the SWAI.

Summary.—The Cochlichnus Ichnofacies is composed of assemblages that include the overlapping of vertebrate, invertebrate, and rhizolith traces intimately related to the SWAI. Vertebrate traces can include those of not only birds, but also of mammals, reptiles, amphibians, and extinct fauna such as dinosaurs and pterosaurs. The Cochlichnus Ichnofacies is based on trace-fossil assemblages and lithofacies associations in the GRF and similar continental water-

margin environments through time, ranging from the Carboniferous, with the oldest occurrence of continental *Cochlichnus* (Lucas & others, 2004; Getty & others, 2017), to recent.

CONCLUSIONS

1. The Eocene GRF of Soldier Summit and Spanish Fork Canyons has a diverse ichnofossil assemblage of 19 ichnogenera and 26 ichnospecies. The ichnofossils represent cubichnia, domichnia, fodinichnia, pascichnia, praedichnia, pupichnia, and repichnia behaviors.

2. A new ichnospecies of *Aulichnites* is proposed, *A. tsouloufeidos*, for bilobate trails with side ridges with arcuate projections. Three new ichnogenera with four ichnospecies are also proposed: *Glaroseidosichnus gierlowskii*, for trails of paired, crescent-shaped impressions; *Midorikawapeda semipalmatus*, for certain semipalmated bird tracks; and *Tsalavoutichnus* (*Ts. ericksonii*, *Ts. leptomonopati*), for sinusoidal series of ovoid impressions forming trails and often associated with bird tracks.

3. Four ichnocoenoses were constructed, representing different communities of organisms associated with low energy settings: The *Conichnus* and *Presbyorniformipes* ichnocoenoses representative of environments below the SWAI; the *Cochlichnus* Ichnocoenosis representative of environments at the SWAI; and the *Treptichnus* Ichnocoenosis representative of environments just above the SWAI.

4. The Soldier Summit and Spanish Fork Canyon Eocene GRF specimens most closely match what is currently known from the Parachute Creek Member of the GRF. Compared with other ancient lacustrine settings, the Eocene GRF invertebrate ichnofossils most closely compare with Cretaceous Jinju Formation of Korea, whereas bird ichnofossils most closely compare with the Eocene Laguna Brava Formation.

5. A new Cochlichnus Ichnofacies was erected and assigned to the Eocene GRF, representing periaquatic environments in low energy settings. The Cochlichnus Ichnofacies is composed of vertebrate, invertebrate, and rhizolith traces intimately related to the SWAI and is based on trace-fossil assemblages and lithofacies associations in the GRF and similar continental shoreline deposits.

REFERENCES

Ainsworth, R. B., S. T. Hasiotis, K. J. Amos, C. B. E. Krapf, T. H. D. Payenberg, M. L. Sandstrom, B. K. Vakarelov, & S. C. Lang. 2012. Tidal signatures in an intracratonic playa lake: GEOLOGY 40:607–610.

Alpert, S. P., & J. N. Moore. 1975. Lower Cambrian trace fossil evidence for predation on trilobites: Lethaia 8(3):223–230.

Anderson, A. M. 1975. Turbidites and arthropod trackways in the Dwyka glacial deposits (Early Permian) of southern Africa: Transactions of the Geological Society of South Africa 78:265–273.

Anderson, A. 1976. Fish trails from the Early Permian of South Africa: Palaeontology 19:397–409.

Aramayo, S. A., & T. Manera de Bianco. 1987. Hallazgo de una icnofauna continental (Pleistoceno tardío) en la localidad de Pehuén-Co (partido de Coronel Rosales), provincia de Buenos Aires, Argentina. Parte II. Carnivora, Artiodactyla y Aves, IV Congreso Latinoamericano de Paleontología, Santa Cruz de la Sierra, Bolivia. p. 532–547.

Azpeitia-Moros, F. 1933. Conchas bivalvas de agua dulce de España y Portugal. Tomos 1 y 2: Memorias del Instituto Geológico y Minero de España. 762 p.

Azuma, Y., Y. Arakawa, Y. Tomida, & P. J. Currie. 2002. Early Cretaceous bird tracks from the Tetori Group, Fukui Prefecture, Japan: Memoir of the Fukui Prefectural Dinosaur Museum 1:1–6.

Bader, J. W. 2009. Structural and tectonic evolution of the Douglas Creek arch, the Douglas Creek fault zone, and environs, northwestern Colorado and northeastern Utah: Rocky Mountain Geology 44:121–145.

Bednarczyk, W., & T. Przybyłowicz. 1980. On the development of Middle Cambrian sediments in the Gdańsk Bay area: Acta Geologica Polonica 30(4):391–415, 24 pl.

Benner, J. S., J. C. Ridge, & N. K. Taft. 2008. Late Pleistocene freshwater fish (Cottidae) trackways from New England (USA) glacial lakes and a reinterpretation of the ichnogenus *Broomichnium* Kuhn: Palaeogeography, Palaeoclimatology, Palaeoecology 260:375–388.

Berg, M. D. V. 2008. Basin-wide Evaluation of the Uppermost Green River Formation's Oil-shale Resource, Uinta Basin, Utah and Colorado: Utah Geological Survey. 19 p.

Berger, W. 1957. Eine spiralförmige Lebensspur aus dem Rupel der bayrischen Beckenmolasse. Neues Jahrbuch für Geologie und Paläontologie Monatshefte 1957:538–540.

Billings, E. 1862. On some new species of fossils from different parts of the Lower, Middle, and Upper Silurian rocks of Canada, Palaeozoic fossils, Volume 1:1861–1865. Geological Survey of Canada Advance Sheets. p. 96–168.

Birkeland, P. W. 1999. Soils and Geomorphology. Oxford University Press. New York. 430 p.

Blackstone, D. L., Jr. 1983. Laramide compressional tectionics, southeastern Wyoming: Contributions to Geology, University of Wyoming 22:1–38.

Blakey, R. C., & W. Ranney. 2008. Ancient landscapes of the Colorado Plateau (Grand Canyon): Grand Canyon Association. 176 p.

Bohacs, K. M., S. T. Hasiotis, & T. M. Demko. 2007. Continental Ichnofossils of the Green River andWasatch Formations, Eocene,Wyoming: A Preliminary Survey, Proposed Relation to Lake–Basin Type, and Application to Integrated Paleo–Environmental Interpretation: The Mountain Geologist 44:79–108.

Bohn, S., L. Pauchard, & Y. Couder. 2005. Hierarchical crack pattern as formed by successive domain divisions. Physical Review E 71 046214. 7 p.

Bottjer, D. J., J. W. Hagadorn, & S. Q. Dornbos. 2000. The Cambrian substrate revolution: GSA Today 10:1–7.

Bradley, W. H. 1931. Origin and microfossils of the oil shale of the Green River Formation of Colorado and Utah. United States Government Printing Office. Washington, D. C. 58 p.

Brady, L. F. 1947. Invertebrate tracks from the Coconino Sandstone of northern Arizona: Journal of Paleontology 21:466–472.

Bromley, R. G. 1996. Trace fossils: biology, taphonomy and applications 2nd Edition. Chapman & Hall. London. 361 p.

Bromley, R., & U. Asgaard. 1979. Triassic freshwater ichnocoenoses from Carlsberg Fjord, east Greenland: Palaeogeography, Palaeoclimatology, Palaeoecology 28:39–80.

Brown, R. W. 1934. Celliforma spirifer, the fossil larval chambers of mining bees: Journal of the Washington Academy of Sciences 24:532– 539.

Buatois, L. A., G. Jalfin, & F. G. Aceñolaza. 1997. Permian nonmarine invertebrate trace fossils from southern Patagonia, Argentina: ichnologic signatures of substrate consolidation and colonization sequences: Journal of Paleontology 71:324–336.

Buatois, L. A., & M. G. Mángano. 1993. The ichnotaxonomic status of *Plangtichnus* and *Treptichnus*: Ichnos: An International Journal of Plant & Animal 2:217–224.

Buatois, L. A., & M. G. Mángano. 1995. The paleoenvironmental and paleoecological significance of the lacustrine Mermia ichnofacies: an archetypical subaqueous nonmarine trace fossil assemblage: Ichnos 4:151–161.

Buatois, L. A., & M. G. Mángano. 1998. Allostratigraphic and sedimentologic applications of trace fossils to the study of incised estuarine valleys: An example from the Virgilian Tonganoxie Sandstone member of eastern Kansas: Current Research in Earth Sciences 241:1–27.

Buatois, L. A., & M. G. Mángano. 2002. Trace fossils from Carboniferous floodplain deposits in western Argentina: implications for ichnofacies models of continental environments: Palaeogeography, Palaeoclimatology, Palaeoecology 183:71-86.

Buatois, L.A. and Mángano, M.G. (2003). Caracterización icnológicay paleoambiental de la localidad tipo de Orchesteropus atavus, Huerta de Huachi, provincia de San Juán, Argentina: AMEGHINIANA 40:53–70.

Buatois, L. A., & M. G. Mángano. 2004. Animal-substrate interactions in freshwater environments: applications of ichnology in facies and sequence stratigraphic analysis of fluvio-lacustrine successions. *In* D. McIlroy, ed., The Application of Ichnology to Palaeoenvironmental and Stratigraphic Analysis. Geological Society, London, Special Publications 228. p. 311–333.

Buatois, L. A., & M. G. Mángano. 2011. Ichnology: organism-substrate interactions in space and time. Cambridge University Press. New York. 358 p.

Buatois, L. A., M. G. Mángano, C. G. Maples, & W. P. Lanier. 1998. Taxonomic reassessment of the ichnogenus *Beaconichnus* and additional examples from the Carboniferous of Kansas, U.S.A: Ichnos 5(4):287–302.

Buatois, L. A., M. G. Mángano, W. Xiantao, & Z. Guocheng. 1995. *Vagorichnus*, a new ichnogenus for feeding burrow systems and its occurrence as discrete and compound ichnotaxa in Jurassic lacustrine turbidtes of Central China: Ichnos: An International Journal for Plant and Animal Traces 3:265–272.

Butts, E. 1891. Recently discovered foot-prints of the amphibian age, in the Upper Coal Measure Group of Kansas City, Missouri: Kansas City Scientist 5:17–19.

Cashion, W. B., 1995. Stratigraphy of the Green River Formation, eastern Uinta Basin, Utah and Colorado – A summary. *In* W. R. Averett, ed., The Green River Formation in Piceance Creek and eastern Uinta Basins. Grand Junction Geological Society. Grand Junction, Colorado. p. 15–21.

Carmona, N. B., M. G. Mángano, L. A. Buatois, & J. J. Ponce. 2010. Taphonomy and paleoecology of the bivalve trace fossil *Protovirgularia* in deltaic heterolithic facies of the Miocene Chenque formation, Patagonia, Argentina: Journal of Paleontology 84(4):730–738.

Chamberlain, C. K. 1971. Morphology and ethology of trace fossils from the Ouachita Mountains, southeast Oklahoma: Journal of Paleontology 45(2):212–246.

Chamberlain, C. K. 1975. Trace Fossils in DSDP Cores of the Pacific: Journal of Paleontology 49(6):1074–1096.

Chisholm, J. I. 1985. Xiphosurid burrows from the lower coal measures (Westphalian A) of West Yorkshire: Palaeontology 28(4):619–628.

Cockerell, T. D. A. 1921. Eocene insects from the Rocky Mountains: Proceedings of the U.S. National Museum 59:29–38.

Cohen, A. S. 2003. Paleolimnology: The history and evolution of lake systems: Oxford University Press. New York. 500 p.

Cope, E. D. 1884. The Vertebrata of the Tertiary formations of the west: Repon U.S. Geological Survey ofthe Territories 3:l-1009.

Covacevich, V., & C. Lamperein. 1970. Hallazgo de icnitas en Península Fildes, Isla Rey Jorge, Archipiélago Shetland del Sur, Antartica: Instituto Antartico Chile o, ser. Científica 1:55–74.

Crews, S. G., & F. G. Ethridge. 1993. Laramide tectonics and humid alluvial fan sedimentation, NE Uinta Uplift, Utah and Wyoming: Journal of Sedimentary Research 63:420–436.

Crimes, T. P., & M. M. Anderson. 1985. Trace Fossils from Late Precambrian-Early Cambrian Strata of Southeastern Newfoundland (Canada): Temporal and Environmental Implications: Journal of Paleontology 59(2): 310–343.

Currie, P. L. 1981. Bird footprints from the Gething Formation (Aptian, Lower Cretaceous) of northeastern British Columbia, Canada: Journal of Vertebrate Paleontology 1:257-264.

Curry, H. D. 1957. Fossil tracks of Eocene vertebrates, southwestern Uinta Basin, Utah. Guidebook to the Geology of the Uinta Basin: Eighth Annual Field Conference. p. 42–47.

D'Alessandro, A., & R. G. Bromley. 1987. Meniscate trace fossils and the Muensteria-Taenidium problem: Palaeontology 30(4):743–763.

Dalman, S. G., & S. G. Lucas. 2015. Lower Jurassic arthropod resting trace from the Hartford Basin of Massachusetts, USA: Ichnos 22(3–4): 177–182.

Danjon, F., H. Sinoquet, C. Godin, F. Colin, & M. Drexhage. 1999. Characterisation of structural tree root architecture using 3D digitsing and AMAPmod software: Plant and Soil 220:241–258.

Davies, N. S., A. G. Liu, M. R. Gibling, & R. F. Miller. 2016. Resolving MISS conceptions and misconceptions: a geological approach to sedimentary surface textures generated by microbial and abiotic processes: Earth-Science Reviews 154:210–246.

Dawson, J. W. 1873. Impressions and footprints of aquatic animals and imitative markings on Carboniferous rocks: American Journal of Science (25):16–24.

Demanet, F. & V. van Straelen. 1938. Faune Houillère de la Belgique. *In* A. Renier, F. Stockmans, F. Demanet, & V. van Straelen, eds., Flore et Faune Houillères de la Belgique. Musée Royal d'Histoire Naturelle de Belgique. p. 99–246.

Desai, B. G., S. J. Patel, R. Shukala, & D. Surve. 2008. Analysis of ichnoguilds and their significance in interpreting ichnological events: a study from Jhuran Formation (Upper Jurassic), Western Kachchh: Journal Geological Society of India 72:458–466.

De Gibert, J. M., M. A. Fregenal-Martínez, L. A. Buatois, & M. G. Mángano. 2000. Trace fossils and the paleoecological significance in Lower Cretaceous lacustrine conservation deposits, El Montsec, Spain: Palaeogeography, Palaeoclimatology, Palaeoecology 156:89–101.

De Quatrefages, M. A. 1849. Note sur Scolicia prisca (A. de Q.), annelide fossile de la craie: Annales des Sciences Naturelles, 3, Zoologie 12:265–266.

De Stefani, C. 1885. Studi paleozoologici sulle creta superiore e media dell'Appennino settentrionale: Memorie della Classe di Scienze Fisiche, Matematiche e Naturali 4(1):73–121.

De Valais, S., & R. N. Melchor. 2008. Ichnotaxonomy of bird–like footprints: an example from the Late Triassic–Early Jurassic of northwest Argentina: Journal of Vertebrate Paleontology 28:145–159.

Dickinson, W. R., M. A. Klute, M. J. Hayes, S. U. Janecke, E. R. Lundin, M. A. McKittrick, & M. D. Olivares. 1988. Paleogeographic and paleotectonic setting of Laramide sedimentary basins in the central Rocky Mountain region: Geological Society of America Bulletin 100:1023–1039.

Díaz-Martinez, I., O. Suarez-Hernando, B. Martinez-Garcia, J. M. Hernandez, S. G. Fernandez, F. Perez-Lorente, & X. Murelaga. 2015. Early Miocene shorebird-like footprints from the Ebro Basin, La Rioja, Spain: paleoecological and paleoenvironmental significance: PALAIOS 30:424–431.

Dittmer, H. J. 1949. Root hair variations in plant species: American Journal of Botony 36(2):152–155.

Doyle, P., J. L. Wood, & G. T. George. 2000. The shorebird ichnofacies: an example from the Miocene of southern Spain: Geological Magazine 137:517–536.

Droser, M. L., S. Jensen, J. G. Gehling, P. M. Myrow, & G. M. Narbonne. 2002. Lowermost Cambrian Ichnofabrics from the Chapel Island Formation, Newfoundland: Implications for Cambrian Substrates, PALAIOS 17:3–15.

Dyni, J. R. 2006. Geology and resources of some world oil shale deposits: U.S. Geological Survey Scientific Investigations Report 2005-5294, 42 p.

Ehrenberg, K. 1944. Ergänzende Bemerkungen zu den seinerzeit aus dem Miozän von Burgschleinitz beschriebenen Gangkernen und Bauten dekapoder Krebse: Palaeontologishe Zeitschrift 23:354–359.

Ekdale, A. A. 1988. Pitfalls of paleobathymetric interpretations based on trace fossil assemblages: PALAIOS 3:464–472.

Ekdale, A. A., R. G. Bromley, & D. B. Loope. 2007. Ichnofacies of an ancient erg: A climatically influenced trace fossil association in the Jurassic Navajo Sandstone, southern Utah, USA. *In* W. Miller III, ed., Trace fossils: concepts, problems, prospects. Elsevier. Amsterdam. p. 562–574.

Ekdale, A. A., R. G. Bromley, & S. G. Pemberton. 1984. Ichnology: The Use of Trace Fossils in Sedimentology and Stratigraphy. SEPM Short Course 15. Tulsa, Oklahoma. 317 p.

Elbroch, M., & E. Marks. 2001. Bird tracks & sign: A guide to North American species. Stackpole Books. Mechanicsburg. 456 p.

Ellenberger, P. 1972. Contribution à la classification des pistes de Vertebres du Trias: les types du Stormberg d'Afrique du Sud. I. Palaeovertebrata, Memoire Extraordinaire, Montpellier. 104 p.

Elliot, R. E. 1985. An interpretation of the trace fossil *Cochlichnus kochi* (Ludwig) from the East Pennine Coalfield of Britain: Proceedings of the Yorkshire Geological Society 45:183–187.

Emmons, E. 1844. The Taconic System: Based on Observations in New York, Massachusetts, Maine, Vermont and Rhode Island. Carroll and Cook Printers. Albany, New York. 68 p.

Erickson, B. R. 1967. Fossil bird tracks from Utah: Museum Observer 5:6–12.

Falk, A. R., S. T. Hasiotis, E. Gong, J.-D. Lim, & E. D. Brewer. 2017. A new experimental setup for studying avian neoichnology and the effects of grain size and moisture content on tracks: trails using the domestic chicken (*Gallus gallus*): PALAIOS 32(11):689–707.

Falk, A. R., S. T. Hasiotis, & L. D. Martin. 2010. Feeding Traces Associated with Bird Tracks from the Lower Cretaceous Haman Formation, Republic of Korea: PALAIOS 25:730–741.

Falk, A. R., L. D. Martin, & S. T. Hasiotis, 2011. A morphologic criterion to distinguish bird tracks: Journal of Ornithology 152:701–716.

Fenton, C. L., & M. A. Fenton. 1937a. Burrows and trails from Pennsylvanian rocks of Texas:

American Midland Naturalist, 18(6):1079–1084.

Fenton, C. L., & M. A. Fenton. 1937b. *Olivellites*, a Pennsylvanian Snail Burrow: American Midland Naturalist, 18(3):452–453.

Fillion, D., & R. K. Pickerill. 1990. Ichnology of the Upper Cambrian? to Lower Ordovician Bell Island and Wabana groups of eastern Newfoundland, Canada: Calgary: Canadian Society of Petroleum Geologists. 119 p.

Fitch, A. 1850. A historical, topographical and agricultural survey of the County of Washington. Part 2–5: Transactions of the New York Agricultural Society 9:753–944.

Foster, J. R. 2001. Salamander tracks (*Ambystomichnus*?) from the Cathedral Bluffs Tongue of the Wasatch Formation (Eocene), northeastern Green River Basin, Wyoming: Journal of Paleontology 75:901–904.

Frey, R. W., & J. D. Howard. 1981. *Conichnus* and *Schaubcylindrichnus*: Redefined Trace Fossils from the Upper Cretaceous of the Western Interior: Journal of Paleontology 55(4):800–804.

Frey, R. W., & S. G. Pemberton. 1987. The *Psilonichnus* ichnocoenoses and its relationship to adjacent marine and nonmarine ichnocoenoses along the Georgia coast: Bulletin of Canadian Petroleum Geology 35:333–357.

Frey, R. W., S. G. Pemberton, & J. A. Fagerstrom. 1984. Morphological, ethological, and environmental significance of the ichnogenera *Scoyenia* and *Ancorichnus*: Journal of Paleontology 58:511–528.

Frey, R. W., & A. Seilacher. 1980. Uniformity in marine invertebrate ichnology: Lethaia 13:183–207.

Fuchs, T. 1895. Studien über Fucoiden und Hieroglyphen: Akademie der Wissenschaften zu Wien, mathematisch-naturwissen-schaftliche Classe, Denkschriften 62:369–448.

Furniss, G., J. F. Rittel, & D. Winston. 1998. Gas bubble and expansion crack origin of “molar-tooth” calcite structures in the Middle Proterozoic Belt Supergroup, western Montana: Journal of Sedimentary Research 68(1):104–114.

Garvey, J. M., & S. T. Hasiotis. 2008. An ichnofossil assemblage from the Lower Carboniferous Snowy Plains Formation, Mansfield Basin, Australia: Palaeogeography, Palaeoclimatology, Palaeoecology 258:257–276.

Germs, G. J. B. 1972. Trace Fossils from the Nama Group, South-West Africa: Journal of Paleontology 46(6):864–870.

Getty, P. R., & A. M. Bush. 2017. On the ichnotaxonomic status of *Haplotichnus indianensis* (Miller, 1889): Ichnos 0:1–5.

Getty, P. R., T. D. McCarthy, S. Hsieh, & A. M. Bush. 2016. A new reconstruction of continental *Treptichnus* based on exceptionally preserved material from the Jurassic of Massachusetts: Journal of Paleontology 90:269–278.

Getty, P. R., R. Sproule, M. R. Stimson, & P. C. Lyons. 2017. Invertebrate trace fossils from the Pennsylvanian Rhode Island Formation of Massachusetts, USA: Atlantic Geology 53:185–206.

Gibbard, P. L. 1977. Fossil tracks from varved sediments near Lammi, South Finland.

Gibbard, P. L., & A. J. Stuart. 1974. Trace fossils from proglacial lake sediments: Boreas 3:69–74.

Gilmore, C. W. 1926. Fossil footprints from the Grand Canyon: Smithsonian Miscellaneous Collections 77:1–41.

Gilmore, C. W. 1938. Fossil snakes of North America: Geological Society of America Special Papers 9:1–96.

Gingras, M. K., K. L. Bann, J. A. MacEachern, & S. G. Pemberton. 2007. A Conceptual Framework for the Application of Trace Fossils. In J. A. MacEachern, K. L. Bann, M. K. Gingras, and S. G. Pemberton, eds., Applied Ichnology: SEPM Short Course Notes 52. SEPM 52:1–26.

Głuszek, A. 1995. Invertebrate trace fossils in the continental deposits of an Upper Carboniferous coal–bearing succession, Upper Silesia, Poland: Studia Geologica Polonica 108:171–202.

Grande, L. 1984. Paleontology of the Green River Formation, with a review of the fish fauna. The Geological Survey of Wyoming. Laramie, Wyoming. 333 p.

Grande, L., & H. P. Buchheirn. 1994. Paleontological and sedimentological variation in early Eocene Fossil Lake: Contributions to Geology 30:33–56.

Hakes, W. G. 1977. Trace fossils in Late Pennsylvanian cyclothems, Kansas. *In* T. P. Crimes, and J. C. Harper, eds., Trace Fossils 2: Proceedings from the 25th International Geological Conference. Geological Journal. Special Issue 9. p. 209–226.

Haldeman, S. S. 1840. Supplement to number one of "A monograph of the Limniades, or freshwater univalve shells of North America": Containing decriptions of apparently new animals in different classes and the names and characters of the subgenera in *Paludina* and *Anculosa*. J. Dobson. Philadelphia. 3 p.

Hall, J. 1847. Palaeontology of New York. Volume I. Containing descriptions of the organic remains of the Lower Division of of the New York System (equivalent of the Lower Silurian rocks of Europe). C. van Benthuysen. Albany, New York. 338 p.

Hallam, A. 1970. *Gyrochorte* and other trace fossils in the Forest Marble (Bathonian) of Dorset, England. *In* T. P. Crimes, & J. C. Harper, eds., Trace fossils. Geological Journal Special Publication 3:189–200.

Hamer, J. M. M., & N. D. Sheldon. 2010. Neoichnology at lake margins: implications for paleo-lake systems: Sedimentary Geology 228:319–327.

Hammersburg, S. R., S. T. Hasiotis, & R. A. Robison. 2018. Ichnotaxonomy of the Cambrian Spence Shale Member of the Langston Formation, Wellsville Mounttains, northern Utah, USA: Paleontological Contributions. 260 manuscript pages.

Han, Y., & R. K. Pickerill. 1994. Taxonomic reassessment of Protovirgularia M'Coy 1850 with new examples from the Paleozoic of New Brunswick, eastern Canada: Ichnos: An International Journal of Plant & Animal 3:203–212.

Häntzschel, W. 1975. Trace Fossils and Problematica. *In* C. Teichert, ed., Treatise on Invertebrate Paleontology. Part W: Miscellanea (Supplement 1). University of Kansas

Press and Geological Society of America. Lawrence, Kansas & Boulder, Colorado. 269 p.

Hasiotis, S. T. 2002. Continental Trace Fossils. SEPM Short Course 51. Tulsa, Oklahoma. 132 p.

Hasiotis, S. T. 2003. Complex ichnofossils of solitary an social soil organisms: understanding their evolution and roles in terrestrial ecosystems: Palaeogeography, Palaeoclimatology, Palaeoecology 192:259–320.

Hasiotis, S. T. 2004. Reconnaissance of Upper Jurassic Morrison Formation ichnofossils, Rocky Mountain Region, USA: paleoenvironmental, stratigraphic, and paleoclimatic significance of terrestrial and freshwater ichnocoenoses: Sedimentary Geology 167:177–268.

Hasiotis, S. T. 2007. Continental ichnology: fundamental processes and controls on trace fossil distribution. *In* W. M. III, ed., Trace fossils: concepts, problems, prospects. Elsevier. Amsterdam. p. 262–278.

Hasiotis, S. T. 2008. Reply to the Comments by Bromley et al. of the paper “Reconnaissance of the Upper Jurassic Morrison Formation ichnofossils, Rocky Mountain Region, USA: Paleoenvironmental, stratigraphic, and paleoclimatic significance of terrestrial and freshwater ichnocoenoses” by Stephen T. Hasiotis: Sedimentary Geology 208:61–68.

Hasiotis, S. T., W. Cressler, & J. R. Beerbower. 1999. Terrestrial and freshwater ichnofossils as soil biota proxies in Devonian ecosystems: A major transformation in the organization of Lower Paleozoic continental ecosystems: Geologcial Society of America Northeast Section Meeting, Providence, Rhode Island 31:22.

Hasiotis, S. T., J. I. Kirkland, G. W. Windscheffel, & C. Safris. 1998. Fossil caddisfly cases (Insecta: Trichoptera), Upper Jurassic Morrison Formation, Fruita Paleontological Area, Colorado: Modern Geology 22:493–502.

Hasiotis, S. T., M. J. Kraus, & T. M. Demko. 2007. Chapter 11 – Climatic controls on continental trace fossils. *In* W. Miller, ed., Trace Fossils: Concepts, Problems, Concepts. Elsevier. Amsterdam. p. 172–195.

Hasiotis, S. T., J. G. McPherson, & M. R. W. Reilly. 2013. Using ichnofossils to reconstruct the depositional history of sedimentary successions in alluvial, coastal-plain, and deltaic settings: International Petroleum Technology Conference 17016. 48 p.

Hasiotis, S. T., & C. E. Mitchell. 1993. A comparison of crayfish burrow morphologies: Triassic and Holocene fossil, paleo- and neo-ichnological evidence, and the identification of their burrowing signatures: Ichnos: An International Journal of Plant & Animal 2:291–314.

Hasiotis, S., & B. Platt. 2012. Exploring the sedimentary, pedogenic, and hydrologic factors that control the occurrence and role of bioturbation in soil formation and horizonation in continental deposits: An integrative approach: The Sedimentary Record 10:4–9.

Hasiotis, S. T., B. F. Platt, D. I. Hembree, & M. J. Everheart. 2007. The Trace-Fossil Record of Vertebrates, Trace Fossils: Concepts, Problems, Prospects. Elsevier Press. Amsterdam. p. 196–218.

Hasiotis, S. T., B. F. Platt, M. Reilly, K. Amos, S. Lang, D. Kennedy, J. A. Todd, & E. Michel. 2012. Actualistic studies of the spatial and temporal distribution of terrestrial and aquatic organism traces in continental environments to differentiate lacustrine from fluvial,

eolian, and marine deposits in the geologic record. *In* O. W. Baganz, Y. Bartov, K. M. Bohacs, and D. Nummedal, eds., Lacustrine sandstone reservoirs and hydrocarbon systems. AAPG Memoir 95. p. 433–489.

Heer, O. 1864–1865. Die urwelt der Schweiz. F. Schulthess. Zürich. 622 p.

Heer, O. 1877. Flora fossilis Helvetiae. Die Vorweltliche Flora der Schweiz. Wurster, Zürich. 182p.

Heinberg, C. 1973. The internal structure of the trace fossils *Gyrochorte* and *Curvolithus*: Lethaia 6:227–238.

Hiscott, R. N., N. P. James, & S. G. Pemberton. 1984. Sedimentology and ichnology of the Lower Cambrian Bradore Formation, coastal Labrador: fluvial to shallow-marine transgressive sequence: Bulletin of Canadian Petroleum Geology 32(1):11–26.

Hitchcock, E. 1858. Ichnology of New England: a Report on the Sandstone of the Connecticut Valley Especially Its Fossil Footmarks Made to the Government of the Commonwealth of Massachusetts. White. Boston. 220 p.

Hitchcock, E. 1865. Supplement to the Ichnology of New England: A Report to the Government of Massachusetts, in 1863. Wright & Potter. Boston. 96 p.

Hofmann, R., M. G. Mángano, O. Elicki, & R. Shinaq. 2012. Paleoecologic and biostratigraphic significance of trace fossils from shallow-to marginal-marine environments from the middle Cambrian (Stage 5) of Jordan: Journal of Paleontology 86(6):931–955.

Huh, H., I. S. Paik, C. H. Chung, J. B. Park, & B. S. Kim. 2001. Dinosaur tracks from Islands in Yeosu, Jeollanam-do, Korea: Journal of the Geological Society of Korea 37:653–658.

Huh, M., I. S. Paik, Y.-K. Ko, K. S. Kim, K.-H. Pack, C. H. Cheong, & K. G. Hwang. 2002. A Research Report on the Yeosu Dinosaur Sites, Korea: Korea Dinosaur Research Center, Chonnam National University and Yeosu City, Kwangju, Korea. 350 p.

Huh, M., M. G. Lockley, K. S. Kim, J. Y. Kim, & S.-G. Gwak. 2012. First Report of Aquatilavipes from Korea: New Finds from Cretaceous Strata in the Yeosu Islands Archipelago: Ichnos: An International Journal for Plant and Animal Traces 19:43-49.

Hwang, K.-G., M. Huh, M. G. Lockley, D. M. Unwin, & J. L. Wright. 2002. New pterosaur tracks (Pteraichnidae) from the Late Cretaceous Uhangri Formation, southwestern Korea: Geological Magazine 139:421–435.

Jackson, A. M., S. T. Hasiotis, & P. P. Flaig. 2016. Ichnology of a Paleopolar, River-Dominated, Shallow Marine Deltaic Succession in the Mackellar Sea: The Mackellar Formation (Lower Permian), Central Transantarctic Mountains, Antarctica: Palaeogeography, Palaeoclimatology, Palaeoecology 441(2):266–291.

Jaeger, E. 1946. Tracks and trailcraft. Macmillan. New York. 381 p.

James, U. P. 1879. Description of new species of fossils and remarks on some others, from the Lower and Upper Silurian rocks of Ohio: Palaeontologist 3:17–24.

Jensen, S. 1997. Trace fossils from the Lower Cambrian Mickwitzia sandstone, south-central Sweden. Fossils and Strata 42. Scandinavian University Press. Oslo. 111 p.

Jensen, S. 2001. *Conichnus* Männil 1966, not *Conichnus* Myannil 1966: Ichnos: An International Journal for Plant and Animal Traces 8:141–142.

Jepsen, G. L. 1966. Early eocene bat from Wyoming: Science 154:1333–1339.

Johnson, R. C. 1985. Early Cenozoic history of the Uinta and Piceance Creek basins, Utah and Colorado, with special reference to the development of Eocene Lake Uinta. *In* R. M. Flores, S. S. Kaplan, eds., Cenozoic Paleogeography of the West-Central United States. Denver, Colorado. p. 247–276.

Jones, M., & S. T. Hasiotis. 2018. Terrestrial behavior and trackway morphology of Neotropical bats: Acta Chiropterologica 20. 50 manuscript pages.

Keighley, D., S. Flint, J. Howell, & A. Moscariello. 2003. Sequence stratigraphy in lacustrine basins: a model for part of the Green River Formation (Eocene), southwest Uinta Basin, Utah, U.S.A.: Journal of Sedimentary Research 73(6):987–1006.

Keighley, D. G., & R. K. Pickerill. 1995. Commentary: The ichnotaxa *Palaeophycus* and *Planolites*: Historical perspectives and recommendations: Ichnos 3(4):301–309.

Keighley, D. G., & R. K. Pickerill. 1998. Systematic ichnology of the Mabou and Cumberland groups (Carboniferous) of western Cape Breton Island, eastern Canada, 2: surface markings: Atlantic Geology 34(2):83–112.

Kim, B. K. 1969. A study of several sole marks in the Haman Formation: 지질학회지 5:243–258.

Kim., J. Y., D. G. Keighley, R. K. Pickerill, W. Hwang, & K.-S. Kim. 2005. Trace fossils from marginal lacustrine deposits of the Creataceous Jinju Formation, souther coast of Korea: Palaeogeography, Palaeoclimatology, Palaeoecology 218:105–124.

Kim, J. Y., M. G. Lockley, S. J. Seo, K. S. Kim, S. H. Kim, & K. S. Baek. 2012. A paradise of Mesozoic birds: the world's richest and most diverse Cretaceous bird track assemblage from the Early Creataceous Haman Formation of the Gajin Tracksite, Jinju, Korea: Ichnos 19:28–42.

Kordos, L. 1985. Footprints in the Lower Miocene sandstone of Ipolytarnóc: Geologica Hungarica 46:257–415.

Kordos, L., & P. Prakfalvi. 1990. Újabb adatok az európai neogén Lábnyomos rétegek ismeretéhez. [A contribution to the knowledge of Neogene beds with footprints marks in Europe]. Àll. Földtani Intézet évi Jelentèse az 1988, vol. I. Amsterdam. p. 201- 212.

Krapovickas, V., P. L. Ciccioli, M. G. Mángano, C. A. Marsicano, & C. O. Limarino. 2009. Paleobiology and paleoecology of an arid–semiarid Miocene South American ichnofauna in anastomosed fluvial deposits: Palaeogeography, Palaeoclimatology, Palaeoecology 284(3):129–152.

Kraus, M., & S. T. Hasiotis. 2006. Significance of different modes of rhizolith preservation to interpreting paleoenvironmental and paleohydrologic settings: examples from Paleogene paleosols, Bighorn Basin, Wyoming, U.S.A.: Journal of Sedimentary Research 76:663–646.

Krestew, K. 1928. Über das Carbon des Iskur-Défilés in Bulgarien und seine Altersstellung: Jahrbuch der Koniglich Preussischen Geologischen Landesanstalt und Bergakademie zu Berlin 49:551–579.

Książkiewicz, M. 1970. Observations on the ichnofauna of the Polish Carpathians. *In* T.P. Crimes, C. Harper, eds., Trace Fossils. Geological Journal Special Issue 3:283-322.

Książkiewicz, M. 1977. Trace fossils in the flysch of the Polish Carpathians: Palaeontologia Polonica 36:1–270.

Lamond, R. E., & L. Tapanila. 2003. Embedment cavities in lacustrine stromatolites: evidence of animal interactions from Cenozoic carbonates in U.S.A. and Kenya: PALAIOS 18:445–453.

Langston, W., Jr., & H. Rose. 1978. A yearling crocodilian from the middle Eocene Green River Formation of Colorado: Journal of Paleontology:122–125.

Lanier, W. P., H. R. Feldman, & A. W. Archer. 1993. Tidal sedimentation from a fluvial to estuarine transition, Douglas Group, Missourian–Vergilian, Kansas: Journal of Sedimentary Petrology 63:860–873.

Leggitt, V. L., R. E. Biaggi, & H. P. Buchheim. 2007. Palaeoenvironments associated with caddisfly-dominated microbial-carbonate mounds from the Tipton Shale Member of the Green River Formation: Eocene Lake Gosiute: Sedimentology 54:661–669.

Leggitt, V. L., & R. A. Cushman. 2001. Complex caddisfly-dominated bioherms from the Eocene Green River Formation: Sedimentary Geology 145:337–396.

Leggitt, V. L., & M. A. Loewen. 2002. Eocene Green River Formation "*Oocardium* tufa" reinterpreted as complex arrays of calcified caddisfly (Insecta: Trichoptera) larval cases: Sedimentary Geology 148:139–146.

Lerner, A. J., & S. G. Lucas. 2015. A *Selenichnites* ichnoassociation from early Permian tidal flats of the prehistoric trackways national monument of south-central New Mexico. *In,* S. G. Lucas and W. A. DiMichele, eds., Carboniferous-Permian Transition in the Robledo Mountains, Southern New Mexico. New Mexico Museum of Natural History and Science Bulletin 65. p. 141–152.

Lesquereux, L. 1876. Species of fossil marine plants from the Carboniferous measures: Geological Survey of Indiana Annual Report 7:134–145.

Lim, J.-D., Z. Zhou, L. D. Martin, K.-S. Baek, & S.-Y. Yang. 2000. The oldest known tracks of web-footed birds from the Lower Creataceous of South Korea: Naturwissenschaften 87:256–259.

Linck, O., 1949. Lebens-spuren aus dem Schilfsandstein (Mittl. Keuper km 2) NW-Wurttembergs und ihre Bedeutung fur die Bildungsgeschichte der Stufe. Verein für vaterländische Naturkunde in Württemberg 97–101:1–1000.

Lockley, M. G., & J. D. Harris. 2010. On the trail of early birds: A review of the fossil footprint record of avian morphological and behavioral evolution. *In* P.K. Ulrich and J.H. Willett, eds., Trends in Ornithology Research. Nova Science Publishers, Inc. New York. p. 1–63.

Lockley, M. G., K. Houck, S.-Y. Yang, M. Matsukawa, & S.-K. Lim. 2006. Dinosaur-dominated footprint assemblages from the Cretaceous Jindong Formation, Hallyo Haesang National Park area, Goseong County, South Korea: evidence and implications: Cretaceous Research 27(1):70-101.

Lockley, M. G., M. Huh, S.-K. Lim, S.-Y. Yang, & D. Unwin. 1997. First report of pterosaur tracks from Asia, Chollanam Province Korea: Journal of the Paleontological Society of Korea, Special Publication 2:17–32.

Lockley, M. G., A. P. Hunt, & C. Meyer. 1994. Vertebrate Tracks and the Ichnofacies Concept: Implications for paleoecology and palichnostratigraphy. *In* S. K. Donovan, ed., The Paleobiology of Trace Fossils. John Hopkins. Baltimore. p. 242–268.

Long, E. E. 1965. Stratigraphy of the Ohio Range, Antarctica. *In* J. B. Hadley, ed., Geology and Paleontology of the Antarctic. Antarctic Research Series, v. 6, A.G.U. Publiciation 1299. Washington. p. 71–116.

Loope, D. B. 1988. Rhizoliths in ancient eolianites: Sedimentary Geology 56:301–314.

Lucas, S. G., A. J. Lerner, M. Bruner, & P. Shipman. 2004. Middle Pennsylvanian ichnofauna from eastern Oklahoma, USA: Ichnos 11:45–55.

Lucas, S. G., & G. E. Schultz. 2007. Miocene vertebrate footprints from the Texas panhandle. *In* S. G. Lucas, J. A. Spielmann, and M. G. Lockley, eds., Cenozoic Vertebrate Tracks and Traces. New Mexico Museum of Natural History and Science Bulletin 42. Albuquerque. p. 177–183.

Lull, R. S. 1915. Triassic life of the Connecticut Valley: State of Connecticut, State Geological and Natural History Survey Bulletin 24:1–285.

MacEachern, J. A., S. G. Pemberton, M. K. Gingras, & K. L. Bann. 2007. The ichnofacies paradigm: a fifty-year retrospective. *In* W. Miller, ed., Trace Fossils: Concepts, Problems, Prospects. Elsevier p. 172–195.

MacEachern, J. A., I. Raychaudhuri, & S. G. Pemberton. 1992. Stratigraphic applications of the Glossifungites Ichnofacies: delineating discontinuities in the rock record. *In* S. G. Pemberton, ed., Applications of Ichnology to Petroleum Exploration. Society of Economic Palaeontologies and Mineralogists, Core Workshop 17. p. 169–198.

Mack, G. H., W. C. James, & H. C. Monger. 1993. Classification of paleosols: Geologcal Society of America Bulletin 105:129–136.

MacNaughton, R. B. 2003. Planispiral burrows from a Recent lacustrine beach, Gander Lake Newfoundland: Canadian Field-Naturalist 117(4):577–581.

Macsotay, O. 1967. Huellas problematicas y su valor paleoecologico en Venezuela: Geos 16:7–79.

Mángano, M. G., L. A. Buatois, C. G. Maples, & W. P. Lanier. 1997. *Tonganoxichnus*, a new insect trace fossil from the Upper Carboniferous of eastern Kansas, USA: Lethaia 30:113–125.

Mángano, M. G., L. A. Buatois, & A. K. Rindsberg. 2003. Carboniferous *Psammichnites*: systematic re-evaluation, taphonomy and autecology: Ichnos 9:1–22.

Männil, R. M. 1966. O vertikalnykh norkakh zaryvaniya v Ordovikskikh izvestnyakakh Pribaltiki [A small vertically excavated cavity in Baltic Ordovician limestone]. *In* R. F. Hecker, ed., Organizm i sreda v geologischeskom proshlom. Paleontologicheskiy Institut. Akademiya Nauk SSSR. 1966, p. 200–207.

Mansilla, H. G., S. de Valais, W. Stinnesbeck, N. A. Varela, & M. A. Leppe. 2012. New Avian tracks from the lower to middle Eocene at Fossil Hill, King George Island, Antarctica: Antarctic Science 24:500–506.

Martin, A. J. 2009. Neoichnology of an Arctic fluvial point bar, North Slope, Alaska (USA): Geological Quarterly, 53:383–396.

Martin, A. J., G. M. Vazquez–Prokopec, & M. Page. 2010. First known feeding trace of the eocene bottom–dwelling fish Notogoneus osculus and its paleontological significance: PLoS One 5:1–8.

Matthew, G. F. 1903. An attempt to classify Palaeozoic batrachian footprints: Transactions of the Royal Society of Canada 2 (9) 4:109–121.

McCoy, F. 1850. On some genera and species of Silurian Radiata in the collection of the University of Cambridge: Annals and Magazine of Natural History, Series 2 6:270–290.

McCrea, R.T., & W. A. S. Sarjeant. 2001. New Ichnotaxa of Bird and Mammal Footprints from the Lower Cretaceous (Albian) Gates Formation of Alberta. Mesozoic Vertebrate Life. Indiana University Press. p. 453–478.

Mehl, M. G. 1931. Additions to the vertebrate record of the Dakota Sandstone: American Journal of Science 21:441–452.

Melchor, R. N. 2004. Trace fossil distribution in lacustrine deltas: examples from the Triassic rift lakes of the Ischigualasto-Villa Unión basin, Argentina. *In* D. McIlroy, ed., The Application of Ichnology to Palaeoenvironmental and Stratigraphic Analysis. Geological Society Special Publications 228. London. p. 335–354.

Melchor, R. N., E. Bedatou, S. de Valais, & J. F. Genise. 2006. Lithofacies distribution of invertebrate and vertebrate trace–fossil assemblages in an Early Mesozoic ephemeral fluvio–lacustrine system from Argentina: Implications for the Scoyenia ichnofacies: Palaeogeography, Palaeoclimatology, Palaeoecology 239:253–285.

Melchor, R. N., R. Buchwaldt, & S. Bowring. 2013. A Late Eocene date for Late Triassic bird tracks: Nature 495:E1–E2.

Melchor, R. N., M. C. Cardonatto, & G. Visconti. 2012. Palaeonvironmental and palaeoecological significance of flamingo-like footprints in shallow-lacustrine rocks: an example from the Oligocene–Miocene Vinchina Formation, Argentina: Palaeogeography, Palaeoclimatology, Palaeoecology 315-316:181–198.

Melchor, R. N., S. de Valais, & J. F. Genise. 2002. Bird–like fossil footprints from the Late Triassic: Nature 417:936–938.

Melchor, R. N., S. de Valais, & J. F. Genise. 2013. Retraction: Bird–like fossil footprints from the Late Triassic: Nature 501:262.

Metz, R. 1981. Why not raindrop impressions?: Journal of Sedimentary Petrology 51(1):0265–0268.

Metz, R. 1987. Sinusoidal trail formed by a recent biting midge (family Ceratopogonidae): trace fossil implications: Journal of Paleontology 61:312–314.

Metz, R. 1998. Nematode trails from the late Triassic of Pennyslvania: Ichnos: An International Journal form Plant and Animal Traces 5:303–308.

Metz, R. 2000. Triassic trace fossils from lacustrine shoreline deposits of the Passaic Formation, Douglassville, Pennsylvania: Ichnos: An International Journal for Plant and Animal Traces 7:253–266.

Michelau, P. 1955. *Belorhaphe kochi* (Ludwig 1869), eine Wurmspur im europaischen Karbon: Geologische Jahrbuch 71:299–33.

Miller, S. A. 1889. North American Geology and Paleontology-for the use of Amateurs, Students and Scientists. 664 p.

Miller, S. A., & C. B. Dyer. 1878. Contributions to paleontology, no. 1: Journal of the Cincinnati Society of Natural History 1:24–39.

Minter, N. J., M. G. Lockley, M. Huh, K.-G. Hwang, & J. Y. Kim. 2012. *Lithographus,* an abundant arthropod trackway from the Cretaceous Haenam tracksite of Korea: Ichnos: An International Journal for Plant and Animal Traces 19:115–120.

Morgan, G. S., & T. E. Williamson. 2007. Middle Miocene (Late Barstovian) mammal and bird tracks from the Benavidez Ranch local fauna, Zia Formation, Albuquerque Basin, Sandoval County, New Mexico. *In* S. G. Lucas, J. A. Spielmann, M. G. Lockley, eds., Cenozoic Vertebrate Tracks and Traces. New Mexico Museum of Natural History and Science Bulletin 42. Albuquerque. p. 319–330

Moussa, M. T. 1968. Fossil Tracks from the Green River Formation (Eocene) near Soldier Summit, Utah: Journal of Paleontology 42:1433–1438.

Moussa, M. T. 1970. Nematode fossil trails from the Green River Formation (Eocene) in the Uinta Basin, Utah: Journal of Paleontology 44:304–307.

Muñiz Guinea, F., M. G. Mángano, L. A. Buatois, V. Podeniene, J. A. Gámez Vintaned, & E. Mayoral Alfaro. 2014. Compound biogenic structures resulting from ontogenetic variation: An example from a modern dipteran: Spanish Journal of Paleontology 29:83–94.

Munsell Color (firm). 2009. Munsell soil-color charts with genuine Munsell® color chips. Munsell Color. Grand Rapids.

Mustoe, G. E. 2002. Eocene Bird, Reptile, and Mammal Tracks from the Chuckanut Formation, Northwest Washington: PALAIOS 17:403–413.

Narbonne, G. M., & J. D. Aitken. 1990. Ediacaran fossils from the Sekwi Brook area, Mackenzie mountains, northwestern Canada: Palaeontology 33(4):945–980.

Nicholson, H. A. 1873. Contributions to the study of the errant annelides of the older Palaeozoic rocks: Royal Society of London Proceedings 21:288–290.

Noffke, N. 2010. Geobiology: Microbial mats in sandy deposits from the Archean Era to today. Springer-Verlag. Heidelberg. 194 p.

Nopsca, F. B. 1923. Die Familien der Reptilien: Fortschritte der Geologie und Palaèontologie 2:1–210.

Olson, S. L. 1977. A Lower Eocene Frigatebird from the Green River Formation of Wyoming (Pelecaniformes: Fregatidae): Smithsonian Contributions To Paleobiology 35:1–33.

Olson, S. L. 2014. Tracks of a Stilt–Like Bird from the Early Eocene Green River Formation of Utah: Possible Earliest Evidence of the Recurvirostridae (Charadriiformes): Waterbirds 37:340–345.

Panin, N., & E. Avram. 1962. Noi urme de vertebrate in Miocenul Subcarpatilor Rominesti: Studii si Cercetari de Geologie 7:455–484.

Parizot, M., P. G. Eriksson, T. Aifa, S. Sarkar, S. Banerjee, O. Catuneanu, W. Altermann, A. J. Bumby, E. M. Bordy, J. L van Rooy, & A. J. Boshoff. Suspected microbial mat-related crack-like sedimentary structures in the Palaeoproterozoic Magaliesberg Formation sandstones, South Africa: Precambrian Research 138:274-296.

Pazos, P. J. 2002. Palaeoenvironmental framework of the glacial-postglacial transition (Late Paleozoic), in the Paganzo-Calingasta basin (southern South America) and the great Karoo-Kalahari basin (southern Africa): ichnological implications: Gondwana Research 5:619–640.

Pemberton, S. G., & R. W. Frey. 1982. Trace fossil nomenclature and the *Planolites*-*Palaeophycus* dilemma: Journal of Paleontology 56(4):843–881.

Pemberton, S. G., & R. W. Frey. 1985. The Glossifungites ichnofacies: modern examples from the Georgia coast, USA. *In* H. A. Curran, ed., Biogenic Structures: Their Use in Interpreting Depositional Environments. Society of Economic Paleontologists and Mineralogists, Special Publications 35. Tulsa, Oklahoma. p. 237-259.

Pemberton, S. G., R. W. Frey, & R. G. Bromley. 1988. The ichnotaxonomy of *Conostichus* and other plug-shaped ichnofossils: Canadian Journal of Earth Sciences 25(6):866–892.

Pemberton, S. G., & B. Jones. 1988. Ichnology of the Pleistocene Ironshore Formation, Grand Cayman Island, British West Indies: Journal of Paleontology 62(4):495–505.

Pemberton, S. G., M. Spila, A. J. Pulham, T. Saunders, J. A. MacEachern, D. Robbins, & I. K. Sinclair. 2001. Ichnology and sedimentology of shallow to marginal marine systems: Ben Nevis and Avalon reservoirs, Jeanne d'Arc Basin. Geological Association of Canada Short Course Notes 15. 343 p.

Pickerill, R. K., & L. R. Fyffe. 1999. The stratigraphic significance of trace fossils from the Lower Paleozoic Baskahegan Lake Formation near Woodstock, west-central New Brunswick: Atlantic Geology 35:205–214.

Poschmann, M. 2015. The corkscrew-shaped trace fossil *Helicodromites* Berger, 1957, from Rhenish Lower Devonian shallow-marine facies (Upper Emsian; SW Germany): Paläontologische Zeitschrift 89(3):635–643.

Prantl, F. 1945. Dve záhadné zkamenliny (stopy) z vrstev chrustenických—dδ2: Rozpravy II, Třidy Ceské Akademie 55(1):3–8.

Pregitzer, K. S., J. L. DeForest, A. J. Burton, M. F. Allen, R. W. Ruess, & R. L. Hendrick. 2002. Fine root architectrure of nine North American trees: Ecological Monographs 72(2):293–309.

Retallack, G. J., 2001. Soils of the past: an introduction to paleopedology, 2nd edition. Blackwell Science. Oxford. 512 p.

Retrum, J. B., S. T. Hasiotis, & R. L. Kaesler. 2011. Neoichnological experiments with the freshwater ostracode *Heterocypris incongruens*: Implications for reconstructing aquatic settings PALAIOS 26(8):509–518.

Richter, R. 1937. Marken und Spuren aus allen Zeiten, I–II: Senckenbergiana 19:150–169.

Ride, W. D. L., C. W. Sabrosky, G. Bernardi, & R. V. Melville. 1985. International Code of Zoological Nomenclature. Third Edition. International Trust for Zoological Nomenclature and British Museum (Natural History). London. 338 p.

Rindsberg, A. K., & D. C. Kopaska-Merkel. 2005. *Treptichnus* and *Arenicolites* from the Steven C. Minkin Paleozoic footprint site (Langsettian, Alabama, USA): Pennsylvanian Footprints in the Black Warrior Basin of Alabama: Alabama Paleontological Society Monograph 1:121–141.

Robison, R. A. 1991. Middle Cambrian biotic diversity: examples from four Utah Lagerstätten. *In* A. M. Simonetta, & S. Conway Morris, eds., The early evolution of Metazoa and the significance of problematic taxa. Cambridge University Press. Cambridge. p. 77–98.

Roehler, H. W., J. H. Hanley, & J. G. Honey. 1988. Geology of the Cottonwood Creek Delta in the Eocene Tipton Tongue of the Green River Formation, southeast Washakie Basin, Wyoming: US Geological Survey Bulletin 1669. 14 p.

Romano, M. & M. A. Whyte. 1990. *Selenichnites*, a new name for the ichnogenus *Selenichnus* Romano and Whyte, 1987: Proceedings of the Yorkshire Geological Society 48:221.

Salter, J. W. 1857. On Annelide-burrows and Surface-markings from the Cambrian Rocks of the Longmynd. No. 2: Quarterly Journal of the Geological Society 13(1-2):199–206.

Sarjeant, W. A. S., & W. Langston, Jr. 1994. Vertebrate footprints and invertebrate traces from the Chadronian (Late Eocene) of Trans–Pecos TX: Texas Memorial Museum Bulletin 36. 86 p.

Sarjeant, W., R. Reynolds, & M. Kissell-Jones. 2002. Fossil creodont and carnivore footprints from California, Nevada, and Wyoming. *In* R. E. Reynolds, ed., Between the Basins: Exploring the Western Mojave and Southern Basin and Range Province. California State University, Desert Studies Consortium. Fullerton. p. 37–50.

Sarjeant, W. A. S., & R. E. Reynolds. 2001. Bird Footprints from the Miocene of California. *In* R.E. Reynolds, ed., The Changing Face of the East Mojave Desert. California State University, Desert Studies Consortium. Fullerton, California. p. 21–40.

Sarkar, S., P. Samanta, & W. Altermann. 2011. Setulfs, modern and ancient: formative mechanism, preservation bias and palaeoenvironmental implications: Sedimentary Geology 238:71–78.

Schaetzl, R., & S. Anderson. 2005. Soils: Genesis and Geomorphology. Cambridge University Press. New York. 817 p.

Schwarzbach, M. 1938. Tierfährten aus eiszeitlichen Bändertonen: Zeitschrift für Geschiebeforschung und Flachlandsgeologie 14:143–152.

Scott, J. J., & M. E. Smith. 2015. Trace Fossils of the Eocene Green River Lake Basins, Wyoming, Utah, and Colorado. *In* M. E. Smith and A. R. Carroll, eds., Stratigraphy and Paleolimnology of the Green River Formation, Western USA. Springer. Netherlands. p. 313–350.

Scudder, S. H. 1890a. Physiognomy of the American Tertiary Hemiptera: Proceedings of the Boston Society of Natural History 24:562–579.

Scudder, S. H. 1890b. The tertiary insects of North America: US Government Printing Office. 734 p.

Seilacher, A. 1953. Studien zur palichnologie. I. über die methoden der palichnologie: Neues Jahrbuch für Geologie und Paläontologie, Abhandlungen 96:421–452.

Seilacher, A. 1955a. 4. Spuren und Lebensweise der Trilobiten. In O. H. Schindewolf, & A. Seilacher, eds., Beiträge zur Kenntnis des Kambriums in der Salt Range (Pakistan). Akademie der Wissenschaften und der Literatur zu Mainz, mathematisch-naturwissenschftliche Klasse, Abhandlungen 10:342–372.

Seilacher, A. 1955b. 5. Spuren und Fazies im Unterkambrium. *In* O. H. Schindewolf, and A. Seilacher, eds., Beiträge zur Kenntnis des Kambriums in der Salt Range (Pakistan). Akademie der Wissenschaften und der Literatur zu Mainz, mathematisch-naturwissenschaftliche Klasse, Abhandlungen 10:373–399.

Seilacher, A. 1963. Lebensspuren und Salinitatsfazies: Fortschritte in der Geologic Rheinland und Westfalens 10:81–94.

Seilacher, A. 1967. Bathymetry of trace fossils: Marine geology 5(5-6):413–428.

Seilacher, A. 2007. Trace fossil analysis. Springer. Berlin Heidelberg. 226 p.

Seilacher, A., & C. Hemleben. 1966. Beitrage zur sedimentation und fossilsfuhrung des Hunsrucksciefers 14. Spurenfaunau nd Bildungstiefe der Hunsruckschiefer (Unterdevon): Notizblatt des HessischenL andesamtes fur Bodenforschungz u Wiesbaden 94:40–53.

Seilacher, A. T., & E. Seilacher. 1994. Bivalvian trace fossils: a lesson from actuopaleontology: Courier Forschungsinstitut Senckenberg 169:5–15.

Shrock, R. R. 1948. Sequence in layered rocks: a study of features and structures useful for determining top and bottom or order of succession in bedded and tabular rock bodies. McGraw-Hill. New York. 507 p.

Smith, J. J., S. T. Hasiotis, M. J. Kraus, & D. T. Woody. 2008a. Relationship of floodplain ichnocoenoses to paleopedology, paleohydrology, and paleoclimate in the Willwood Formation, Wyoming, during the Paleocene–Eocene Thermal Maximum: PALAIOS 23:683–699.

Smith, J. J., S. T. Hasiotis, M. J. Kraus, & D. T. Woody. 2008b. Naktodemasis bowni: new ichnogenus and ichnospecies for adhesive meniscate burrows (AMB), and paleoenvironmental implications, Paleogene Willwood Formation, Bighorn Basin, Wyoming: Journal of Paleontology 82(2):267–278.

Smith, J. J., S. T. Hasiotis, M. J. Kraus, & D. T. Woody. 2009. Transient dwarfism of soil fauna during the Paleocene–Eocene Thermal Maximum: Proceedings of the National Academy of Sciences 106:17655–17660.

Smith, M. E., A. R. Carroll, & B. S. Singer. 2008. Synoptic reconstruction of a major ancient lake system: Eocene Green River Formation, western United States: GSA Bulletin 120(1–2):54–84.

Song, J. Y. 2010. Reinterpretation of unusual Uhangri dinosaur tracks from the view of functional morphology: Journal of the Paleontological Society of Korea 26: 95–105.

Stokes, W. L. 1957. Pteradactyl tracks from the Morrison Formation: Journal of Paleontology 31:952–954.

Stokes, W. L. 1978. Impressions of lizard scales from the Green River Formation (Eocene), Uinta Basin, Utah: Journal of Paleontology. p. 407–410.

Tasch, P. 1968. A Permian trace fossil from the Antarctic Ohio Range: Transactions of the Kansas Academy of Science 71:33–37.

Thulborn, T. 2004. Extramorphological features of sauropod dinosaur tracks in the Uhangri Formation (Cretaceous), Korea: Ichnos: An International Journal for Plant and Animal Traces 11: 295–298.

Torell, O. M. 1870. Petrificata Suecana Formationis Cambricae: Lunds Universitets Arsskrift 6:1–14.

Twenhofel, W. H. 1921. Impressions made by bubbles, rain-drops, and other agencies: Bulletin of the Geological Society of America 32:359–372.

Uchman, A. 1998. Taxonomy and ethology of flysch trace fossils: a revision of the Marian Książkiewicz collection and studies of complementary material: Annales Societatis Geologorum Poloniae 68:105–218.

Uchman, A. 1999. Ichnology of the Rhenodanubian Flysch (Lower Cretaceous–Eocene) in Austria and Germany: Beringeria 25:67–173.

Uchman, A. 2005. *Treptichnus*-like traces made by insect larvae (Diptera: Chironomidae, Tipulidae). *In* R. J. Buta, A. K. Rindsberg, D. C. Kopaska-Merkel, eds., Pennsylvanian Footprints in the Black Warrior Basin of Alabama. Alabama Paleontological Society Monograph No. 1. 143–146 p.

Uchman, A., R. G. Bromley, & S. Leszczyński. 1998. Ichnogenus *Treptichnus* in Eocene flysch, carpathians, Poland: Taxonomy and preservation: Ichnos 5(4):269–275.

Uchman, A., V. Kazakauskas, & A. Gaigalas. 2009. Trace fossils from Late Pleistocene varved lacustrine sediments in eastern Lithuania: Palaeogeography, Palaeoclimatology, Palaeoecology 272:199–211.

Uchman, A., M. Pika-Biolzi, & P. A. Hochuli. 2004. Oligocene trace fossils from temporary fluvial plain ponds: An examble from the Freshwater Molasse of Switzerland: Eclogae Geologicae Helvetiae 97(1):133–148.

Vannier, J., I. Calandra, C. Gaillard, & A. Żylińska. 2010. Priapulid worms: Pioneer horizontal burrowers at the Precambrian-Cambrian boundary: Geology 38(8):711–714.

Voigt, S., S. G. Lucas, & K. Krainer. 2013. Coastal-plain origin of trace-fossil bearing red beds in the Early Permian of soutehrn New Mexico: Palaeogeography, Palaeoclimatology, Palaeoecology 369:323–334.

Vyalov, O. S. 1965. Stratigrafiya neogenovix molass Predcarpatskogo probiga: Naukova Dumka (Akademiya Nauk Ukrainskoy SSR Institut Geologii I Geokhimii Goryuchikh Iskopayemykh). Kiev. p. 165.

Vyalov, O. S. 1966. Sledy zhiznedeyatelnosti organizmov I ikh paleontologicheskoe znacheniye: Naukova Dumka (Akademiya Nauk Ukrainskoy SSR Institut Geologii I Geokhimii Goryuchikh Iskopayemykh). Kiev. p. 219.

Walter, V.H. 1985. Zur Ichnologie des Pleistozäns von Liebegast. Freiberger Forschungshefte. p. 101–116.

Weaver, J. E., & W. J. Himmel. 1929. Relation between the development of root systems and shoot under long-and short-day illumination: Plant physiology 4(4):435–457.

Weidmann, M., & M. Reichel. 1979. Traces de pattes d'oiseaux dans la Molasse suisse: Eclogae Geologicae Helvetiae 72:953–971.

Wetzel, R. G. 2001. Limnology: Lake and River Ecosystems, 3rd Edition. Academic Press. San Diego. 1006 p.

Whyte, M. A., & M. Romano. 2001. A dinosaur ichnocoenosis from the Middle Jurassic of Yorkshire, UK: Ichnos: An International Journal of Plant & Animal 8:223–234.

Wilson, J. P., J. P. Grotzinger, W. W. Fischer, K. P. Hand, S. Jensen, A. H. Knoll, J. Abelson, J. M. Metz, N. McLoughlin, P. A. Cohen, & M. M. Tice. 2012. Deep-water incised valley deposits at the Ediacaran-Cambrian Boundary in southern Namibia contain abundant *Treptichnus pedum*: PALAIOS 27(4):252–273.

Wulfsohn, D., & J. R. Nyengaard. 1999. Simple stereological procedure to estimate the number and dimensions of root hairs: Plant and Soil 209(1):129–136.

Yang, S. Y., M. G. Lockley, R. Greben, B. R. Erickson, & S.-K. Lim. 1995. Flamingo and duck–like bird tracks from the Late Cretaceous and Early Tertiary: evidence and implications: Ichnos 4:21–34.

Yaosong, X., S. Yanbin, & Z. Erjun. 1996. Petrological characteristics of the sedimentary volcaniclastic rocks of the Fossil Hill Formation (Eocene) in King George Island, West Antarctica: Antarctic Research 7:99–117.

Yochelson, E. L., & D. E. Schindel. 1978. A re-examination of Pennsylvanian trace fossil *Olivellites*: Journal of Research of the US Geological Survey 6(6):789–796.

Zawiskie, J. M., J. W. Collinson, & W. R. Hammer. 1983. Trace fossils of the Permian Triassic Takrouna Formation, northern Victoria Land, Antarctica. *In* R. L. Oliver, P. R. James, J. B. Jago, eds., Antarctic Earth Science. Australian Academy of Science and Cambridge University Press. Canberra. 215–220 p.

Zonneveld, J. P., M. K. Gingras, & T. W. Beatty. 2010. Diverse ichnofossil assemblages following the P-T mass extinction, Lower Triassic, Alberta and British Columbia, Canada: Evidence for shallow marine refugia on the northwestern coast of Pangaea: PALAIOS 25(6):368–392.

FIGURES AND FIGURE CAPTIONS

Figure 1. Map of middle Eocene Green River Formation; stars mark sample sites. Modified from Grande and Buchheim (1994).

Figure 2. Common bird foot morphotypes. *1*, Anisodactyl; *2*, Incumbent Anisodactyl; *3* Semipalmate; *4*, Zygodactyl; *5*, Palmate; *6*, Totipalmate. Numerals indicate digit number; lines between digits indicate webbing. Modified from Falk, Martin, and Hasiotis (2011).

Figure 3. Track and trackway measurements. *1*, Track measurements: W_t = Track Width, L_t = Track Length; *2*, Trackway Measurements: W_{tw} = Trackway Width; L_s = Stride Length; W_p = Pace Width; L_p = Pace Length, ϕ = Angle of divarication from trackway midline; M = trackway midline. Modified from Falk, Hasiotis, and Martin (2010).

Figure 4. Angle of divarication (AoD) track measurements: θ_1 = AoD between digits I and II, θ_2 = AoD between digits I and III, θ_3 = AoD between digits I and IV, θ_4 = AoD between digits II and III, θ_5 = AoD between digits II and IV, θ_6 = AoD between digits III and IV.

Figure 5. *Acanthichnus cursorius* (Ac), *Aulichnites parkerensis* (Ap), *Aulichnites tsouloufeidos* (At), *Avipeda phoenix* (Ax), *Cochlichnus anguineus* (Ca), *Cochlichnus plegmaeidos* (Cp), *Conichnus conichnus* (Cc), *Glaciichnium liebegastensis* (Gl), *Planolites montanus* (Pm), and rhizolith (Rz) specimens from the Eocene GRF. *1*, Rhizoliths and *Cochlichnus anguineus*, convex hyporelief, GC-C-11; *2*, rhizoliths, concave hyporelief, and *Planolites montanus*, convex hyporelief, GC-C-5; *3*, *Acanthichnus cursorius* and *Avipeda phoenix*, convex hyporelief, GC-C-15; *4*, *Aulichnites parkerensis*, *Aulichnites tsouloufeidos*, *Cochlichnus anguineus*, *Conichnus conichnus*, and *Glaciichnium liebegastensis*, convex hyporelief, GC-C-13; *5*, *Cochlichnus anguineus* turning, concave epirelief, GC-C-6; *6*, *Cochlichnus anguineus* and *Cochlichnus plegmaeidos*, convex hyporelief, GC-C-1.

Figure 6. *Cochlichnus anguineus* (Ca), *Conichnus conichnus* (Co), *Glaciichnium liebegastensis* (Gl), *Glaroseidosichnus gierlowskii* (Gg), *Planolites montanus* (Pm), *Protovirgularia dichotoma* (Pd), *Sagittichnus linki* (Sl), and *Treptichnus bifurcus* (Tb) specimens from the Eocene GRF. *1*, *Cochlichnus anguineus*, *Conichnus conichnus*, *Planolites montanus*, and *Treptichnus bifurcus*, convex hyporelief, GC-C-14; *2*, *Glaciichnium liebegastensis*, convex hyporelief, GC-C-13; *3*, *Cochlichnus anguineus* and *Glaroseidosichnus gierlowskii*, convex hyporelief, GC-C-16; *4*, *Cochlichnus anguineus* in convex hyporelief and *Planolites montanus*, concave and convex hyporelief, GC-C-5; *5*, *Protovirgularia dichotoma*, convex hyporelief, GC-C-15; *6*, *Cochlichnus anguineus* and *Sagittichnus linki*, convex hyporelief, and *Planolites montanus*, concave and convex hyporelief, GC-C-5.

Figure 7. *Alaripeda lofgreni* (Al), c.f. *Aquatilavipes* isp. (Aq), c.f. *Aviadactyla* isp. (Ad), *Aviadactyla vialovi* (Av), *Avipeda phoenix* (Ax), *Conichnus conichnus* (Cc), *Planolites montanus* (Pl), *Treptichnus bifurcus* (Tb), *Tr. pedum* (Tp), and *Tr. vagans* (Tv) specimens from the Eocene GRF, *1, Tr. bifurcus, Tr. pedum*, and *Tr. vagans*, concave epirelief, GC-C-9; *2, Tr. bifurcus*, convex hyporelief, GC-C-9; *3, Alaripeda lofgreni, Conichnus conichnus*, and *Planolites montanus*, convex hyporelief, GC-C-14; *4*, c.f. *Aquatilavipes* isp., convex hyporelief, GC-C-16; *5*, c.f. *Aviadactyla* isp., concave epirelief, GC-C-3; *6, Alaripeda lofgreni, Aviadactyla vialovi, Avipeda phoenix*, and *Planolites montanus*, convex hyporelief, GC-C-14.

Figure 8. *Avipeda phoenix* (Ax), *Fuscinapeda texana* (Ft), *Gruipeda fuenzalidae* (Gf), *Gruipeda gryponyx* (Gr), *Midorikawapeda semipalmatus* (Ms), and *Tsalavoutichnus leptomonopati* (Tl) specimens from the Eocene GRF. *1, Avipeda phoenix*, convex hyporelief, GC-C-15; *2, Fuscinapeda texana*, concave epirelief, GC-C-5; *3, Gruipeda fuenzalidae* with overstepping *Midorikawapeda semipalmatus*, convex hyporelief, GC-C-16; *4*, line drawing of *Gruipeda fuenzalidae* and *Midorikawapeda semipalmatus* in *2*; *5, Gruipeda gryponyx*, convex hyporelief, GC-C-6; *4, Gruipeda gryponyx*, convex hyporelief, GC-C-15; *6, Midorikawapeda semipalmatus* and *Tsalavoutichnus leptomonopati*, convex hyporelief, GC-C-2.

Figure 9. *Presbyorniformipes feduccii* (Pf) and *Tsalavoutichnus ericksonii* (Te) traces. *1, Pe. feduccii* and full length of sinuous *Ts. ericksonii*, convex hyporelief, GC-C-17; *2, Pe. feduccii* and *Ts. ericksonii*, cast of holotype slab, concave epirelief, GC-C-21; *3, Pe. feduccii* with scutellate webbing impressions and reticulate digit impressions, convex hyporelief, GC-C-4; *4, Pe. feduccii* scutellate webbing impressions and digit slip marks with scale lineations, concave epirelief, GC-C-8, arrows point to tuning-fork shaped impressions.

Figure 10. *Presbyorniformipes feduccii* (Pf) traces. *1*, *Pe. feduccii* track with scale patterns on webbing and bottom of digits; *2*, *Pe. feduccii* track with slip mark and scale patterns.

Figure 11. *Cochlichnus anguineus* (Ca), *Midorikawapeda semipalmatus* (Ms), raindrop traces, and microbial mat specimens from the Eocene GRF. *1*, *Midorikawapeda semipalmatus*, concave epirelief, and elephant skin texturing with dark coloration of a microbial mat, GC-C-20; *2*, *Cochlichnus anguineus* in convex epirelief and elephant skin texturing of a microbial mat, GC-C-13; *3*, rounded, overlapping raindrop traces, concave epirelief, GC-C-13; *4*, abiotic texturing, epirelief, GC-C-6.

Figure 12. GRF Ichnocoenoses below, at, and above the SWAI, with water depth maximum ~5 cm; traces include: *Acanthichnus cursorius* (Ac), *Alaripeda lofgreni* (Al), *Aquatilavipes* isp. (Aq), *Aulichnites parkerensis* (Ap), *Aviadactyla vialovi* (Av), *Avipeda phoenix* (Ax), *Cochlichnus anguineus* (Ca), *Conichnus conichnus* (Cc), *Fuscinapeda texana* (Ft), *Glaciichnium liebegastensis* (Gl), *Glaroseidosichnus gierlowskii* (Gg), *Gruipeda dominguensis* (Gr), *Midorikawapeda semipalmatus* (Ms), *Planolites montanus* (Pm), *Presbyorniformipes feduccii* (Pf), *Protovirgularia dichotoma* (Pd), rhizoliths (Rz), *Sagittichnus linki* (Sl), *Treptichnus bifurcus* (Tb), *Tr. pedum* (Tp), *Tr. vagans* (Tv), and *Tsalavoutichnus ericksonii* (Te). *1*, *Conichnus* ichnoceonosis; *2*, *Presbyorniformipes* ichnocoenosis; *3*, *Cochlichnus* ichnocoenosis; *4*, *Treptichnus* ichnocoenosis; *5*, Diagram of the ichnocoenoses occurring at the same time at various water depths, from ~5 cm to exposure; *6*, formation of the overlapping of trace assemblages over time due to short-term water fluctuations on GC-C-14 (hyporelief).

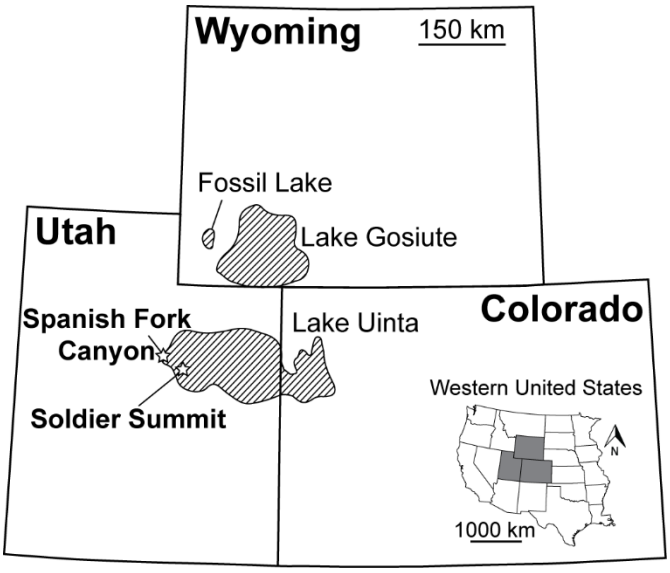
Wyoming
150 km
Fossil Lake
Lake Gosiute
Utah
Spanish Fork
Canyon
Soldier Summit
Lake Uinta
Colorado
Western United States
N
1000 km

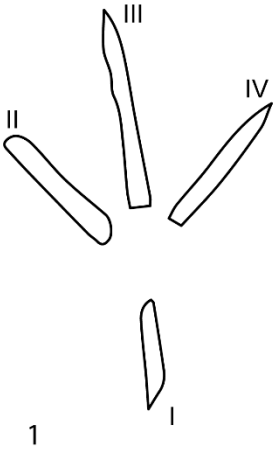

1

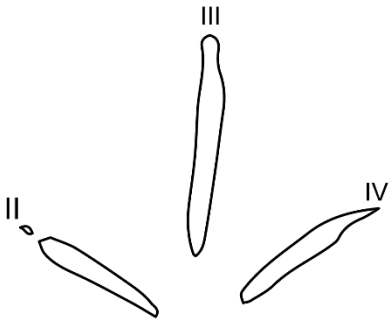

2

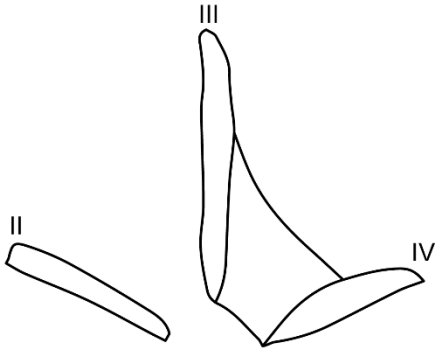

3

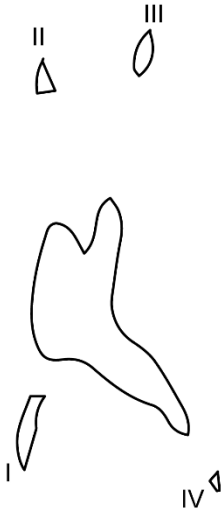

4

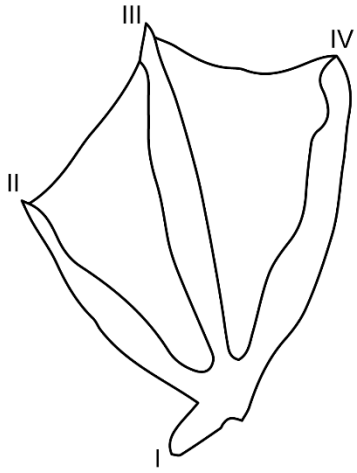

5

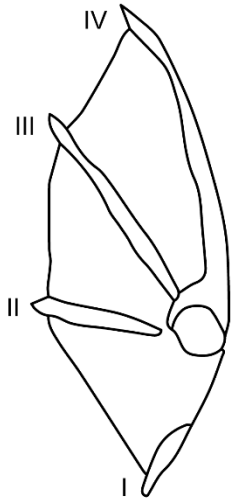

6

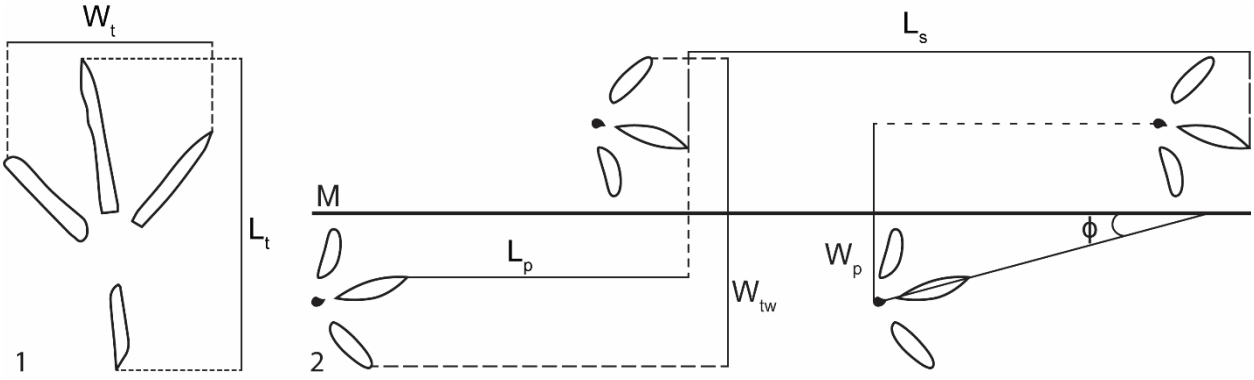
W_t
L_t
1
M
L_p
W_tw
2
L_s
W_p
ϕ

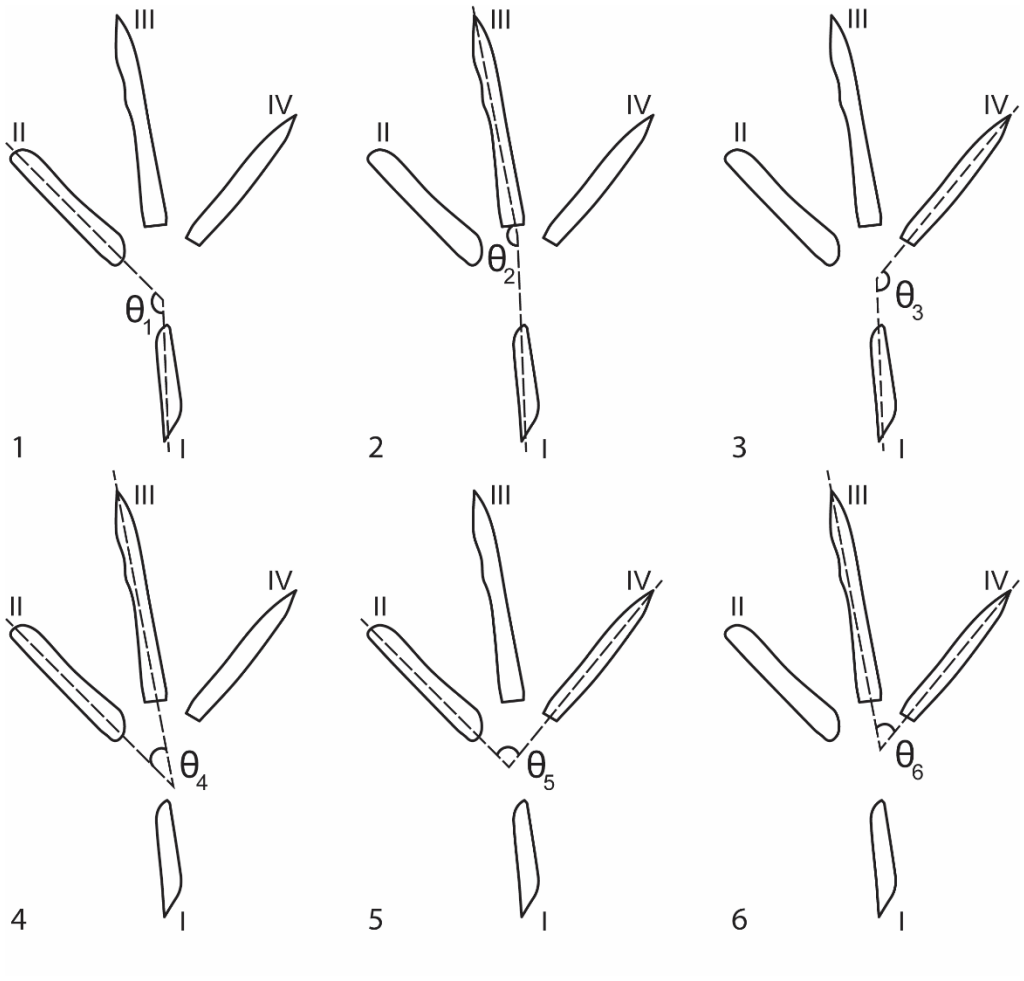
III
IV
II
θ1
I
1
III
IV
II
θ2
I
2
III
IV
II
θ3
I
3
III
IV
II
θ4
I
4
III
IV
II
θ5
I
5
III
IV
II
θ6
I
6

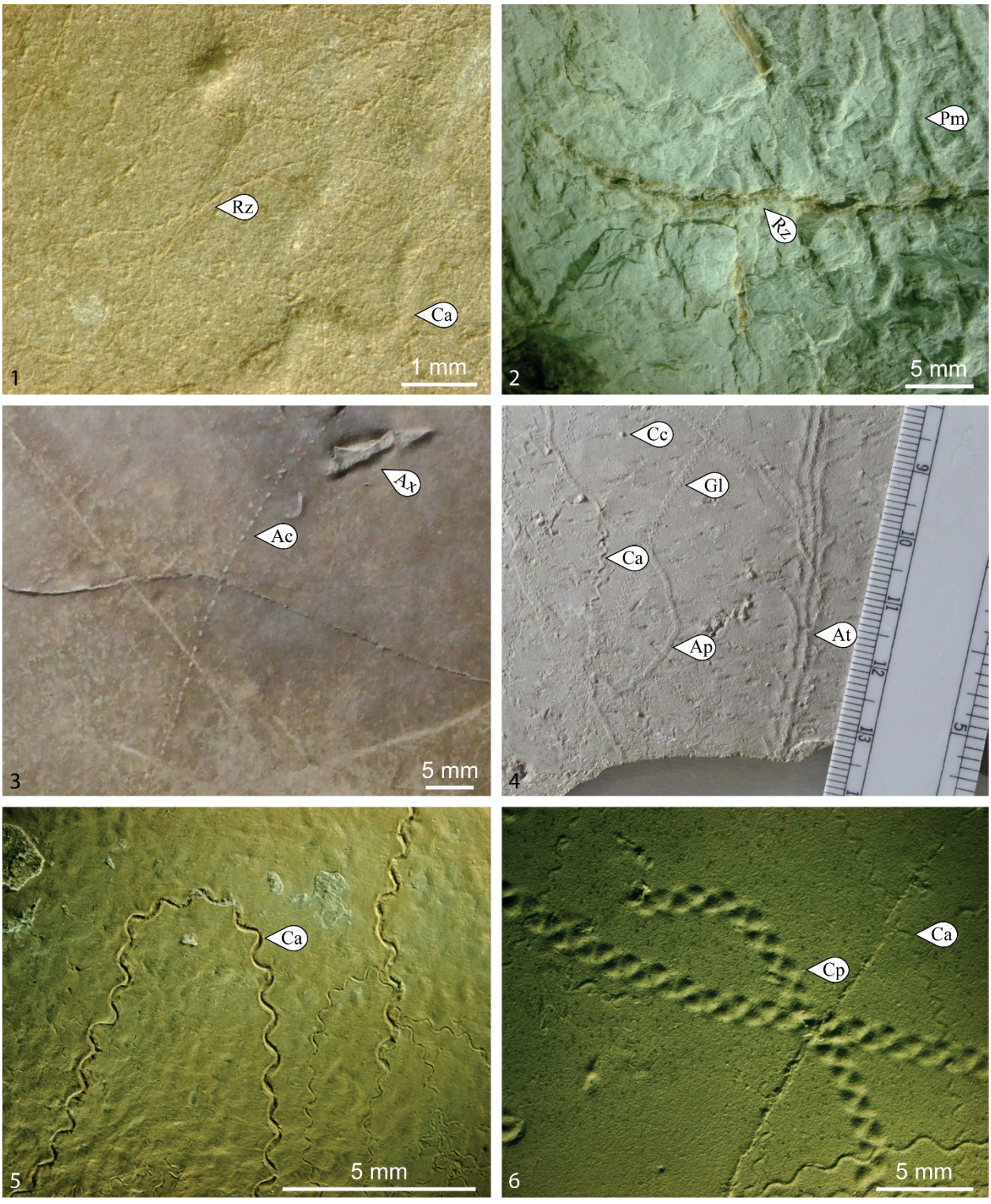
Rz
Ca
1 mm
1
Pm
Rz
5 mm
2
Ax
Ac
5 mm
3
Cc
Gl
Ca
Ap
At
4
Ca
5 mm
5
Ca
Cp
5 mm
6

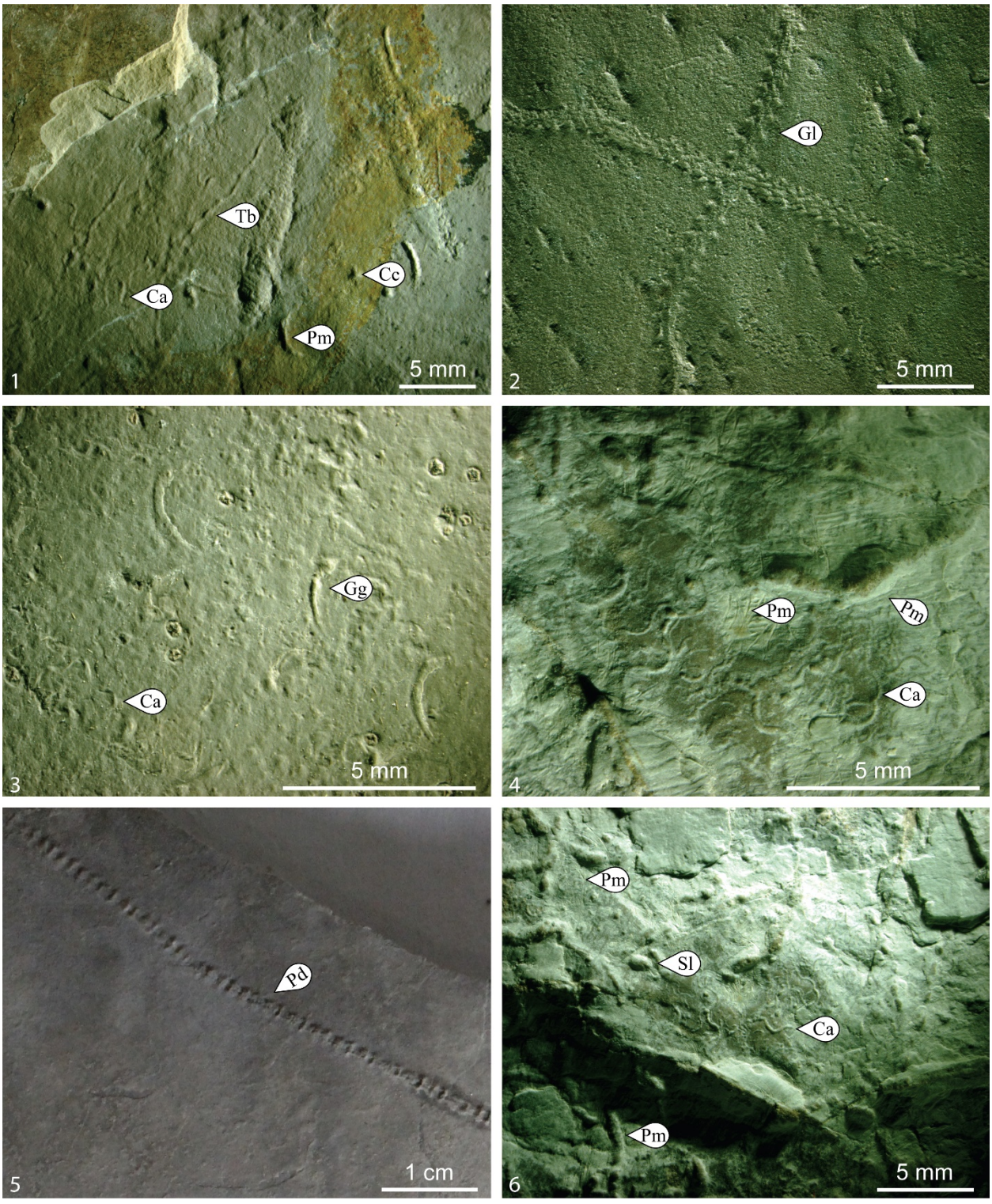
Tb
Cc
Ca
Pm
5 mm
1
Gl
5 mm
2
Gg
Ca
5 mm
3
Pm
Pm
Ca
5 mm
4
Pd
1 cm
5
Pm
Sl
Ca
Pm
5 mm
6

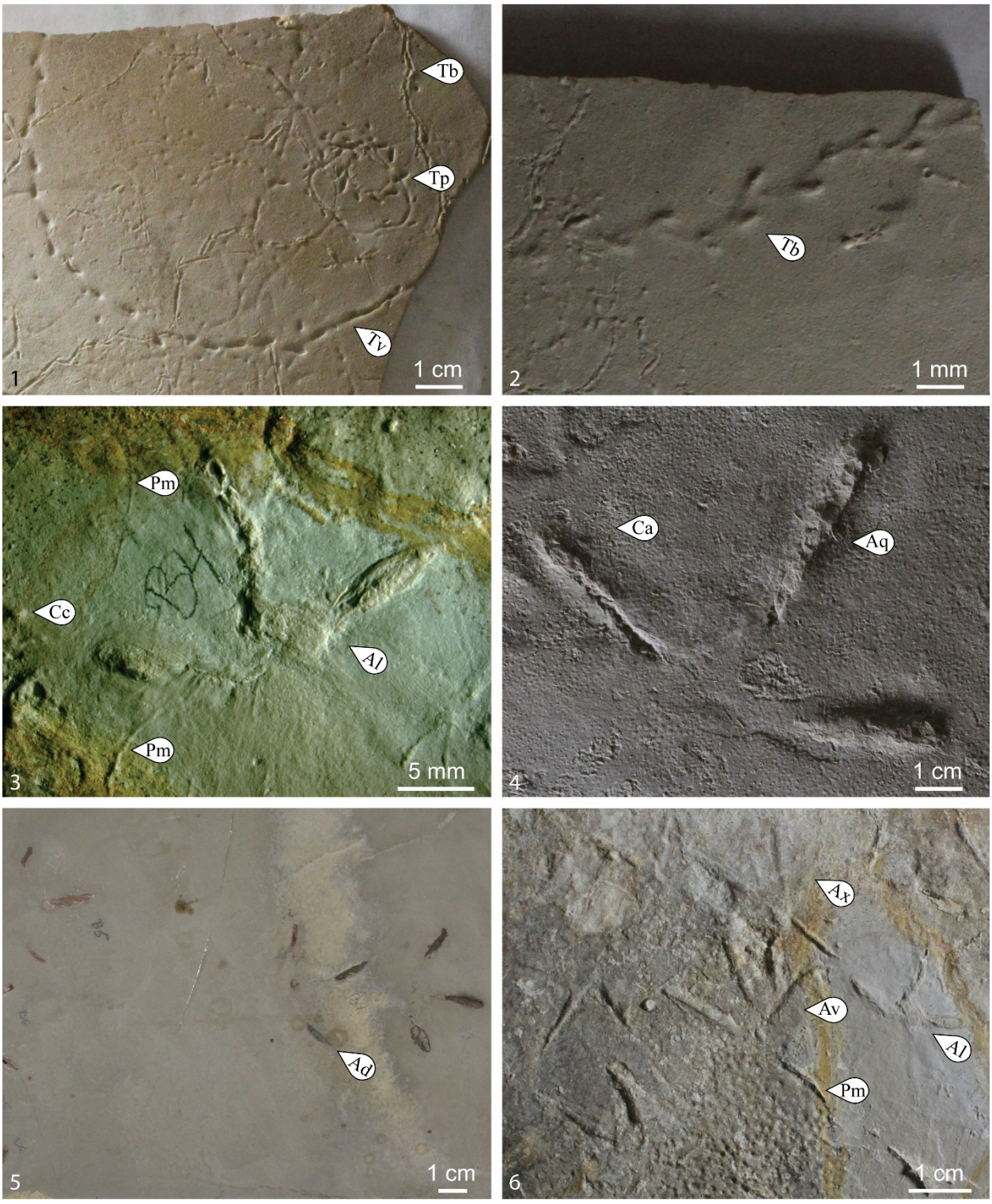
Tb
Tp
Tv
1 cm
1
Tb
1 mm
2
Pm
Cc
Al
Pm
5 mm
3
Ca
Aq
1 cm
4
Ad
1 cm
5
Ax
Av
Al
Pm
1 cm
6

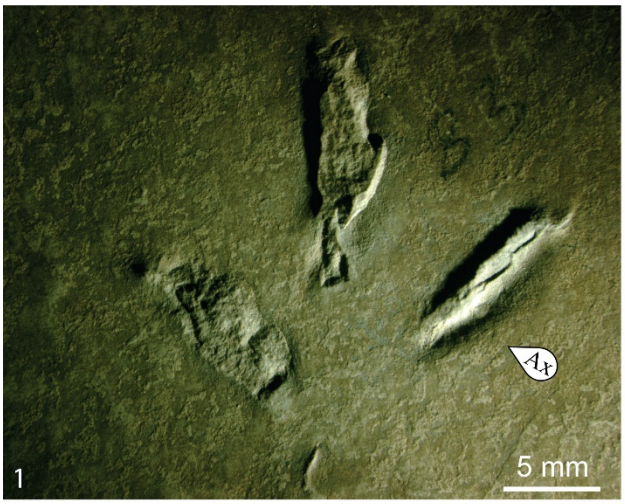
Ax
5 mm
1


Ft
2

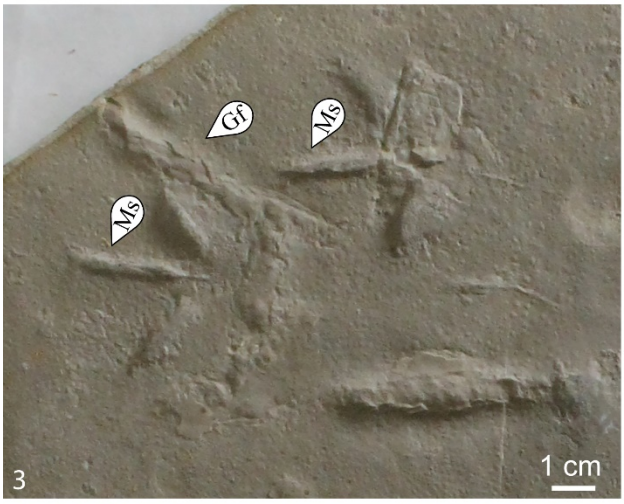
Gf
Ms
Ms
1 cm
3

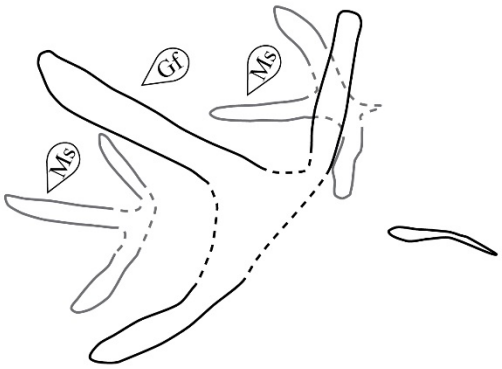
Gf
Ms
Ms
1 cm
4

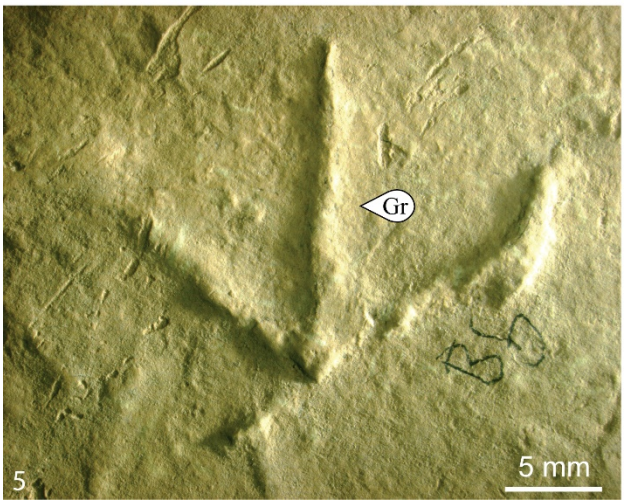
Gr
5 mm
5

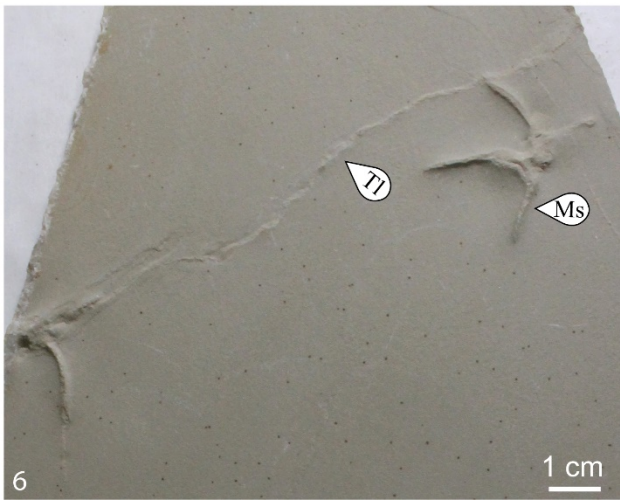
Tl
Ms
1 cm
6


Te
Pf
1 cm
1


3
Pf
Te
2

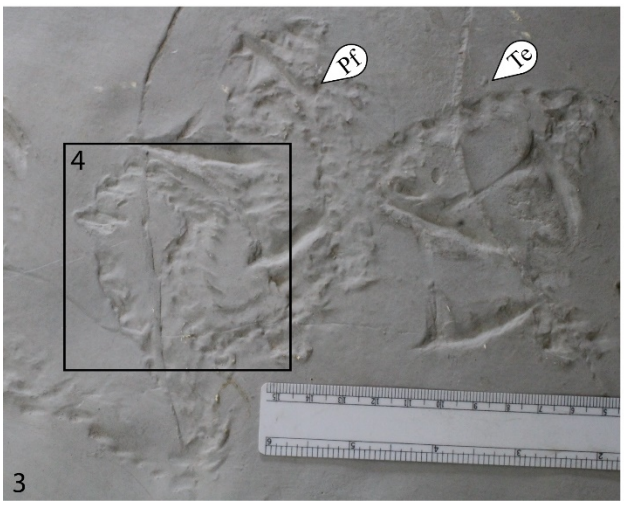
Pf
Te
4
3

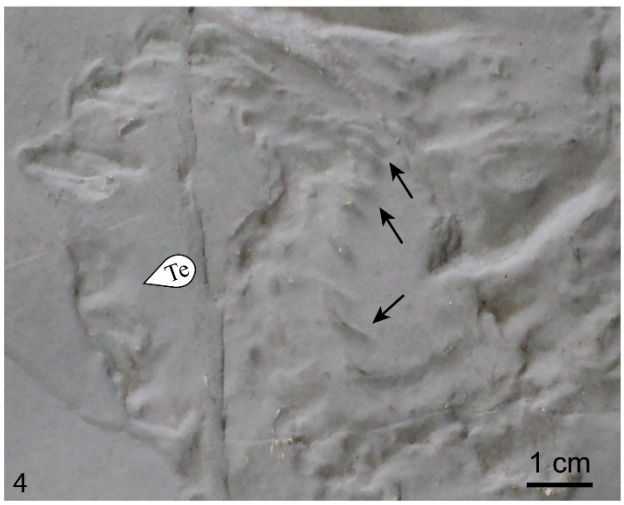
Te
1 cm
4

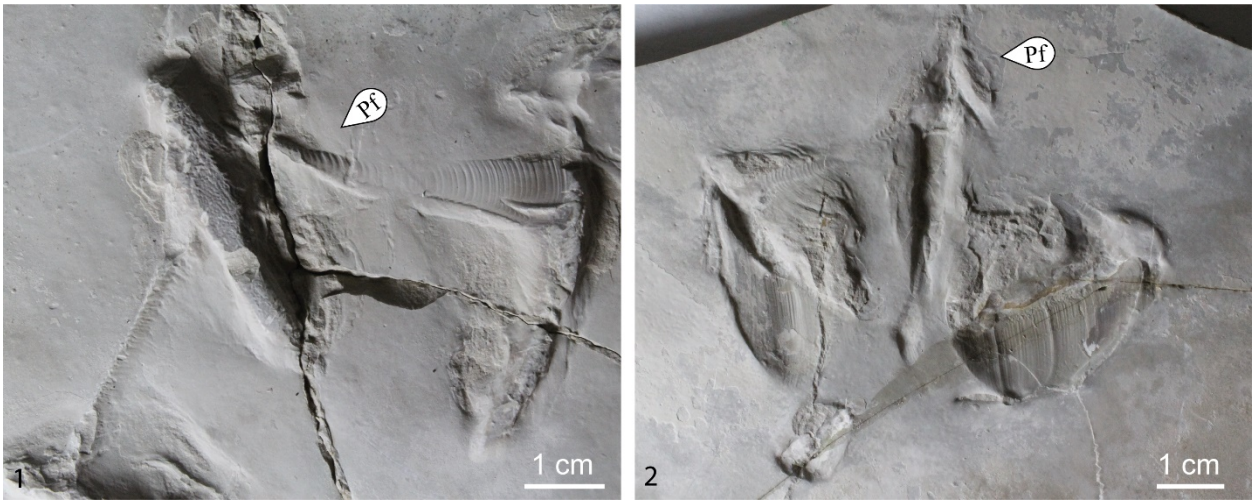
Pf
1 cm
1
Pf
1 cm
2

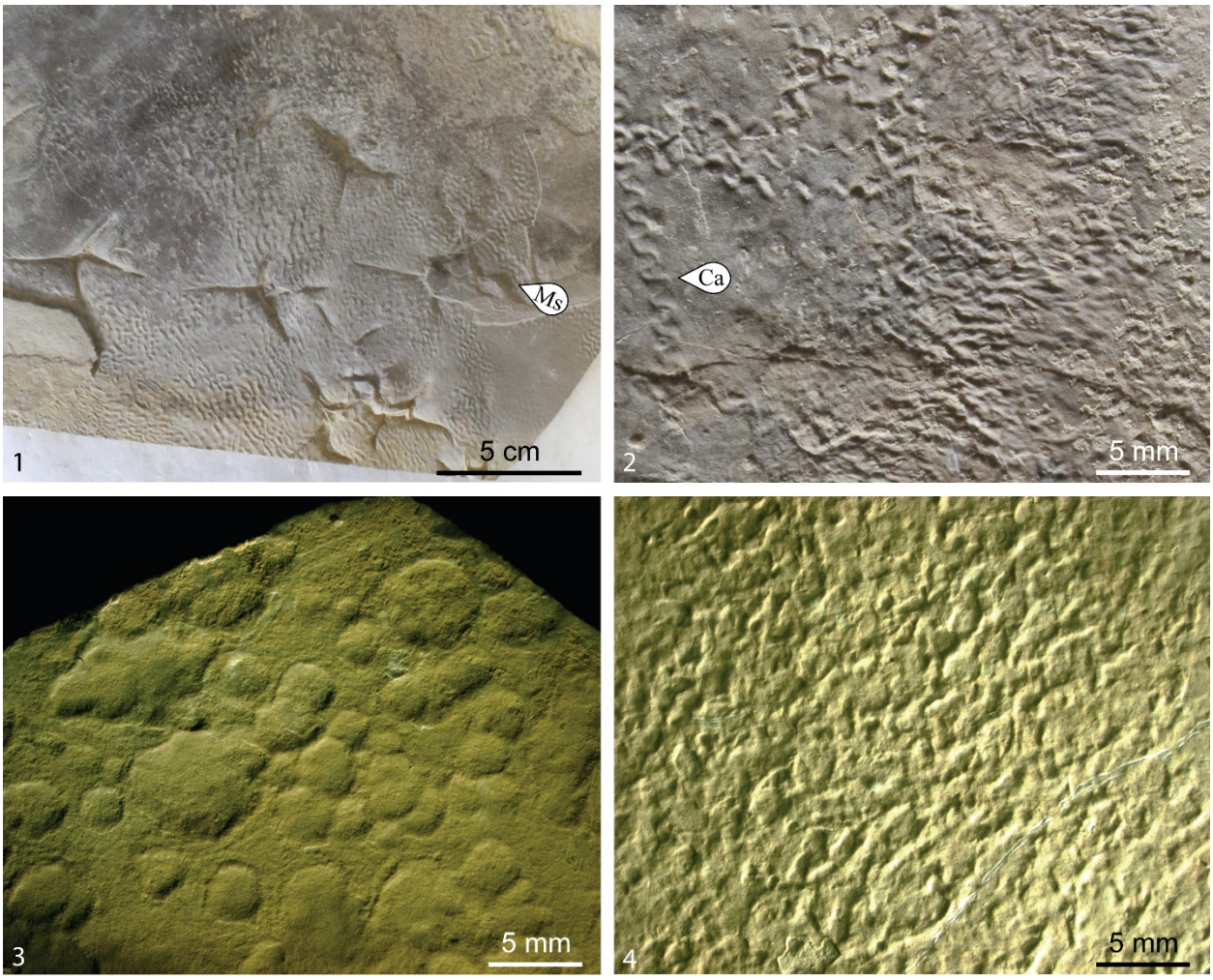
Ms
5 cm
1
Ca
5 mm
2
5 mm
3
5 mm
4

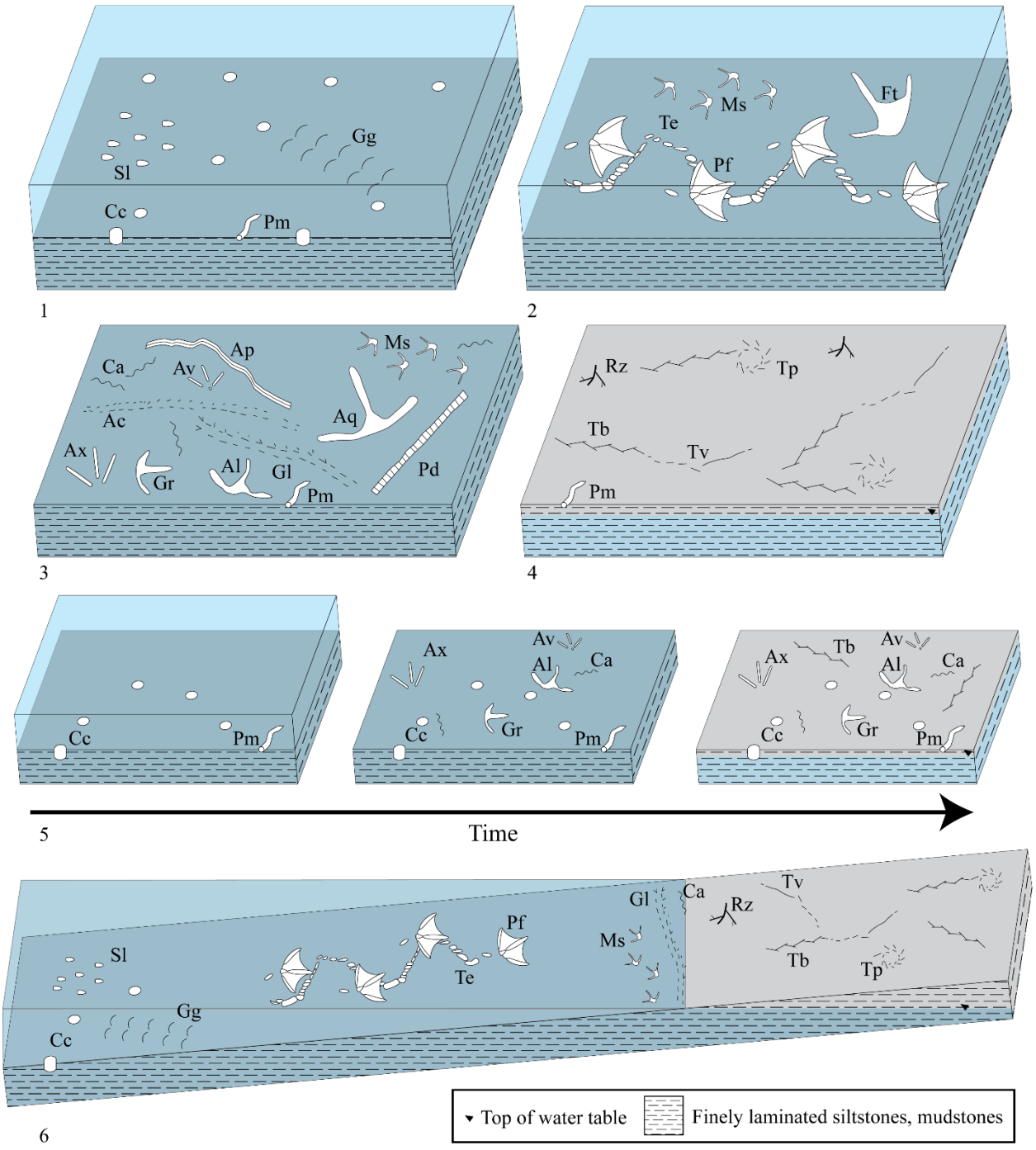
Gg
Sl
Cc
Pm
1
Ms
Te
Ft
Pf
2
Ca
Ap
Av
Ac
Ms
Aq
Ax
Gr
Al
Gl
Pm
Pd
3
Rz
Tp
Tb
Tv
Pm
4
Cc
Pm
Ax
Av
Al
Ca
Cc
Gr
Pm
Ax
Tb
Av
Al
Ca
Cc
Gr
Pm
5
Time
Sl
Gg
Cc
Te
Pf
Gl
Ms
Ca
Rz
Tv
Tb
Tp
6
Top of water table
Finely laminated siltstones, mudstones

TABLES AND TABLE CAPTIONS

Table 1. Known ichnofossils from the GRF.

Table 2. Identified traces by slab and their preservation pattern.

Table 3. Ichnotaxa, relative abundances, ethologies, and potential tracemakers. VR = Very Rare (n = 1), R = Rare (n = 2–5), C = Common (n = 6–20), A = Abundant (n > 20).

Table 4. Established ichnocoenoses for the GRF ichnotaxa.

Table 5. Ages, localities, ichnofacies, and shared ichnotaxa of other lacustrine deposits.

Table 6. Previous work on localities reinterpreted as belonging to the Cochlichnus Ichnofacies.

Reference	Stratigraphy	Location	Trace Fossils
Bohacs, Hasiotis, & Demko, 2007	Green River Formation (Tipton, Wilkins Peak, Laney); Wasatch Formation (Lumen Tongue, Niland Tongue, Cathedral Bluffs)	Greater Green River Basin, WY	Bird trackways, *Camborygma*, *Eatonichnus*, *Fuersichnus*, *Haplotichnus*, insect nests, insect trackways, *Palaeophycus*, *Planolites*, *Scolicia*, *Scoyenia*, *Skolithos*, spider traces, *Steinichnus*, *Tektonargus*
Curry, 1957	Green River Formation (Parachute Creek Member)	Timber Creek, Uinta Basin, UT	Bird tracks, cf. *Presbyorniformipes*, lizard tracks, cf. *Cochlichnus*, mammal tracks
Erickson, 1967	Green River Formation	Tucker (Soldier Summit area), Uinta Basin, UT	*Presbyorniformipes*, *Tsalavoutichnus* (formally bird feeding trace)
Lamond & Tapanila, 2003	Green River Formation (Tipton Member)	Delaney Rim, Washakie Basin, WY	Embedment cavities in stromatolites produced by brine shrimp or insects
Leggitt & Cushman, 2001; Leggitt & Loewan, 2002; Leggitt, Biaggi, & Buchheim, 2007	Green River Formation (Tipton Member)	Essex Mountain, Big Sandy, Little Mesa, Greater Green River Basin, WY	*Tektonargus* (formally Caddisfly larval cases)
Martin Vazquez-Prokopec, & Page, 2010	Green River Formation (Fossil Butte Member)	Dayvault Quarry, Fossil Basin, WY	*Undichna*
Moussa, 1968, 1970	Green River Formation (Parachute Creek)	Soldier Summit, Uinta Basin, UT	Bird tracks, cf. *Cochlichnus*, perissodactyl tracks
Olson, 2014	Green River Formation	Tucker (Soldier Summit area), Uinta Basin, UT	*Juncitarsus* trackway
Roehler, Hanley, & Honey, 1988	Green River Formation (Cottonwood Creek Delta, Tipton Member)	Baggs, Washakie Basin, WY	cf. *Planolites*, rhizoliths
Yang & others, 1995	Green River Formation (Parachute Creek)	Timber Creek, Uinta Basin, UT	*Presbyorniformipes*

Slab ID	Locality	Surface	Ichnofossils	Ichnocoenoses
GC-C-1	Spanish Fork Canyon	Hyporelief	*Cochlichnus anguineus, Cochlichnus plegmaeidos, Planolites montanus*	*Cochlichnus*
GC-C-2	Spanish Fork Canyon	Epirelief	*Cochlichnus anguineus, Planolites montanus*	*Cochlichnus*
		Hyporelief	*Midorikawapeda semipalmatus, Tsalavoutichnus leptomonopati*	*Presbyorniformipes*
GC-C-3	Spanish Fork Canyon	Epirelief	c.f. *Aviadactyla* isp., *Cochlichnus anguineus*	*Cochlichnus*
		Hyporelief	*Cochlichnus anguineus*	*Cochlichnus*
GC-C-4	Soldier Summit	Hyporelief	*Presbyorniformipes feduccii*	*Presbyorniformipes*
GC-C-5	Spanish Fork Canyon	Epirelief	*Fuscinapeda texana*	*Presbyorniformipes*
		Hyporelief	*Cochlichnus anguineus, Planolites montanus, Sagittichnus linki, Treptichnus pedum,* Rhizoliths	*Cochlichnus, Conichnus, Treptichnus*
GC-C-6	Spanish Fork Canyon	Epirelief	*Cochlichnus anguineus, Gruipeda gyrponyx*	*Cochlichnus*
		Hyporelief	*Alaripeda lofgreni, Cochlichnus anguineus, Gruipeda gryponyx*	*Cochlichnus*
GC-C-7	Soldier Summit	Epirelief	*Cochlichnus anguineus*	*Cochlichnus*
		Hyporelief	*Cochlichnus anguineus, Gruipeda gryponyx*	*Cochlichnus*
GC-C-8	Spanish Fork Canyon	Epirelief	*Presbyorniformipes feduccii*	*Presbyorniformipes*
GC-C-9	Spanish Fork Canyon	Epirelief	*Treptichnus bifurcus, T. pedum, T. vagans*	*Treptichnus*
		Hyporelief	*Treptichnus bifurcus*	*Treptichnus*
GC-C-10	Spanish Fork Canyon	Epirelief	*Presbyorniformipes feduccii, Tsalavoutichnus ericksonii*	*Presbyorniformipes*
		Hyporelief	*Cochlichnus anguineus, Cochlichnus plegmaeidos*	*Cochlichnus*
GC-C-11	Spanish Fork Canyon	Hyporelief	*Cochlichnus anguineus, Cochlichnus plegmaeidos*	*Cochlichnus*
GC-C-12	Soldier Summit	Epirelief	*Cochlichnus anguineus, Cochlichnus plegmaeidos*	*Cochlichnus*
GC-C-13		Epirelief	Bird digits, *Cochlichnus anguineus*	*Cochlichnus*

	Spanish Fork Canyon	Hyporelief	*Aulichnites parkerensis, Au. tsouloufeidos, Cochlichnus anguineus, Conichnus conichnus, Glaciichnium liebegastensis*	*Cochlichnus, Conichnus*
GC-C-14	Spanish Fork Canyon	Epirelief	*Cochlichnus anguineus*	*Cochlichnus*
		Hyporelief	*Alaripeda lofgreni, Aviadactyla vialovi, Avipeda phoenix, Cochlichnus anguineus, Conichnus conichnus, Gruipeda gryponyx, Treptichnus bifurcus*	*Cochlichnus, Conichnus, Treptichnus*
GC-C-15	Spanish Fork Canyon	Epirelief	*Alaripeda lofgreni, Aviadactyla vialovi, Avipeda phoenix, Cochlichnus anguineus, Gruipeda gryponyx*	*Cochlichnus*
		Hyporelief	*Acanthichnus cursorius, Avipeda phoenix, Cochlichnus anguineus, Gruipeda gryponyx, Planolites montanus, Protovirgularia dichotoma*	*Cochlichnus*
GC-C-16	Spanish Fork Canyon	Hyporelief	c.f. *Aquatilavipes* isp., *Aviadactyla vialovi, Cochlichnus anguineus, Glaroseidosichnus gierlowskii, Gruipeda fuenzalidae, Midorikawapeda semipalmatus*	*Cochlichnus*
GC-C-17	Spanish Fork Canyon	Hyporelief	*Presbyorniformipes feduccii, Tsalavoutichnus ericksonii*	*Presbyorniformipes*
GC-C-18	Soldier Summit	Epirelief	*Presbyorniformipes feduccii*	*Presbyorniformipes*
		Hyporelief	*Cochlichnus anguineus*	*Cochlichnus*
GC-C-19	Soldier Summit	Epirelief	*Presbyorniformipes feduccii*	*Presbyorniformipes*
GC-C-20	Spanish Fork Canyon	Epirelief	*Midorikawapeda semipalmatus*	*Presbyorniformipes*
GC-C-21	Soldier Summit	Epirelief	*Presbyorniformipes feduccii, Tsalavoutichnus ericksonii*	*Presbyorniformipes*

Ichnofossils	Frequency	Ethology	Tracemaker
Acanthichnus cursorius	VR	Repichnia	Arthropods
Aulichnites parkerensis	VR	Pascichnia	Gastropods
Aulichnites tsouloufeidos	VR	Pascichnia	Gastropods
Cochlichnus anguineus	A	Repichnia	Nematodes
Cochlichnus plegmaeidos	C	Repichnia	Nematodes, Vermiforms
Conichnus conichnus	A	Domichnia	Clams
Glaciichnium liebegastensis	C	Repichnia	Arthropods
Glaroseidosichnus gierlowskii	VR	Repichnia	Arthropods
Planolites montanus	A	Fodinichnia, Repichnia	Vermiforms
Protovirgularia dichotoma	VR	Repichnia	Scaphopods
Sagittichnus lincki	A	Cubichnia	Arthropods, Ostracodes
Treptichnus bifurcus	A	Pupichnia	Insect larvae
Treptichnus pedum	C	Pupichnia	Insect larvae
Treptichnus vagans	R	Pupichnia, Repichnia	Insect larvae
Alaripeda lofgreni	C	Repichnia	Shorebirds
c.f. *Aquatilavipes* isp.	R	Repichnia	Shorebirds
c.f. *Aviadactyla* isp.	C	Repichnia	Shorebirds
Aviadactyla vialovi	C	Repichnia	Shorebirds
Avipeda phoenix	C	Repichnia	Shorebirds
Fuscinapeda texana	VR	Repichnia	Shorebirds
Gruipeda fuenzalidae	VR	Repichnia	Shorebirds
Gruipeda gryponyx	A	Repichnia	Shorebirds
Midorikawapeda semipalmatus	A	Repichnia	Shorebirds
Presbyorniformipes feduccii	A	Repichnia	*Presbyornis*-like shorebird

Tsalavoutichnus ericksonii	C	Fodinichnia, Praedichnia	*Presbyornis*-like shorebird
Tsalavoutichnus leptomonopati	VR	Fodinichnia	Shorebirds
Rhizoliths	A	NA	Plants

Ichnocoenoses	Traces	Slab Horizons	Behaviors	Environmental Interpretation
Cochlichnus	*Acanthichnus cursorius*, *Alaripeda lofgreni,* c.f. *Aquatilavipes* isp. *Aulichnites parkerensis*, *Aviadactyla vialovi*, *Avipeda phoenix, Cochlichnus anguineus*, *C. plegmaeidos*, *Glaciichnium liebegastensis*, *Gruipeda fuenzalidae*, *Gruipeda gryponyx*, *Midorikawapeda semipalmatus, Planolites montanus*, *Protovirgularia dichotoma*, and rhizoliths	GC-C-1 (hyporelief), GC-C-2 (epirelief), GC-C-3 (epirelief), GC-C-6 (epirelief and hyporelief), GC-C-7 (epirelief and hyporelief), GC-C-10 (hyporelief), GC-C-11 (hyporelief), GC-C-12 (epirelief), GC-C-13 (epirelief), GC-C-14 (epirelief), GC-C-15 (epirelief and hyporelief), GC-C-16 (hyporelief), and GC-C-18 (hyporelief)	Pascichnia, Fodinichnia, Repichnia	SWAI
Conichnus	*Conichnus conichnus*, *Sagittichnus linki*, and *Glaroseidosichnus gierlowskii*	GC-C-5 (hyporelief), GC-C-13 (hyporelief), GC-C-14 (hyporelief), and GC-C-16 (hyporelief)	Cubichnia, Repichnia	Aquatic below SWAI, < ~5 cm.
Presbyorniformipes	*Fuscinapeda texana*, *Midorikawapeda semipalmatus*, *Presbyorniformipes feduccii*, *Tsalavoutichnus ericksonii*, and *Ts. leptomonopati*	GC-C-2 (hyporelief), GC-C-4 (hyporelief), GC-C-5 (epirelief), GC-C-8 (epirelief), GC-C-10 (epirelief), GC-C-17 (epirelief and hyporelief), GC-C-18 (epirelief), GC-C-19 (epirelief), and GC-C-21 (epirelief)	Praedichnia, Repichnia	Aquatic below SWAI, < ~5 cm.
Treptichnus	*Treptichnus bifurcus*, *T. pedum*, *T. vagans*	GC-C-5 (hyporelief), GC-C-9 (epirelief and hyporelief), and GC-C-14 (hyporelief)	Pupichnia	Exposure just above SWAI.

Refs	Locality	Geologic Age	Shared Ichnotaxa
Curry, 1957; Erickson, 1967; Moussa, 1968, 1970; Olson, 2014	Parachute Creek Member, Green River Formation	Eocene	*Aquatilavipes*, *Aviadactyla*, *Avipeda*, *Cochlichnus*, *Conichnus*, *Gruipeda*, *Midorikawapeda*, *Planolites*, and *Presbyorniformipes*
Kim, 1969; Lim & others, 2000; Kim & others, 2012	Haman Formation	Upper Cretaceous	*Aquatilavipes*, *Cochlichnus*
Roehler, Hanley, & Honey, 1988; Cushman, 2001; Leggitt & Loewan, 2002; Lamond & Tapanila, 2003; Leggitt, Biaggi, & Buchheim; 2007	Tipton Member, Green River Formation	Eocene	*Planolites*, rhizoliths
Robison, 1991	Blackhawk Formation	Upper Cretaceous	*Aquatilavipes*, *Avipeda*
Foster, 2001	Wasatch Formation, Wyoming	Eocene	*Cochlichnus*
Huh & others, 2001, 2002, 2012	Yeosu Islands Archipelago, Korea	Cretaceous	*Aquatilavipes*, *Cochlichnus*
Azuma & others, 2002	Tetori Group	Lower Cretaceous	*Aquatilavipes*
Melchor, de Valais, & Genise, 2002, 2013; Melchor & others, 2006; de Valais & Melchor, 2008; Melchor, Buchwaldt, & Bowring, 2013	Laguna Brava Formation	Eocene	*Alaripeda*, *Aquatilavipes*, *Avipeda*, *Cochlichnus*, and *Gruipeda*
Hasiotis, 2004, 2008	Morrison Formation	Jurassic	*Cochlichnus*, *Conichnus*, *Planolites*, and rhizoliths
Melchor, 2004	Ischigualasto-Villa Unión Basin, Argentina	Triassic	*Cochlichnus*
Uchman, Pika-Biolzi, & Houchuli, 2004	Lower Freshwater Molasse, Switzerland	Oligocene	*Cochlichnus*, *Treptichnus*
Kim & others, 2005	Jinju Formation, Korea	Cretaceous	*Cochlichnus*, *Planolites*, *Protovirgularia*
Uchman, Kazakauskas, & Gaigalas, 2009	Varved proglacial lake, Lithuania	Upper Pleistocene	*Cochlichnus*, *Glaciichnium*

Martin, Vazquez-Prokopec, & Page, 2010	Fossil Butte Member, Green River Formation	Eocene	None
Mansilla & others, 2012	Fossil Hill, Antarctica	Eocene	*Avipeda*, *Gruipeda*
Melchor, Coronatto, & Visconti, 2012	Vinchina Formation	Oligocene–Miocene	None
Getty & others, 2016	East Berlin Formation	Jurassic	*Treptichnus*

Reference	Geologic Age	Locality	Previous Interpretation
Curry, 1957	Eocene	Parachute Creek Member, Green River Formation	Shorebird Ichnofacies
Erickson, 1967	Eocene	Parachute Creek Member, Green River Formation	Shorebird Ichnofacies
Moussa, 1968, 1970	Eocene	Parachute Creek Member, Green River Formation	Shorebird Ichnofacies
Tasch, 1968	Permian	Antarctic Ohio Range	None
Gibbard, 1977	Holocene	Varved proglacial deposits, Finland	Mermia Ichnofacies
Buatois, Jalfin, & Aceñolaza, 1997	Permian	Laguna Polino Member, La Golondrina Formation, Argentina	Mermia and Scoyenia ichnofacies
Doyle, Wood, & George, 2000	Miocene	Sorbas Member, Sorbas Basin, Spain	Shorebird Ichnofacies
Foster, 2001	Eocene	Wasatch Formation	None
Huh & others, 2001, 2002, 2012	Cretaceous	Yeosu Islands Archipelago, Korea	None
Hasiotis, 2004, 2008	Jurassic	Tidwell Member, Morrison Formation	Proximal Lacustrine Ichnocoenosis
Lucas & others, 2004	Pennsylvanian	Keota Sandstone Member, McAlester Formation, Oklahoma	Mermia and Scoyenia ichnofacies
Uchman, Pika-Biolzi, & Houchuli, 2004	Oligocene	Freshwater Molasse, Switzerland	Mermia Ichnofacies
Kim & others, 2005	Cretaceous	Jinju Formation, Korea	Mermia-Scoyenia Composite
Uchman, Kazakauskas, & Gaigalas, 2009	Pleistocene	Varved proglacial lake, Lithuania	Mermia Ichnofacies
Lerner & Lucas, 2015	Permian	Robeldo Mountains Formation, New Mexico	Tidal Flats
Getty & others, 2017	Pennsylvanian	Rhode Island Formation, Massachusetts	Mermia Ichnofacies

APPENDICES AND APPENDIX CAPTIONS

Appendix 1. Rhizolith measurements.

Appendix 2. *Cochlichnus anguineus* measurements.

Appendix 3. *Cochlichnus plegmaeidos* measurements.

Appendix 4. *Conichnus conichnus* measurements.

Appendix 5. *Glaciichnium liebegastensis* measurements.

Appendix 6. *Planolites montanus* measurements.

Appendix 7. *Sagittichnus linki* measurements.

Appendix 8. *Treptichnus bifurcus* measurements.

Appendix 9. *Alaripeda lofgreni* measurements.

Appendix 10. c.f. *Aviadactyla* isp. measurements.

Appendix 11. *Aviadactyla vialovi* measurements.

Appendix 12. *Avipeda phoenix* measurements.

Appendix 13. *Gruipeda gryponyx* measurements.

Appendix 14. *Midorikawapeda semipalmatus* measurements.

Appendix 15. *Presbyorniformipes feduccii* measurements.

Appendix 16. *Tsalavoutichnus ericksonii* measurements.

Appendix 17. Trackway measurements.

Trace ID	Length (mm)	Width (mm)	Preservation
GC-C-5-Rz-1	48.0	1.0	Concave Hyporelief
GC-C-5-Rz-2	19.8	0.7	Concave Hyporelief
GC-C-5-Rz-3	80.0	2.0	Concave Hyporelief
GC-C-5-Rz-4	19.5	1.6	Concave Hyporelief
GC-C-5-Rz-5	64.2	1.1	Concave Hyporelief
GC-C-5-Rz-6	73.6	1.6	Concave Hyporelief
GC-C-5-Rz-7	62.7	0.7	Concave Hyporelief
GC-C-5-Rz-8	25.2	0.5	Concave Hyporelief
GC-C-11-Rz-1	n/a	0.6	Convex Hyporelief
GC-C-11-Rz-2	n/a	0.5	Convex Hyporelief
GC-C-11-Rz-3	n/a	0.5	Convex Hyporelief
GC-C-11-Rz-4	n/a	0.4	Convex Hyporelief
GC-C-11-Rz-5	n/a	0.5	Convex Hyporelief
GC-C-11-Rz-6	n/a	0.3	Convex Hyporelief
GC-C-11-Rz-7	n/a	0.3	Convex Hyporelief
GC-C-11-Rz-8	n/a	0.5	Convex Hyporelief
GC-C-11-Rz-9	n/a	0.6	Convex Hyporelief
GC-C-11-Rz-10	n/a	0.5	Convex Hyporelief
GC-C-11-Rz-11	n/a	0.4	Convex Hyporelief
GC-C-11-Rz-12	n/a	0.5	Convex Hyporelief
GC-C-11-Rz-13	n/a	0.1	Convex Hyporelief
GC-C-11-Rz-14	n/a	0.1	Convex Hyporelief
GC-C-11-Rz-15	n/a	0.2	Convex Hyporelief
GC-C-11-Rz-16	n/a	0.1	Convex Hyporelief
GC-C-11-Rz-17	n/a	0.2	Convex Hyporelief
GC-C-11-Rz-18	n/a	0.1	Convex Hyporelief
GC-C-11-Rz-19	n/a	0.2	Convex Hyporelief
GC-C-11-Rz-20	n/a	0.3	Convex Hyporelief

Sample ID	Amplitude (mm)	Wavelength (mm)	Preservation
GC-C-1-Coa-1	0.8	1.3	Convex Hyporelief
GC-C-1-Coa-2	1.2	1.2	Convex Hyporelief
GC-C-1-Coa-3	0.8	1.2	Convex Hyporelief
GC-C-1-Coa-4	1.0	1.3	Convex Hyporelief
GC-C-1-Coa-5	0.8	1.4	Convex Hyporelief
GC-C-1-Coa-6	1.3	1.3	Convex Hyporelief
GC-C-1-Coa-7	1.3	1.5	Convex Hyporelief
GC-C-1-Coa-8	1.1	1.7	Convex Hyporelief
GC-C-1-Coa-9	0.9	1.1	Convex Hyporelief
GC-C-1-Coa-10	1.2	1.5	Convex Hyporelief
GC-C-1-Coa-11	0.9	1.8	Convex Hyporelief
GC-C-1-Coa-12	1.3	1.8	Convex Hyporelief
GC-C-1-Coa-13	0.8	1.5	Convex Hyporelief
GC-C-1-Coa-14	1.1	1.4	Convex Hyporelief
GC-C-1-Coa-15	1.3	1.9	Convex Hyporelief
GC-C-1-Coa-16	0.9	1.5	Convex Hyporelief
GC-C-1-Coa-17	0.8	1.1	Convex Hyporelief
GC-C-1-Coa-18	0.9	1.5	Convex Hyporelief
GC-C-1-Coa-19	0.9	1.6	Convex Hyporelief
GC-C-1-Coa-20	1.0	1.5	Convex Hyporelief
GC-C-1-Coa-21	1.0	1.7	Convex Hyporelief
GC-C-1-Coa-22	0.9	1.3	Convex Hyporelief
GC-C-1-Coa-23	1.1	1.8	Convex Hyporelief
GC-C-1-Coa-24	0.8	1.5	Convex Hyporelief
GC-C-1-Coa-25	0.9	1.4	Convex Hyporelief
GC-C-2-Coa-1	1.6	2.2	Concave Epirelief
GC-C-2-Coa-2	0.8	2.2	Concave Epirelief
GC-C-2-Coa-3	0.4	1.4	Concave Epirelief
GC-C-3-Coa-1	0.8	2.2	Concave Epirelief
GC-C-3-Coa-2	0.6	1.6	Concave Epirelief
GC-C-3-Coa-3	0.9	1.5	Concave Epirelief
GC-C-3-Coa-4	1.0	1.6	Concave Epirelief
GC-C-3-Coa-5	0.7	1.7	Concave Epirelief
GC-C-3-Coa-6	1.0	1.5	Concave Epirelief
GC-C-3-Coa-7	0.5	1.3	Convex Hyporelief
GC-C-3-Coa-8	0.7	2.1	Convex Hyporelief
GC-C-6-Coa-1	0.7	1.8	Concave Epirelief
GC-C-6-Coa-2	1.0	1.7	Concave Epirelief
GC-C-6-Coa-3	1.1	1.7	Concave Epirelief
GC-C-6-Coa-4	0.6	1.6	Concave Epirelief

GC-C-6-Coa-5	0.7	1.3	Concave Epirelief
GC-C-6-Coa-6	1.3	1.8	Concave Epirelief
GC-C-6-Coa-7	1.1	2.3	Concave Epirelief
GC-C-6-Coa-8	0.7	2.4	Concave Epirelief
GC-C-6-Coa-9	1.0	2.8	Concave Epirelief
GC-C-6-Coa-10	0.5	1.7	Concave Epirelief
GC-C-6-Coa-11	0.7	1.3	Concave Epirelief
GC-C-6-Coa-12	0.7	1.6	Concave Epirelief
GC-C-6-Coa-13	1.2	1.7	Concave Epirelief
GC-C-6-Coa-14	0.7	1.5	Concave Epirelief
GC-C-6-Coa-15	0.5	1.2	Concave Epirelief
GC-C-6-Coa-16	0.6	1.2	Concave Epirelief
GC-C-6-Coa-17	0.6	1.3	Concave Epirelief
GC-C-6-Coa-18	0.7	1.8	Concave Epirelief
GC-C-6-Coa-19	0.9	2.0	Concave Epirelief
GC-C-6-Coa-20	0.5	1.3	Concave Epirelief
GC-C-6-Coa-21	0.7	1.4	Convex Hyporelief
GC-C-6-Coa-22	0.8	2.1	Convex Hyporelief
GC-C-6-Coa-23	1.0	2.0	Convex Hyporelief
GC-C-7-Coa-1	0.5	1.6	Concave Epirelief
GC-C-7-Coa-2	0.6	0.8	Concave Epirelief
GC-C-7-Coa-3	1.0	1.4	Concave Epirelief
GC-C-7-Coa-4	1.1	1.5	Concave Epirelief
GC-C-7-Coa-5	0.7	1.2	Concave Epirelief
GC-C-7-Coa-6	0.9	1.4	Concave Epirelief
GC-C-7-Coa-7	1.0	1.3	Concave Epirelief
GC-C-7-Coa-8	0.5	1.3	Concave Epirelief
GC-C-7-Coa-9	0.9	1.2	Concave Epirelief
GC-C-7-Coa-10	1.3	1.6	Concave Epirelief
GC-C-7-Coa-11	0.9	1.5	Concave Epirelief
GC-C-7-Coa-12	0.7	1.1	Concave Epirelief
GC-C-7-Coa-13	0.7	1.0	Concave Epirelief
GC-C-7-Coa-14	0.6	1.2	Concave Epirelief
GC-C-7-Coa-15	0.7	1.2	Concave Epirelief
GC-C-7-Coa-16	1.1	1.7	Concave Epirelief
GC-C-7-Coa-17	0.8	1.3	Concave Epirelief
GC-C-7-Coa-18	0.6	1.4	Concave Epirelief
GC-C-7-Coa-19	0.5	1.3	Concave Epirelief
GC-C-7-Coa-20	1.0	2.4	Concave Epirelief
GC-C-10-Coa-1	1.0	2.2	Concave Hyporelief
GC-C-10-Coa-2	0.9	1.4	Concave Hyporelief

GC-C-10-Coa-3	0.7	2.5	Concave Hyporelief
GC-C-10-Coa-4	0.5	1.8	Concave Hyporelief
GC-C-10-Coa-5	1.1	1.9	Concave Hyporelief
GC-C-10-Coa-6	1.0	2.2	Concave Hyporelief
GC-C-10-Coa-7	0.5	1.3	Concave Hyporelief
GC-C-11-Coa-1	0.8	0.8	Convex Hyporelief
GC-C-11-Coa-2	0.8	1.9	Convex Hyporelief
GC-C-11-Coa-3	1.0	1.9	Convex Hyporelief
GC-C-11-Coa-4	1.0	1.6	Convex Hyporelief
GC-C-11-Coa-5	0.8	1.3	Convex Hyporelief
GC-C-11-Coa-6	1.1	1.4	Convex Hyporelief
GC-C-11-Coa-7	1.1	1.5	Convex Hyporelief
GC-C-11-Coa-8	0.6	1.1	Convex Hyporelief
GC-C-11-Coa-9	0.7	1.3	Convex Hyporelief
GC-C-11-Coa-10	0.8	2.0	Convex Hyporelief
GC-C-11-Coa-11	0.7	2.0	Convex Hyporelief
GC-C-11-Coa-12	0.9	1.7	Convex Hyporelief
GC-C-11-Coa-13	1.2	1.6	Convex Hyporelief
GC-C-11-Coa-14	0.9	1.3	Convex Hyporelief
GC-C-11-Coa-15	0.9	1.9	Convex Hyporelief
GC-C-11-Coa-16	0.6	0.8	Convex Hyporelief
GC-C-11-Coa-17	0.6	1.0	Convex Hyporelief
GC-C-12-Coa-1	1.1	1.8	Concave Epirelief
GC-C-12-Coa-2	1.1	2.2	Concave Epirelief
GC-C-12-Coa-3	0.7	1.8	Concave Epirelief
GC-C-12-Coa-4	0.8	1.5	Concave Epirelief
GC-C-12-Coa-5	0.6	1.1	Concave Epirelief
GC-C-12-Coa-6	1.0	1.5	Concave Epirelief
GC-C-12-Coa-7	0.6	1.2	Concave Epirelief
GC-C-12-Coa-8	0.8	2.0	Concave Epirelief
GC-C-12-Coa-9	1.1	1.8	Concave Epirelief
GC-C-12-Coa-10	1.1	1.4	Concave Epirelief
GC-C-12-Coa-11	0.9	1.2	Concave Epirelief
GC-C-12-Coa-12	0.8	1.8	Concave Epirelief
GC-C-12-Coa-13	1.0	1.8	Concave Epirelief
GC-C-12-Coa-14	0.9	1.5	Concave Epirelief
GC-C-12-Coa-15	0.9	1.6	Concave Epirelief
GC-C-12-Coa-16	0.7	1.3	Concave Epirelief
GC-C-12-Coa-17	0.6	1.2	Concave Epirelief
GC-C-12-Coa-18	0.5	1.5	Concave Epirelief
GC-C-12-Coa-19	1.0	1.8	Concave Epirelief

GC-C-12-Coa-20	0.6	1.5	Concave Epirelief
GC-C-12-Coa-21	0.9	1.4	Concave Epirelief
GC-C-12-Coa-22	1.0	1.5	Concave Epirelief
GC-C-12-Coa-23	0.6	1.5	Concave Epirelief
GC-C-12-Coa-24	0.9	1.5	Concave Epirelief
GC-C-12-Coa-25	0.8	1.7	Concave Epirelief
GC-C-12-Coa-26	0.7	1.8	Concave Epirelief
GC-C-12-Coa-27	0.9	1.9	Concave Epirelief
GC-C-12-Coa-28	1.0	1.5	Concave Epirelief
GC-C-12-Coa-29	0.9	1.7	Concave Epirelief
GC-C-12-Coa-30	0.7	2.1	Concave Epirelief
GC-C-12-Coa-31	0.6	1.1	Concave Epirelief
GC-C-12-Coa-32	0.7	1.7	Concave Epirelief
GC-C-12-Coa-33	0.6	1.8	Concave Epirelief
GC-C-12-Coa-34	1.1	1.8	Concave Epirelief
GC-C-12-Coa-35	1.0	1.3	Concave Epirelief
GC-C-12-Coa-36	0.9	1.8	Concave Epirelief
GC-C-12-Coa-37	0.5	1.0	Concave Epirelief
GC-C-12-Coa-38	0.8	1.5	Concave Epirelief
GC-C-12-Coa-39	0.3	1.3	Concave Epirelief
GC-C-13-Coa-1	1.6	1.6	Concave Epirelief
GC-C-13-Coa-2	1.9	2.4	Concave Epirelief
GC-C-13-Coa-3	1.5	2.1	Concave Epirelief
GC-C-13-Coa-4	1.3	2.2	Concave Epirelief
GC-C-13-Coa-5	1.3	2.0	Concave Epirelief
GC-C-13-Coa-6	1.3	1.5	Concave Epirelief
GC-C-13-Coa-7	1.5	1.9	Concave Epirelief
GC-C-13-Coa-8	1.2	2.0	Concave Epirelief
GC-C-13-Coa-9	1.6	2.4	Concave Epirelief
GC-C-13-Coa-10	1.2	2.0	Concave Epirelief
GC-C-13-Coa-11	1.2	2.2	Concave Epirelief
GC-C-13-Coa-12	1.4	2.2	Concave Epirelief
GC-C-13-Coa-13	1.3	2.0	Concave Epirelief
GC-C-13-Coa-14	1.5	2.6	Concave Epirelief
GC-C-13-Coa-15	1.5	1.5	Concave Epirelief
GC-C-13-Coa-16	1.4	1.0	Concave Epirelief
GC-C-13-Coa-17	1.1	2.8	Concave Epirelief
GC-C-13-Coa-18	1.0	1.1	Concave Epirelief
GC-C-13-Coa-19	1.8	2.9	Concave Epirelief
GC-C-13-Coa-20	1.7	1.9	Concave Epirelief
GC-C-13-Coa-21	1.1	1.5	Convex Hyporelief

GC-C-13-Coa-22	0.7	1.5	Convex Hyporelief
GC-C-13-Coa-23	1.5	2.0	Convex Hyporelief
GC-C-13-Coa-24	0.5	1.0	Convex Hyporelief
GC-C-13-Coa-25	0.7	1.4	Convex Hyporelief
GC-C-13-Coa-26	1.7	1.8	Convex Hyporelief
GC-C-13-Coa-27	1.2	1.6	Convex Hyporelief
GC-C-13-Coa-28	1.1	2.0	Convex Hyporelief
GC-C-13-Coa-29	1.1	1.5	Convex Hyporelief
GC-C-13-Coa-30	1.3	2.2	Convex Hyporelief
GC-C-13-Coa-31	0.7	1.9	Convex Hyporelief
GC-C-13-Coa-32	1.1	2.2	Convex Hyporelief
GC-C-13-Coa-33	1.1	1.4	Convex Hyporelief
GC-C-13-Coa-34	0.7	1.4	Convex Hyporelief
GC-C-13-Coa-35	0.6	2.4	Convex Hyporelief
GC-C-13-Coa-36	0.7	1.0	Convex Hyporelief
GC-C-13-Coa-37	0.6	0.7	Convex Hyporelief
GC-C-13-Coa-38	0.5	1.0	Convex Hyporelief
GC-C-13-Coa-39	0.8	1.6	Convex Hyporelief
GC-C-13-Coa-40	0.8	1.3	Convex Hyporelief
GC-C-14-Coa-1	1.0	1.8	Convex Hyporelief
GC-C-14-Coa-2	0.5	1.1	Convex Hyporelief
GC-C-14-Coa-3	0.5	1.5	Convex Hyporelief
GC-C-14-Coa-4	0.8	1.5	Convex Hyporelief
GC-C-14-Coa-5	0.9	1.1	Convex Hyporelief
GC-C-15-Coa-1	1.3	1.7	Convex Hyporelief
GC-C-15-Coa-2	0.9	2.7	Convex Hyporelief
GC-C-15-Coa-3	1.3	1.5	Convex Hyporelief
GC-C-15-Coa-4	1.0	1.6	Convex Hyporelief
GC-C-15-Coa-5	0.8	1.2	Convex Hyporelief
GC-C-15-Coa-6	0.9	1.8	Convex Hyporelief
GC-C-15-Coa-7	0.7	1.7	Concave Epirelief
GC-C-15-Coa-8	0.6	1.0	Concave Epirelief
GC-C-15-Coa-9	0.6	1.8	Concave Epirelief
GC-C-15-Coa-10	0.6	1.3	Concave Epirelief
GC-C-15-Coa-11	0.8	1.4	Concave Epirelief
GC-C-18-Coa-1	0.7	1.7	Convex Hyporelief

Sample ID	Length (mm)	Width (mm)	Preservation
GC-C-1-Cop-1	19.5	1.6	Convex Hyporelief
GC-C-1-Cop-2	18.2	1.6	Convex Hyporelief
GC-C-1-Cop-3	79.8	1.6	Convex Hyporelief
GC-C-1-Cop-4	35.8	1.6	Convex Hyporelief
GC-C-10-Cop-1	22.7	2.2	Convex Hyporelief
GC-C-11-Cop-1	37.1	1.4	Convex Hyporelief
GC-C-12-Cop-1	69.8	1.7	Concave Epirelief
GC-C-12-Cop-2	45.4	1.6	Concave Epirelief
GC-C-12-Cop-3	8.2	1.3	Concave Epirelief

Trace ID	Diameter (mm)	Preservation
GC-C-13-Coc-1	0.9	Convex Hyporelief
GC-C-13-Coc-2	0.7	Convex Hyporelief
GC-C-13-Coc-3	0.5	Convex Hyporelief
GC-C-13-Coc-4	0.6	Convex Hyporelief
GC-C-13-Coc-5	0.9	Convex Hyporelief
GC-C-13-Coc-6	0.9	Convex Hyporelief
GC-C-13-Coc-7	0.9	Convex Hyporelief
GC-C-13-Coc-8	0.5	Convex Hyporelief
GC-C-13-Coc-9	0.7	Convex Hyporelief
GC-C-13-Coc-10	0.7	Convex Hyporelief
GC-C-13-Coc-11	0.6	Convex Hyporelief
GC-C-13-Coc-12	0.6	Convex Hyporelief
GC-C-13-Coc-13	0.6	Convex Hyporelief
GC-C-13-Coc-14	0.8	Convex Hyporelief
GC-C-13-Coc-15	1.0	Convex Hyporelief
GC-C-13-Coc-16	1.0	Convex Hyporelief
GC-C-13-Coc-17	1.0	Convex Hyporelief
GC-C-13-Coc-18	0.8	Convex Hyporelief
GC-C-13-Coc-19	1.3	Convex Hyporelief
GC-C-13-Coc-20	1.3	Convex Hyporelief
GC-C-14-Coc-1	0.7	Convex Hyporelief
GC-C-14-Coc-2	0.7	Convex Hyporelief
GC-C-14-Coc-3	0.7	Convex Hyporelief
GC-C-14-Coc-4	0.9	Convex Hyporelief
GC-C-14-Coc-5	0.7	Convex Hyporelief
GC-C-14-Coc-6	0.9	Convex Hyporelief
GC-C-14-Coc-7	0.9	Convex Hyporelief
GC-C-14-Coc-8	0.6	Convex Hyporelief
GC-C-14-Coc-9	0.9	Convex Hyporelief
GC-C-14-Coc-10	0.8	Convex Hyporelief
GC-C-14-Coc-11	0.6	Convex Hyporelief
GC-C-14-Coc-12	0.6	Convex Hyporelief
GC-C-14-Coc-13	0.9	Convex Hyporelief
GC-C-14-Coc-14	0.9	Convex Hyporelief
GC-C-14-Coc-15	1.0	Convex Hyporelief
GC-C-14-Coc-16	0.7	Convex Hyporelief
GC-C-14-Coc-17	0.7	Convex Hyporelief
GC-C-14-Coc-18	0.6	Convex Hyporelief
GC-C-14-Coc-19	0.7	Convex Hyporelief
GC-C-14-Coc-20	0.4	Convex Hyporelief

Sample ID	Length (mm)	Width (mm)	Preservation
GC-C-13-Gll-1	1.7	101.5	Convex Hyporelief
GC-C-13-Gll-2	1.9	217.8	Convex Hyporelief
GC-C-13-Gll-3	1.3	103.5	Convex Hyporelief
GC-C-13-Gll-4	1.7	272.5	Convex Hyporelief
GC-C-13-Gll-5	1.3	201.8	Convex Hyporelief
GC-C-13-Gll-6	1.0	70.5	Convex Hyporelief
GC-C-13-Gll-7	1.3	65.6	Convex Hyporelief
GC-C-13-Gll-8	1.3	122.3	Convex Hyporelief
GC-C-13-Gll-9	1.4	37.2	Convex Hyporelief
GC-C-13-Gll-10	1.3	123.4	Convex Hyporelief
GC-C-13-Gll-11	1.4	111.7	Convex Hyporelief
GC-C-13-Gll-12	1.7	30.2	Convex Hyporelief
GC-C-13-Gll-13	1.6	25.3	Convex Hyporelief
GC-C-13-Gll-14	1.4	33.2	Convex Hyporelief

Sample ID	Length (mm)	Width (mm)	Preservation
GC-C-1-Plm-1	16.8	1.5	Convex Hyporelief
GC-C-2-Plm-1	173.0	3.5	Convex Epirelief
GC-C-2-Plm-2	67.9	3.5	Convex Epirelief
GC-C-2-Plm-3	69.7	0.8	Convex Epirelief
GC-C-2-Plm-4	88.4	1.3	Convex Epirelief
GC-C-14-Plm-1	9.4	1.0	Convex Hyporelief
GC-C-14-Plm-2	7.2	0.6	Convex Hyporelief
GC-C-14-Plm-3	7.8	0.7	Convex Hyporelief
GC-C-14-Plm-4	2.8	0.6	Convex Hyporelief
GC-C-14-Plm-5	4.2	0.9	Convex Hyporelief
GC-C-14-Plm-6	44.4	0.9	Convex Hyporelief
GC-C-14-Plm-7	39.1	0.9	Convex Hyporelief
GC-C-15-Plm-1	54.1	0.4	Convex Hyporelief
GC-C-15-Plm-2	34.6	0.4	Convex Hyporelief
GC-C-15-Plm-3	29.8	0.6	Convex Hyporelief

Trace ID	Diameter (mm)	Preservation
GC-C-5-Sal-1	0.5	Convex Hyporelief
GC-C-5-Sal-2	0.7	Convex Hyporelief
GC-C-5-Sal-3	0.9	Convex Hyporelief
GC-C-5-Sal-4	0.5	Convex Hyporelief
GC-C-5-Sal-5	0.4	Convex Hyporelief
GC-C-5-Sal-6	0.9	Convex Hyporelief
GC-C-5-Sal-7	0.9	Convex Hyporelief
GC-C-5-Sal-8	0.8	Convex Hyporelief
GC-C-5-Sal-9	0.7	Convex Hyporelief
GC-C-5-Sal-10	0.7	Convex Hyporelief
GC-C-5-Sal-11	0.7	Convex Hyporelief
GC-C-5-Sal-12	0.7	Convex Hyporelief
GC-C-5-Sal-13	0.8	Convex Hyporelief
GC-C-5-Sal-14	0.5	Convex Hyporelief
GC-C-5-Sal-15	0.5	Convex Hyporelief
GC-C-5-Sal-16	0.9	Convex Hyporelief
GC-C-5-Sal-17	0.9	Convex Hyporelief
GC-C-5-Sal-18	0.6	Convex Hyporelief
GC-C-5-Sal-19	0.9	Convex Hyporelief
GC-C-5-Sal-20	0.8	Convex Hyporelief

Sample ID	Length (mm)	Width (mm)	Preservation
GC-C-9-Trb-1	131.2	0.8	Concave Epirelief
GC-C-9-Trb-2	130.6	1.2	Concave Epirelief
GC-C-9-Trb-3	197.3	1.1	Concave Epirelief
GC-C-9-Trb-4	111.4	2.1	Concave Epirelief
GC-C-9-Trb-5	168.0	1.1	Concave Epirelief
GC-C-9-Trb-6	63.2	1.0	Concave Epirelief
GC-C-9-Trb-7	100.1	1.4	Concave Epirelief
GC-C-9-Trb-8	50.0	0.5	Concave Epirelief
GC-C-9-Trb-9	65.7	1.6	Concave Epirelief
GC-C-9-Trb-10	51.5	1.2	Concave Epirelief
GC-C-9-Trb-11	148.1	1.3	Concave Epirelief
GC-C-9-Trb-12	102.6	0.9	Concave Epirelief
GC-C-9-Trb-13	53.7	0.8	Concave Epirelief
GC-C-9-Trb-14	29.4	1.3	Concave Epirelief
GC-C-9-Trb-15	66.9	2.2	Concave Epirelief
GC-C-9-Trb-16	6.4	1.0	Concave Epirelief
GC-C-9-Trb-17	18.6	0.9	Concave Epirelief
GC-C-9-Trb-18	16.1	0.8	Concave Epirelief
GC-C-9-Trb-19	83.8	1.3	Concave Epirelief
GC-C-9-Trb-20	66.3	0.9	Convex Hyporelief
GC-C-9-Trb-21	260.2	1.2	Convex Hyporelief
GC-C-9-Trb-22	183.0	0.7	Convex Hyporelief
GC-C-9-Trb-23	105.5	1.4	Convex Hyporelief
GC-C-9-Trb-24	138.3	1.8	Convex Hyporelief
GC-C-9-Trb-25	102.7	1.4	Convex Hyporelief
GC-C-9-Trb-26	143.3	1.8	Convex Hyporelief
GC-C-9-Trb-27	141.1	8.0	Convex Hyporelief
GC-C-9-Trb-28	14.2	0.6	Convex Hyporelief
GC-C-9-Trb-29	22.8	0.5	Convex Hyporelief
GC-C-9-Trb-30	194.9	1.4	Convex Hyporelief
GC-C-9-Trb-31	94.9	1.6	Convex Hyporelief
GC-C-9-Trb-32	53.2	1.5	Convex Hyporelief
GC-C-9-Trb-33	47.5	2.2	Convex Hyporelief
GC-C-9-Trb-34	17.4	0.7	Convex Hyporelief
GC-C-9-Trb-35	91.8	1.6	Convex Hyporelief
GC-C-9-Trb-36	42.7	3.6	Convex Hyporelief
GC-C-9-Trb-37	60.8	1.3	Convex Hyporelief
GC-C-9-Trb-38	169.4	1.6	Convex Hyporelief
GC-C-9-Trb-39	14.7	0.9	Convex Hyporelief
GC-C-9-Trb-40	48.7	0.9	Convex Hyporelief

GC-C-14-Trb-1	14.4	0.2	Convex Hyporelief
GC-C-14-Trb-2	11.5	0.3	Convex Hyporelief

Sample ID	Length (mm)	Width (mm)	AOD II–IV (degrees)	Preservation
GC-C-6-All-1	15.3	19.8	200.2	Convex Hyporelief
GC-C-6-All-2	15.4	16.6	146.0	Convex Hyporelief
GC-C-6-All-3	14.8	24.5	131.3	Convex Hyporelief
GC-C-14-All-1	12.2	24.3	129.1	Convex Hyporelief
GC-C-14-All-2	17.4	22.0	134.6	Convex Hyporelief
GC-C-15-All-1	21.6	21.7	126.2	Concave Epirelief
GC-C-15-All-2	16.7	24.4	147.6	Concave Epirelief

Sample ID	Length (mm)	Width (mm)	AOD II–IV (degrees)	Preservation
GC-C-3-Av-1	24.4	35.2	123.1	Concave Epirelief
GC-C-3-Av-2	24.4	n/a	n/a	Concave Epirelief
GC-C-3-Av-3	24.4	35.2	117.4	Concave Epirelief
GC-C-3-Av-4	24.4	35.2	123.6	Concave Epirelief
GC-C-3-Av-5	24.4	34.8	111.8	Concave Epirelief
GC-C-3-Av-6	24.4	34.8	121.7	Concave Epirelief

Sample ID	Length (mm)	Width (mm)	AOD II–IV (degrees)	Preservation
GC-C-14-Avv-1	17.4	20.9	112.6	Convex Hyporelief
GC-C-14-Avv-2	19.8	28.4	101.6	Convex Hyporelief
GC-C-14-Avv-3	37.6	17.4	103.3	Convex Hyporelief
GC-C-14-Avv-4	16.5	19.8	98.8	Convex Hyporelief
GC-C-14-Avv-5	14.6	21.6	115.0	Convex Hyporelief
GC-C-14-Avv-6	25.8	20.6	110.6	Convex Hyporelief
GC-C-14-Avv-7	21.9	26.5	97.4	Convex Hyporelief
GC-C-15-Avv-1	21.0	29.6	131.8	Concave Epirelief
GC-C-16-Avi-1	16.2	23.8	131.1	Convex Hyporelief
GC-C-16-Avi-2	37.3	34.5	99.0	Convex Hyporelief
GC-C-16-Avi-3	16.0	22.9	97.0	Convex Hyporelief
GC-C-16-Avi-4	22.6	33.9	100.5	Convex Hyporelief
GC-C-16-Avi-5	16.3	23.0	102.4	Convex Hyporelief
GC-C-16-Avi-6	23.6	31.3	137.8	Convex Hyporelief

Sample ID	Length (mm)	Width (mm)	AOD II–IV (degrees)	Preservation
GC-C-14-Avp-1	30.5	33.0	93.5	Concave Epirelief
GC-C-14-Avp-2	22.2	23.0	90.0	Convex Hyporelief
GC-C-14-Avp-3	37.6	17.4	82.4	Convex Hyporelief
GC-C-15-Avp-1	19.1	23.6	91.9	Convex Hyporelief
GC-C-15-Avp-2	19.4	23.5	83.5	Convex Hyporelief
GC-C-15-Avp-3	23.2	26.3	94.8	Concave Epirelief
GC-C-16-Avp-1	21.4	26.1	72.5	Convex Hyporelief

Sample ID	Length (mm)	Width (mm)	AOD II–IV (degrees)	Preservation
GC-C-6-Grg-1	17.9	24.6	118.7	Concave Epirelief
GC-C-6-Grg-2	17.9	24.6	101.5	Concave Epirelief
GC-C-6-Grg-3	17.9	24.6	103.9	Concave Epirelief
GC-C-6-Grg-4	n/a	n/a	n/a	Concave Epirelief
GC-C-6-Grg-5	18.6	22.1	108.9	Convex Hyporelief
GC-C-6-Grg-6	15.0	n/a	98.4	Convex Hyporelief
GC-C-6-Grg-7	15.0	19.7	100.7	Convex Hyporelief
GC-C-6-Grg-8	17.0	n/a	105	Convex Hyporelief
GC-C-6-Grg-9	16.2	18.1	102.1	Convex Hyporelief
GC-C-6-Grg-10	18.1	22.0	103.4	Convex Hyporelief
GC-C-6-Grg-11	22.9	35.1	113.5	Convex Hyporelief
GC-C-6-Grg-12	13.8	19.7	117.0	Convex Hyporelief
GC-C-6-Grg-13	19.1	30.4	112.8	Convex Hyporelief
GC-C-7-Grg-1	14.0	21.6	102.7	Convex Hyporelief
GC-C-7-Grg-2	14.0	21.6	93.4	Convex Hyporelief
GC-C-14-Grg-1	32.1	40.4	95.5	Concave Epirelief
GC-C-14-Grg-2	37.6	17.4	95.8	Convex Hyporelief
GC-C-14-Grg-3	17.3	22.1	95.5	Convex Hyporelief
GC-C-15-Grg-1	19.0	23.7	110.2	Concave Epirelief
GC-C-15-Grg-2	19.9	23.7	116.7	Concave Epirelief
GC-C-15-Grg-3	24.1	31.6	126.7	Concave Epirelief
GC-C-15-Grg-4	29.3	31.4	98.0	Concave Epirelief
GC-C-15-Grg-5	23.1	27.4	101.5	Convex Hyporelief
GC-C-15-Grg-6	24.1	31.7	104.7	Convex Hyporelief
GC-C-15-Grg-7	30.5	35.2	122.3	Convex Hyporelief
GC-C-15-Grg-8	24.7	29.8	124.8	Convex Hyporelief

Sample ID	Length (mm)	Width (mm)	AOD II–IV (degrees)	Preservation
GC-C-2-Mis-1	24.5	32.0	116.4	Convex Hyporelief
GC-C-2-Mis-2	24.5	34.8	113.8	Convex Hyporelief
GC-C-2-Mis-3	24.5	n/a	n/a	Convex Hyporelief
GC-C-2-Mis-4	n/a	n/a	n/a	Convex Hyporelief
GC-C-2-Mis-5	24.5	33.8	110.1	Convex Hyporelief
GC-C-16-Mis-1	18.0	26.0	118.6	Convex Hyporelief
GC-C-16-Mis-2	18.1	26.2	130.9	Convex Hyporelief
GC-C-16-Mis-3	19.7	26.4	126.2	Convex Hyporelief
GC-C-16-Mis-4	23.7	36.2	106.1	Convex Hyporelief
GC-C-16-Mis-5	25.6	37.7	119.6	Convex Hyporelief
GC-C-16-Mis-6	27.0	37.1	109.6	Convex Hyporelief
GC-C-16-Mis-7	25.4	38.2	113.4	Convex Hyporelief
GC-C-16-Mis-8	21.3	25.0	105.2	Convex Hyporelief
GC-C-20-Mis-1	33.2	29.0	125.4	Concave Epirelief
GC-C-20-Mis-2	46.7	34.6	119.2	Concave Epirelief
GC-C-20-Mis-3	41.7	32.1	130.4	Concave Epirelief
GC-C-20-Mis-4	43.9	36.4	139.4	Concave Epirelief
GC-C-20-Mis-5	40.3	31.4	129.6	Concave Epirelief
GC-C-20-Mis-6	23.7	n/a	n/a	Concave Epirelief
GC-C-20-Mis-7	32.0	31.8	119.5	Concave Epirelief
GC-C-20-Mis-8	21.1	31.7	132.9	Concave Epirelief
GC-C-20-Mis-9	40.3	31.3	146.7	Concave Epirelief
GC-C-20-Mis-10	43.6	29.5	176.0	Concave Epirelief
GC-C-20-Mis-11	43.6	37.4	154.6	Concave Epirelief
GC-C-20-Mis-12	43.7	35.0	116.9	Concave Epirelief
GC-C-20-Mis-13	33.3	31.3	149.2	Concave Epirelief

Sample ID	Length (mm)	Width (mm)	AOD II–IV (degrees)	Preservation
GC-C-4-Prf-1	44.1	63.7	117.7	Convex Hyporelief
GC-C-4-Prf-2	60.3	75.6	96.0	Convex Hyporelief
GC-C-4-Prf-3	n/a	n/a	n/a	Convex Hyporelief
GC-C-4-Prf-4	62.2	73.0	93.6	Convex Hyporelief
GC-C-4-Prf-5	62.0	73.5	106.6	Convex Hyporelief
GC-C-8-Prf-1	53.3	72.0	107.3	Concave Epirelief
GC-C-10-Prf-1	61.0	77.4	103.6	Concave Epirelief
GC-C-10-Prf-2	n/a	74.6	94.6	Concave Epirelief
GC-C-10-Prf-3	n/a	n/a	n/a	Concave Epirelief
GC-C-10-Prf-4	52.0	65.1	82.5	Concave Epirelief
GC-C-10-Prf-5	n/a	n/a	n/a	Concave Epirelief
GC-C-17-Prf-1	59.4	73.9	86.8	Convex Hyporelief
GC-C-17-Prf-2	n/a	73.7	n/a	Convex Hyporelief
GC-C-17-Prf-3	86.1	n/a	n/a	Concave Epirelief
GC-C-17-Prf-4	n/a	78.2	n/a	Concave Epirelief
GC-C-17-Prf-5	80.0	n/a	n/a	Concave Epirelief
GC-C-18-Prf-1	63.4	80.1	101.9	Concave Epirelief
GC-C-19-Prf-1	53.0	65.8	73.9	Concave Epirelief
GC-C-19-Prf-2	59.2	72.7	95.67	Concave Epirelief
GC-C-21-Prf-1	60.0	76.3	96.0	Concave Epirelief
GC-C-21-Prf-2	59.8	76.3	95.9	Concave Epirelief
GC-C-21-Prf-3	59.8	76.3	86.0	Concave Epirelief
GC-C-21-Prf-4	59.9	72.0	78.4	Concave Epirelief
GC-C-21-Prf-5	59.9	72.0	97.8	Concave Epirelief
GC-C-21-Prf-6	59.9	72.0	92.3	Concave Epirelief

Sample ID	Total Length (mm)	Linear Length (mm)	Sinuosity Index	Width (mm)	Amplitude (mm)	Preservation
GC-C-10-Tse-1	102.2	83.7	0.82	8.7	271.0	Concave Epirelief
GC-C-10-Tse-2	89.9	87.4	0.97	8.7	165.0	Concave Epirelief
GC-C-17-Tse-1	293.8	223.5	0.76	13.0	102.0	Convex Hyporelief
GC-C-21-Tse-1	792.8	650.0	0.82	7.35	147.0	Concave Epirelief

Trace	Slab ID	Tracks	Pace Length (mm)	Stride Length (mm)	Pace Width (mm)	Trackway Width (mm)	ϕ (degrees)
c.f. *Aviadactyla* isp.	GC-C-3	2	115.0	n/a	9.0	38.0	27.9, 2.1
c.f. *Aviadactyla* isp.	GC-C-3	2	97.0	n/a	25.0	63.0	4.3, 9.4
Gruipeda gryponyx	GC-C-6	4	62.5, 35.9, 73.3	93.5, 106.4	17.7, 15.0	35.7	7.7, 18, 10.6,
Midorikawapeda semipalmatus	GC-C-2	3	66.2, 81.4	148.3	16.3	33.1	13.1, 12.0, 17.9
Midorikawapeda semipalmatus	GC-C-2	2	n/a	n/a	14.5	n/a	18.4
Midorikawapeda semipalmatus	GC-C-16	4	78.5, 85.3, 42.9	156.7, 122.8	31.9, 17.5, 27.2	63.2	15.4, 15.6, 9.7, 9.6
Midorikawapeda semipalmatus	GC-C-16	3	82.8, 82.8	173.6	27.2. 23.9	42.8	21.7, 18.6, 17.4
Presbyorniformipes feduccii	GC-C-4	2	160.0	n/a	15.0	190.0	4.8, 6.9
Presbyorniformipes feduccii	GC-C-10	3	98.5	n/a	41.9, 25.3	101.1	4.2, 8.8
Presbyorniformipes feduccii	GC-C-17	2	n/a	n/a	15.3	98.8	5.1
Presbyorniformipes feduccii	GC-C-21	7	84.0, 81.0, 82.0, 96.0, 115.0	140.0, 142.0, 154.0, 188.0	27.0, 29.0, 17.0, 13.0, 21.0	122.0	3.8, 3.8, 14.9, 1.9, 6.2